SURVIVING IRREPARABLE DNA DAMAGE:

GENETIC MECHANISMS TO ESCAPE

PROGRAMMED CELL DEATH

by

Riddhita Chakraborty

A dissertation submitted to the faculty of
The University of Utah
in partial fulfillment of the requirements for the degree of

Doctor of Philosophy

Department of Biology

The University of Utah

December 2014

The University of Utah Graduate School

STATEMENT OF DISSERTATION APPROVAL

The dissertation of **Riddhita Chakraborty**

has been approved by the following supervisory committee members:

Kent G. Golic	, Chair	**10/21/2014** Date Approved
Markus Babst	, Member	**10/22/2014** Date Approved
Mark M. Metzstein	, Member	**10/22/2014** Date Approved
Michael D. Shapiro	, Member	**10/27/2014** Date Approved
Leslie E. Sieburth	, Member	**10/23/2014** Date Approved

and by **M. Denise Dearing** , Chair/Dean of

the Department/College/School of **Biology**

and by David B. Kieda, Dean of The Graduate School.

ABSTRACT

A cell with an irreparably damaged genome is genetically programmed to undergo cell death, called apoptosis. This is to make sure that such cells are not propagating the damaged DNA to their daughter cells, because it will lead to accumulation of genetic instability and is thus detrimental to the tissue or the organ, and to the organism as a whole. In spite of the highly efficient genetic programming to get succumbed to apoptosis, it has been sometimes found that some cells can escape from the fate of apoptosis and continue to survive and proliferate. Accumulation of such cells forms one of the first steps towards the development of cancer. For my dissertation, I have tried to identify the genetic mechanisms that aid a cell to survive DNA damage beyond repair. Thus, this study will help us understand the genetic routes to predisposition towards carcinogenesis and possibly identify new drug targets for cancer therapeutics.

Using a highly tractable genetic model organism, the fruitfly, *Drosophila melanogaster*, I first modeled irreparable DNA damage in the form of a single telomere loss – a mode of DNA damage that cannot be repaired by the DNA repair machinery. This served us as a system to assay the fate of cells following the DNA damage. In this background, I carried out a genetic screen to identify genes that help survival of cells withstanding telomere loss. Here I identified a

singular gene, *corp*, that inhibits P53-dependent cell death by negatively regulating the tumor suppressor, P53. I characterized Corp as the functional analog of vertebrate Mdm2 in the *Drosophila* system. I identified another gene through the screen - *fs(1)Yb*, that reduces cell survival following telomere loss possibly by inducing the DDR pathway following telomere loss.

Overall, my findings indicate that there are distinct genetic pathways that negatively or positively regulate cell survival following irreparable DNA damage. A tilt towards or away from them causes abnormal proliferation of cells containing damaged genome, thus predisposing an organism to cancer development.

I dedicate my thesis to my parents, Krishna Chakraborty and Biplab Chakraborty,

for their constant love and support to help me stand where I am today.

TABLE OF CONTENTS

LIST OF TABLES

LIST OF GENE NAMES AND FUNCTIONS

GENE	PROTEIN	CELLULAR MECHANISM
chk1/grp	Chk1	DNA damage response
chk2/loki/mnk	Chk1	DNA damage response
p53	P53	transcription, DNA repair, apoptosis
brca1	BRCA1	DNA damage response
cdc25	Cdc25	cell cycle control
nbs1	Nbs1	DNA DSB response
cdc2	Cdc2	cell cycle control
14-3-3σ	14-3-3σ	adapter protein, DNA damage responsive
p21	P21	G2 arrest
atm/*tefu*	ATM	DNA damage response
atr/*mei-41*	ATR	DNA damage response
Ku70/*Ku80*	Ku70/Ku80	NHEJ, telomere maintenance
mre11	Mre11	DNA DSB response
rad50	Rad50	DNA DSB response
bax	Bax	pro-apoptotic
noxa	Noxa	pro-apoptotic
puma	Puma	pro-apoptotic

apaf-1	APAF-1	pro-apoptotic
bad	Bad	pro-apoptotic
fas	Fas	death-receptor, pro-apoptotic
dr5	Dr5	death-receptor, pro-apoptotic
bcl-2	BcL-2	anti-apoptotic
corp	Corp	P53 negative regulator
mdm2	Mdm2	P53 negative regulator
hid	Hid	pro-apoptotic
reaper	Reaper	pro-apoptotic
pavarotti	Pavarotti	kinesin motor function
CG1632	CG1632	LDL receptor, proteolysis
pdcd4	Pdcd4	stem cell differentiation
CG8924	CG8924	transcriptional proliferation
med18	MED18	RNA pol II transcriptional mediator
CG2701	CG2701	Ubiquitin system component (?)
fs(1)Yb	Fs(1)Yb	germline stem cell maintenance
piwi	Piwi	piRNA synthesis
armi	Armi	piRNA synthesis
hiphop	Hiphop	telomere maintenance
CG14814	CG14814	not known
crebB17A	CrebB-17A	c-AMP regulated transcription
SmG	SmG	mitotic spindle organization
mthl1	Mthl1	early development function, morphogenesis

ACKNOWLEDGEMENTS

As I stand now, a stone's throw from the finish line of my graduate career, I would like to take the time to look back and extend my heartiest acknowledgements to all those who inspired me, extended their supportive hands, and put their belief in me to endure to the end of this journey that I started six years back.

First and foremost, I would thank my doctoral adviser, my guru, Dr. Kent Golic. A naïve as I was, he taught me to appreciate genetics in the truest essence and the art of doing scientific research. His invaluable guidance and patience through my mistakes tremendously helped me to develop my skills over years to start practicing logical hypothesis-driven research. Besides, he has been an exceedingly supportive and understanding mentor and I truly consider myself very fortunate to have secured a position as a graduate student in his laboratory years ago. Next I would acknowledge Mary Golic. She always made me see the Golic lab as my most comfortable and safest nook. Her warmth and kind-heartedness made me not only able to survive but also to stand straight in some of the most stressful periods of my life. I think, I would always fall short of words in trying to thank Kent and Mary. In a nutshell, without them I wouldn't be standing where I am today.

Next, I would like to thank my committee members, Dr. Leslie Sieburth, Dr. Markus Babst, Dr. Mark Metzstein, and Dr. Mike Shapiro. I have been very lucky to have these wonderful scientists on my committee who made my yearly committee meetings such an enjoyable and great learning experience, which always made me look forward to the next year's meeting. I particularly thank Mark for prompting me to attend my first *Drosophila* conference and for kindly giving me the various fly stocks I needed. I thank Markus for allowing me to carry out my Western blot experiments in his lab.

I would next thank the present and some of the past Golic lab members, Dr. Simon Titen, Dr. Rebeccah Kurzhals, Dr. Heng Xie, Adam Lin, Jayaram Bhandari, Jenny Wilson, Zachary Lee, Arun Kannanganat, and Hunter Hill. Simon, Rebeccah, and Heng never grew tired of answering my zillion questions, be it on labwork or on coursework. I thank them for their contribution towards my education as a scientist. Even outside science, they became an integral part of my life in the new continent: from getting acquainted with the lifestyle in the States to solving nitty-gritties of daily life. Adam and Jay have always extended their helping hands whenever I needed them. All these people have always made me see the Golic lab as a part of my family.

I thank Dr. Julie Hollien for helping me with learning the cell culture techniques and her important input in troubleshooting with qPCR. My heartful thanks to my buddies from the Hollien lab, Jinny Li, Kristin Moore, and Deepika Goddam, for cell culture and qPCR troubleshooting. Thanks to Shrawan Mageswaran and Matthew Curtiss from the Babst lab for troubleshooting during

Western blot experiments. My thanks to Dr. Colin Dale for letting me use the qPCR facility in his lab.

I thank our collaborators, Dr. Lei Zhou and Dr. Ying Li, University of Florida, for their supportive work. I thank Dr. Tin Tin Su and Dr. Andreas Bergmann for sharing their unpublished data with us and Dr. Haifan Lin for kindly gifting us the *fs(1)Yb* mutants.

I thank the University of Utah Core facilities for DNA sequencing and primer facilities. I thank the *Drosophila* Stock Centers of Bloomington and Vienna and all the scientific vendors for all their reagents to make my research smoother. I highly express my gratitude toward our graduate coordinator, Shannon Nielsen, for her help and support with all administrative paperwork and truthfully reminding me of all the deadlines throughout the period of my doctoral work.

I would thank Dr. Gordon Lark for sharing with me his scientific philosophies and experiences that have highly influenced me and made me feel a part of the global scientific fraternity, instead of taking science as a mere rat race. I would also like to mention here and acknowledge some of my scientific forefathers whose biographies and works have always inspired and influenced me into doing and enjoying the extraordinary art of *Drosophila* genetics: Dr. Thomas Hunt Morgan, Dr. Alfred Sturtevant, Dr. Edward Novitski, Dr. Seymour Benzer, and Dr. Larry Sandler. I thank my teachers and supervisors in India, Dr. Debashis Banerjee, Dr. Asok Mukherjee, Dr. Rathindranath Baral, Dr. Chanchal Dasgupta, and Dr. Uma Dasgupta, who have always instigated my scientific

inquisitiveness and encouraged me to do good science. I would also thank my biology tutor during my high school days, Gopal Chandra Paul, who planted in me the initial interests in biology, particularly in genetics. Thank you all for making me dream high.

Finally, I thank my parents for their love, protection, support, and encouragement all through my life to stand where I stand today.

Last but not the least, I acknowledge those without whom my research could not have been conducted, those who bore all the pain to direct us onto our path of scientific discoveries: my tiny friends, the fruitflies.

CHAPTER 1

INTRODUCTION

The survival and evolution of life depends on the faithful inheritance of information through DNA from mother to daughter cells both in the soma and through the germline, with not only accurate DNA replication and distribution of genetic material, but also keeping the mutation load in cells to a minimum. The beauty of the living system lies in that it has a highly evolved intrinsic surveillance system by which it can sense damage to its DNA and respond accordingly, thereby maintaining the fidelity of its genome.

Cellular response to DNA damage

Cellular metabolites, intracellular accumulated ROS, or external environmental factors like X-ray, UV irradiation, and toxic mutagenic chemicals are constantly inflicting damage to the genome of an organism. Cells are, however, well-armed to combat such constant insults. There are primarily three branches of this multifaceted damage response pathway that the cells exhibit in response to DNA damage: cell cycle arrest, DNA repair, and programmed cell death or apoptosis (Jackson and Bartek, 2009).

A detailed study has been made on the signal transducers following DNA damage that triggers the damage response pathways at their downstream. One of the classes of signal transducers comprises phospho-inositide kinase (PIK)-related proteins that include ATM and ATR. Downstream of ATM and ATR are two structurally unrelated proteins with overlapping substrate specificity: checkpoint serine/threonine kinases CHK2 and CHK1 activate a cascade of downstream effector proteins, like p53, BRCA1, Cdc25, Nbs1, etc. that execute

the functions of DNA damage responses (Figure 1). Initially, the term checkpoint referred to the 'control mechanism enforcing dependency in the cell cycle' (Hartwell and Weinert, 1989) but later, it was also found to control DNA repair and apoptotic induction as well. These pathways are, to a large extent, conserved from mammals to lower invertebrates like *Drosophila* and single-celled eukaryotes, such as yeast. Several of the checkpoint genes are essential for organismal survival, implying that this pathway has important roles to play in functions that are tightly linked to normal cellular physiology. Inactivation of the checkpoint pathways leads to cancer development in mammals.

Cell cycle arrest ensures that the damaged DNA is not replicated and that the cells with damaged DNA are not proliferating. In mammals, Chk1 and Chk2 both play a role in preventing mitotic entry following DNA damage. Evidence shows that Chk2 and Chk1 induce inhibitory phosphorylation of Cdc25, which then fails to dephosphorylate Cdc2. Arrest at the G2 phase of cell cycle is primarily maintained and regulated by phosphorylated Cdc2 (Brown et al., 1999; Chaturvedi et al., 1999; Matsuoka et al., 1998; Nurse, 1997; Sanchez et al., 1997). Further, Chk2-activated p53 induces 14-3-3σ and p21 that play important roles in maintaining G2 arrest in response to DNA damage (Bunz et al., 1998; Chan et al., 1999). ATR phosphorylates Chk1 at Ser 345 in response to UV light both *in vivo* and *in vitro* and mice lacking *chk1* die in early embryogenesis like *ATR*$^{-/-}$ mice (Kim et al., 1999; Liu et al., 2000; Takai et al., 2000). *chk1* mutant embryonic stem cells are incapable of preventing mitotic entry after irradiation, implying that Chk1 is required for G2/M phase transition checkpoint in response

to DNA damage (Liu et al., 2000). Similarly, in *Drosophila*, *ATR*/*mei-41* induces *Chk1*/*grp*, which are essential to induce cell cycle arrest in response to DNA damage (de Vries, 2005; Song, 2005; Song et al., 2004). *grp* mutants fail to delay anaphase onset following I-CreI-induced double-strand breaks (Royou et al., 2005). The *ATM*/*tefu* and *Chk2*/*mnk* pathway also play a role in cell cycle arrest, but is not absolutely indispensable (Bi, 2005; de Vries, 2005; Song et al., 2004; Xu et al., 2001).

The wide variety of DNA lesions necessitates multiple DNA repair mechanisms (Jackson and Bartek, 2009). For DNA single-strand lesions, the mismatched base or region of missing base pairs is recognized and several mismatch-repair methods are applied to fix it: (1) Following detection of mismatches, the insertion-deletion loop triggers a single-strand incision that is worked upon by nuclease, polymerase, and ligase enzymes to repair the damage (Jiricny, 2006). (2) Base-excision repair: Here, the DNA glycosylase enzyme recognizes the damaged base and mediates its removal (David et al., 2007). (3) Nucleotide excision repair: After recognition of the DNA helix-distorting lesions, the damage is excised as a 20-30 base-pair long oligonucleotide, thus producing a single-stranded DNA, which is then acted upon by DNA polymerase, associated factors, and finally ligase for fixing the damage (Hoeijmakers, 2001). For DNA double-strand break (DSB) repair, two principle methods are used: (1) non-homologous end joining (NHEJ) and (2) homologous recombination (HR). NHEJ is error-prone and can occur at any phase of the cell cycle. Here, the DSB is recognized by Ku proteins, which then activate DNA protein kinases, leading to

recruitment of end-processing enzymes, polymerases and DNA ligase IV to join any two double-strand breaks without sequence specificity (Hefferin and Tomkinson, 2005; Lieber, 2008). Ku70 and Ku80 deficient mice showed profound deficiency in DNA DSB repair and exhibited dwarfism, also indicating their roles in growth control (Nussenzweig et al., 1996; Ouyang et al., 1997). HR, which is confined to S and G2 phase of cell cycle, is a comparatively faithful mode of repair as it uses the sister chromatid to mediate the repair process. ssDNA, generated by the Mre11-Rad50-Nbs1 (MRN complex), invades the undamaged template strand, is extended by polymerase, and following nuclease, helicase, and ligase activity, strand resolution occurs (San Filippo et al., 2008). The DNA repair pathway components are highly conserved in *Drosophila* (Sekelsky et al., 2000). Loss-of-function mutations of *mre11*, *rad50*, and *nbs* in *Drosophila* failed to repair irradiation-induced DNA damage (Mukherjee et al., 2009). Chk2-mediated P53 activation induces the transcription of a wide array of DNA repair pathway components in single- or double-strand repair, like, *Mre11*, *Rad50*, and *Ku70/Ku80* (Brodsky et al., 2004). Interestingly, a *mei-41*-mediated, *Chk1*/*Chk2*-independent DNA repair mechanism through HR has been also reported (LaRocque et al., 2007).

The role of P53 in DNA repair has been widely studied (Sengupta and Harris, 2005). Isogenic matched cell lines exposure to a chemical DNA damaging agent showed slower base excision repair when they lacked *p53* and the repair mechanism involves binding to specific transcription factors (Seo et al., 2002; Wang et al., 1995). Disruption of the components of the MRN complex also

causes failure to repair DNA double-strand breaks (D'Amours and Jackson, 2002; Tauchi et al., 2002; Williams et al., 2007; Yuan and Chen, 2010).

Thus, to summarize so far, upon being sensed, DNA damage triggers checkpoint mechanisms that arrest cell cycle progression and repair the damaged DNA before entering into the next mitotic cycle. However, if the DNA damage is beyond repair, the cells may succumb to apoptosis and are thus eliminated in order to stem the spread of genetic aberrations and thereby maintain genomic stability.

DNA damage beyond repair

The inability to repair damage usually leads to various types of disorders and predisposition towards tumor development. Programmed cell death is a last line of defense against the development of cancer. P53 is extremely essential for induction of apoptosis following irreparable DNA damage (Fridman and Lowe, 2003; Vousden and Lu, 2002; Yoshida and Miki, 2010). Humans lacking one copy of *p53* are predisposed to develop cancers and *p53* knockout mice also develop cancers at a higher rate (Donehower et al., 1992; Jackson and Bartek, 2009; Sancar et al., 2004; Zhou and Elledge, 2000). Irradiation-induced *chk2*$^{-/-}$ thymocytes do not have stabilized and activated *p53* and have no induction of its downstream genes in the apoptotic pathway (Hirao, 2000). In mammals, P53 positively regulates both intrinsic (mitochrondrially-regulated) and extrinsic (cell-surface receptor-mediated) apoptotic pathways by transcriptional activation of multiple genes and also by transcriptional independent mechanisms (Chipuk and

Green, 2006; Haupt, 2003; Yoshida and Miki, 2010). For example, P53 induces the pro-apoptotic genes *Bax*, *Noxa*, *Puma*, and *Apaf-1* and counteracts the anti-apoptotic *Bad* in the intrinsic pathway (Li et al., 2008; Miyashita and Reed, 1995; Nakano and Vousden, 2001; Oda et al., 2000; Robles et al., 2001) and the death receptors Fas and DR5 (Haupt, 2003) in the extrinsic pathway. P53 also binds to the anti-apoptotic BcL-2 and compromises the latter's ability to stabilize the mitochondrial membrane (Wolff et al., 2008), resulting in cytochrome C release – that promotes the pro-apoptotic cascade activation.

Most of the DDR pathways, including cell cycle arrest, DNA repair, and apoptosis, are conserved in the *Drosophila* model. However, in flies, P53 does not participate in cell cycle arrest (Sogame et al., 2003); following activation by Chk2 in response to DNA damage, it induces DNA repair or apoptosis (Brodsky et al., 2004; Kurzhals et al., 2011; Peters et al., 2002; Titen and Golic, 2008). Besides, the existence of P53-independent apoptotic pathways have also been reported (McNamee and Brodsky, 2009; Titen and Golic, 2008; van Bergeijk et al., 2012; Wichmann et al., 2006).

Surviving irreparable DNA damage

In spite of the multistep checkpoints, a fraction of cells may still continue to survive with irreparable DNA damage (Ahmad and Golic, 1999; Kurzhals et al., 2011; Titen and Golic, 2008). One way by which this can happen is if the DDR pathway genes are mutated. There may also be some more defined genetic pathways that allow the survival of such cells. It will be very interesting to identify

and characterize such pathways, as they will help us elucidate pathways to carcinogenesis or other complex human diseases.

Dissertation outline

In my dissertation, I have made an attempt to understand the genetic mechanisms that regulate a cell's life or death decision in response to irreparable DNA damage. In Chapter 2, I will start by describing a genetic method that I have used to assay the fate of somatic cells with respect to surviving or succumbing to cell death following induction of nonrepairable DNA damage in the form of a single telomere loss. In this background of telomere loss, I will present the putative genes that I have identified as enhancers and suppressors of cell death, using a highly efficient genetic misexpression (*EP*) screen. In Chapter 3, I will describe the characterization of one of the candidate genes from the screen, called *corp*. I will show how Corp functions in a negative feedback loop on the tumor suppressor P53 and functions as the functional analog of the vertebrate Mdm2. In Chapter 4, I will show my work on the characterization of another candidate gene, *fs(1)Yb*, identified as a inducer of apoptotic phenotype in the screen. In Chapter 5, I will address the roles played by *p53* and *corp* on the viability of the animals when they are exposed to DNA damaged, caused by ionizing radiation. Finally in Chapter 6, I perform a critical analysis of all my findings and discuss how they contribute to answering the bigger question addressed at the beginning of this dissertation, that is, how a cell survives irreparable DNA damage. In the Appendices, I present the entire data sheet of

EP screen results and a list of the *Drosophila* stocks that I have constructed, for future reference and use.

Figure 1. DNA damage response pathways. Insult to the DNA triggers a damage response through signal transducers (like *ATM*, *ATR*, and checkpoint kinases) and effectors (like *p53*, *Cdc25*, *nbs1* and *BRCA1*) that activate multiple downstream pathways to combat the damage – cell cycle arrest, DNA repair, and apoptosis. Apoptotic response occurs particularly in response to irreparable damage. These pathways are mostly conserved from mammals to lower invertebrates.

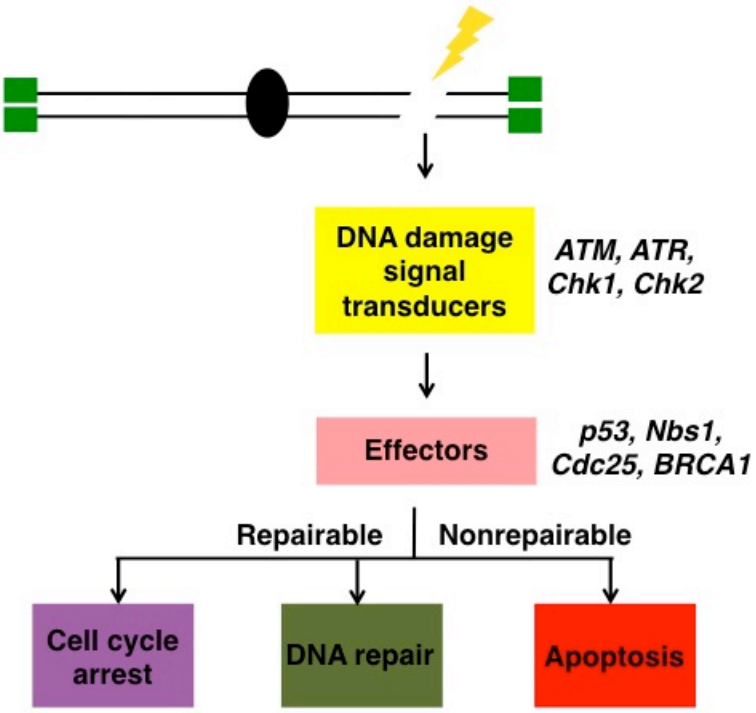
DNA damage signal transducers
ATM, ATR, Chk1, Chk2
Effectors
p53, Nbs1, Cdc25, BRCA1
Repairable
Nonrepairable
Cell cycle arrest
DNA repair
Apoptosis

References

Ahmad, K.K., and Golic, K.G.K. (1999). Telomere loss in somatic cells of Drosophila causes cell cycle arrest and apoptosis. Genetics *151*, 1041–1051.

Bi, X. (2005). Drosophila ATM and Mre11 Are Essential for the G2/M Checkpoint Induced by Low-Dose Irradiation. Genetics *171*, 845–847.

Brodsky, M.H., Weinert, B.T., Tsang, G., Rong, Y.S., McGinnis, N.M., Golic, K.G., Rio, D.C., and Rubin, G.M. (2004). Drosophila melanogaster MNK/Chk2 and p53 Regulate Multiple DNA Repair and Apoptotic Pathways following DNA Damage. Molecular and Cellular Biology *24*, 1219–1231.

Brown, A.L., Lee, C.H., Schwarz, J.K., Mitiku, N., Piwnica-Worms, H., and Chung, J.H. (1999). A human Cds1-related kinase that functions downstream of ATM protein in the cellular response to DNA damage. Proc. Natl. Acad. Sci. U.S.a. *96*, 3745–3750.

Bunz, F., Dutriaux, A., Lengauer, C., Waldman, T., Zhou, S., Brown, J.P., Sedivy, J.M., Kinzler, K.W., and Vogelstein, B. (1998). Requirement for p53 and p21 to sustain G2 arrest after DNA damage. Science *282*, 1497–1501.

Chan, T.A., Hermeking, H., Lengauer, C., Kinzler, K.W., and Vogelstein, B. (1999). 14-3-3|[sigma]| is required to prevent mitotic catastrophe after DNA damage. Nature *401*, 616–620.

Chaturvedi, P.P., Eng, W.K.W., Zhu, Y.Y., Mattern, M.R.M., Mishra, R.R., Hurle, M.R.M., Zhang, X.X., Annan, R.S.R., Lu, Q.Q., Faucette, L.F.L., et al. (1999). Mammalian Chk2 is a downstream effector of the ATM-dependent DNA damage checkpoint pathway. Oncogene *18*, 4047–4054.

Chipuk, J.E., and Green, D.R. (2006). Dissecting p53-dependent apoptosis. Cell Death Differ *13*, 994–1002.

D'Amours, D., and Jackson, S.P. (2002). The mre11 complex: at the crossroads of dna repair and checkpoint signalling. Nat. Rev. Mol. Cell Biol. *3*, 317–327.

David, S.S., O'Shea, V.L., and Kundu, S. (2007). Base-excision repair of oxidative DNA damage. Nature *447*, 941–950.

de Vries, H.I. (2005). Grp/DChk1 is required for G2-M checkpoint activation in Drosophila S2 cells, whereas Dmnk/DChk2 is dispensable. Journal of Cell Science *118*, 1833–1842.

Donehower, L.A.L., Harvey, M.M., Slagle, B.L.B., McArthur, M.J.M., Montgomery, C.A.C., Butel, J.S.J., and Bradley, A.A. (1992). Mice deficient for p53 are developmentally normal but susceptible to spontaneous tumours. Nature *356*, 215–221.

Fridman, J.S., and Lowe, S.W. (2003). Control of apoptosis by p53. Oncogene *22*, 9030–9040.

Hartwell, L.H., and Weinert, T.A. (1989). Checkpoints: controls that ensure the order of cell cycle events. Science *246*, 629–634.

Haupt, S. (2003). Apoptosis - the p53 network. Journal of Cell Science *116*, 4077–4085.

Hefferin, M.L., and Tomkinson, A.E. (2005). Mechanism of DNA double-strand break repair by non-homologous end joining. DNA Repair (Amst) *4*, 639–648.

Hirao, A. (2000). DNA Damage-Induced Activation of p53 by the Checkpoint Kinase Chk2. Science *287*, 1824–1827.

Hoeijmakers, J.H. (2001). Genome maintenance mechanisms for preventing cancer. Nature *411*, 366–374.

Jackson, S.P., and Bartek, J. (2009). The DNA-damage response in human biology and disease. Nature *461*, 1071–1078.

Jiricny, J. (2006). The multifaceted mismatch-repair system. Nat. Rev. Mol. Cell Biol. *7*, 335–346.

Kim, S.T., Lim, D.S., Canman, C.E., and Kastan, M.B. (1999). Substrate Specificities and Identification of Putative Substrates of ATM Kinase Family Members. Journal of Biological Chemistry *274*, 37538–37543.

Kurzhals, R.L., Titen, S.W.A., Xie, H.B., and Golic, K.G. (2011). Chk2 and p53 are haploinsufficient with dependent and independent functions to eliminate cells after telomere loss. PLoS Genet *7*, e1002103–e1002103.

LaRocque, J.R., Jaklevic, B., Su, T.T., and Sekelsky, J. (2007). Drosophila ATR in double-strand break repair. Genetics *175*, 1023–1033.

Li, Y.-Z., Lu, D.-Y., Tan, W.-Q., Wang, J.-X., and Li, P.-F. (2008). p53 initiates apoptosis by transcriptionally targeting the antiapoptotic protein ARC. Molecular and Cellular Biology *28*, 564–574.

Lieber, M.R. (2008). The mechanism of human nonhomologous DNA end joining. J. Biol. Chem. *283*, 1–5.

Liu, Q., Guntuku, S., Cui, X.S., Matsuoka, S., Cortez, D., Tamai, K., Luo, G., Carattini-Rivera, S., DeMayo, F., Bradley, A., et al. (2000). Chk1 is an essential kinase that is regulated by Atr and required for the G(2)/M DNA damage checkpoint. Genes & Development *14*, 1448–1459.

Matsuoka, S., Huang, M., and Elledge, S.J. (1998). Linkage of ATM to cell cycle

regulation by the Chk2 protein kinase. Science *282*, 1893–1897.

McNamee, L.M., and Brodsky, M.H. (2009). p53-Independent Apoptosis Limits DNA Damage-Induced Aneuploidy. Genetics *182*, 423–435.

Miyashita, T., and Reed, J.C. (1995). Tumor suppressor p53 is a direct transcriptional activator of the human bax gene. Cell *80*, 293–299.

Mukherjee, S., LaFave, M.C., and Sekelsky, J. (2009). DNA damage responses in Drosophila nbs mutants with reduced or altered NBS function. DNA Repair (Amst).

Nakano, K., and Vousden, K.H. (2001). PUMA, a novel proapoptotic gene, is induced by p53. Mol. Cell *7*, 683–694.

Nurse, P. (1997). Checkpoint pathways come of age. Cell *91*, 865–867.

Nussenzweig, A., Chen, C., da Costa Soares, V., Sanchez, M., Sokol, K., Nussenzweig, M.C., and Li, G.C. (1996). Requirement for Ku80 in growth and immunoglobulin V(D)J recombination. Nature *382*, 551–555.

Oda, E., Ohki, R., Murasawa, H., Nemoto, J., Shibue, T., Yamashita, T., Tokino, T., Taniguchi, T., and Tanaka, N. (2000). Noxa, a BH3-only member of the Bcl-2 family and candidate mediator of p53-induced apoptosis. Science *288*, 1053–1058.

Ouyang, H., Nussenzweig, A., Kurimasa, A., Soares, V.D.C., Li, X., Cordon-Cardo, C., Li, W.H., Cheong, N., Nussenzweig, M., Iliakis, G., et al. (1997). Ku70 Is Required for DNA Repair but Not for T Cell Antigen Receptor Gene Recombination In Vivo. Journal of Experimental Medicine *186*, 921–929.

Peters, M., DeLuca, C., Hirao, A., Stambolic, V., Potter, J., Zhou, L., Liepa, J., Snow, B., Arya, S., Wong, J., et al. (2002). Chk2 regulates irradiation-induced, p53-mediated apoptosis in Drosophila. Proc Natl Acad Sci USA *99*, 11305–11310.

Robles, A.I., Bemmels, N.A., Foraker, A.B., and Harris, C.C. (2001). APAF-1 is a transcriptional target of p53 in DNA damage-induced apoptosis. Cancer Res. *61*, 6660–6664.

Royou, A., Macias, H., and Sullivan, W. (2005). The Drosophila Grp/Chk1 DNA Damage Checkpoint Controls Entry into Anaphase. Current Biology.

San Filippo, J., Sung, P., and Klein, H. (2008). Mechanism of Eukaryotic Homologous Recombination. Annu. Rev. Biochem. *77*, 229–257.

Sancar, A.A., Lindsey-Boltz, L.A.L., Unsal-Kaçmaz, K.K., and Linn, S.S. (2004). Molecular mechanisms of mammalian DNA repair and the DNA damage

checkpoints. Biochemistry *73*, 39–85.

Sanchez, Y., Wong, C., Thoma, R.S., Richman, R., Wu, Z., Piwnica-Worms, H., and Elledge, S.J. (1997). Conservation of the Chk1 checkpoint pathway in mammals: linkage of DNA damage to Cdk regulation through Cdc25. Science *277*, 1497–1501.

Sekelsky, J.J., Brodsky, M.H., and Burtis, K.C. (2000). DNA Repair in Drosophila. The Journal of Cell Biology.

Sengupta, S., and Harris, C.C. (2005). p53: traffic cop at the crossroads of DNA repair and recombination. Nat. Rev. Mol. Cell Biol. *6*, 44–55.

Seo, Y.R., Fishel, M.L., Amundson, S., Kelley, M.R., and Smith, M.L. (2002). Implication of p53 in base excision DNA repair: in vivo evidence. Oncogene *21*, 731–737.

Sogame, N., Kim, M., and Abrams, J.M. (2003). Drosophila p53 preserves genomic stability by regulating cell death. Proc. Natl. Acad. Sci. U.S.a. *100*, 4696–4701.

Song, Y.-H. (2005). Drosophila melanogaster: a Model for the Study of DNA Damage Checkpoint Response. Mol. Cells *19*, 3651–3660.

Song, Y.-H., Mirey, G., Betson, M., Haber, D.A., and Settleman, J. (2004). The Drosophila ATM ortholog, dATM, mediates the response to ionizing radiation and to spontaneous DNA damage during development. Curr. Biol. *14*, 1354–1359.

Takai, H., Tominaga, K., Motoyama, N., Minamishima, Y.A., Nagahama, H., Tsukiyama, T., Ikeda, K., Nakayama, K., Nakanishi, M., and Nakayama, K. (2000). Aberrant cell cycle checkpoint function and early embryonic death in Chk1(-/-) mice. Genes & Development *14*, 1439–1447.

Tauchi, H., Kobayashi, J., Morishima, K.-I., van Gent, D.C., Shiraishi, T., Verkaik, N.S., vanHeems, D., Ito, E., Nakamura, A., Sonoda, E., et al. (2002). Nbs1 is essential for DNA repair by homologous recombination in higher vertebrate cells. Nature *420*, 93–98.

Titen, S.W.A., and Golic, K.G. (2008). Telomere Loss Provokes Multiple Pathways to Apoptosis and Produces Genomic Instability in Drosophila melanogaster. Genetics *180*, 1821–1832.

van Bergeijk, P., Heimiller, J., Uyetake, L., and Su, T.T. (2012). Genome-Wide Expression Analysis Identifies a Modulator of Ionizing Radiation-Induced p53-Independent Apoptosis in Drosophila melanogaster. PLoS ONE *7*, e36539.

Vousden, K.H., and Lu, X. (2002). Live or let die: the cell's response to p53. Nat. Rev. Cancer. *2*, 594–604.

Wang, X.W., Yeh, H., Schaeffer, L., Roy, R., Moncollin, V., Egly, J.M., Wang, Z., Friedberg, E.C., Evans, M.K., Taffe, B.G., et al. (1995). p53 modulation of TFIIH–associated nucleotide excision repair activity. Nat Genet *10*, 188–195.

Wichmann, A., Jaklevic, B., and Su, T.T. (2006). Ionizing radiation induces caspase-dependent but Chk2- and p53-independent cell death in Drosophila melanogaster. Proc. Natl. Acad. Sci. U.S.a. *103*, 9952–9957.

Williams, R.S., Williams, J.S., and Tainer, J.A. (2007). Mre11–Rad50–Nbs1 is a keystone complex connecting DNA repair machinery, double-strand break signaling, and the chromatin template. Biochem. Cell Biol. *85*, 509–520.

Wolff, S., Erster, S., Palacios, G., and Moll, U.M. (2008). p53's mitochondrial translocation and MOMP action is independent of Puma and Bax and severely disrupts mitochondrial membrane integrity. Cell Res *18*, 733–744.

Xu, J., Xin, S., and Du, W. (2001). Drosophila Chk2 is required for DNA damage-mediated cell cycle arrest and apoptosis. FEBS Letters *508*, 394–398.

Yoshida, K.K., and Miki, Y.Y. (2010). The cell death machinery governed by the p53 tumor suppressor in response to DNA damage. Cancer Sci *101*, 831–835.

Yuan, J., and Chen, J. (2010). MRE11-RAD50-NBS1 Complex Dictates DNA Repair Independent of H2AX. Journal of Biological Chemistry *285*, 1097–1104.

Zhou, B.-B.S., and Elledge, S.J. (2000). The DNA damage response: putting checkpoints in perspective. Nature *408*, 433–439.

CHAPTER 2

IDENTIFYING NOVEL GENES THAT MODULATE CELL SURVIVAL FOLLOWING IRREPARABLE DNA DAMAGE IN *DROSOPHILA MELANOGASTER*

Abstract

The DNA damage response machinery responds to irreparably damaged or broken DNA by activating the apoptotic pathway so that such cells are eliminated, to help maintain the fidelity of the genome. A chromosome lacking a single telomere represents irreparable DNA damage and triggers apoptotic response. However, there is evidence that some cells can survive telomere loss and continue to proliferate. This is detrimental to the health of the organism as it induces genomic instability, genetic imbalance, and predisposes cells towards carcinogenesis. So, it is essential to understand the underlying mechanisms by which a cell can survive telomere loss. To do that, we first built a tractable genetic model of a single telomere loss in somatic cells. We found that some cells do survive after a single telomere loss. Then I used this system to carry out a genetic misexpression screen to identify genes that behave as inducers or suppressors cell death after telomere loss. I identified four suppressors and three inducers through this screen.

Introduction

The normal ends of chromosomes are protected and do not participate in chromosomal rearrangements. However, when broken ends are created by ionizing radiation, they cannot substitute for normal ends (Muller, 1940). This formed the earliest definition of telomere. Telomeres were rediscovered later structurally as nucleic acid-protein complexes that protect the end of linear chromosomes from end-to-end fusions and solve the end replication problem

(Blackburn, 2001). They consist of repetitive sequences at the chromosome termini that are bound by proteins, which can recognize the terminal repeats. Such a protein is telomerase, which plays a role in extending the repeat sequences at the chromosome ends. Most dipterans, however, do not have telomerase; instead, the ends are maintained by repeated transposition of retrotransposons (Biessmann and Mason, 2003). Despite this difference, the telomere capping proteins that protect the chromosome from end-to-end fusion events are mostly conserved between the eukaryotes (Cenci et al., 2005) and loss of the telomere triggers the similar instability response, suggesting that telomere maintenance is an essential phenomenon in a general biological perspective.

A missing telomere poses a unique challenge to the repair machinery. It cannot be repaired by methods that reattach two broken ends. In the 1930s, while Barbara McClintock was using cytogenetics to follow the fate of broken chromosomes in maize, she demonstrated that chromosomes that have lost their normal ends undergo end-to-end fusion, forming anaphase bridges that subsequently break, and a breakage-fusion-bridge (BFB) cycle follows (McClintock, 1939). A single missing telomere is capable of inducing persistent genomic instability in the cells. This genomic instability cannot be repaired and forms a hallmark of cancer (Al-Mulla et al., 1999; Artandi and DePinho, 2010; Murnane, 2010; Ong et al., 1998; Schneider and Kulesz-Martin, 2004). There is evidence of aberrant karyotypes including fusion events involving other chromosomes, polyploidy, and chromosomal rearrangements in cells that

originally had a single telomere loss (Hackett and Greider, 2003; Sabatier et al., 2005; Sandell, 1993; Titen and Golic, 2008). Such cells usually undergo apoptosis to stem the spread of the unstable genome to the daughter cells; however, cancer cells exemplify instances where they escape apoptosis and continue to survive and proliferate. In *Drosophila*, a fraction of somatic cells have been found to survive after telomere loss (Ahmad and Golic, 1999; Kurzhals et al., 2011; Titen and Golic, 2008). It is important to understand how they can survive, because that can help us understand the development of cancer.

Here, I induce irreparable DNA damage in the form of a single telomere loss specifically in the developing eye to build a tractable system for quantitatively assaying the fate of cells: that is, to find out if they can survive or succumb to cell death. We call this the BARTL (Bar + Telomere Loss) assay and found that some cells can survive and reconstitute a partial eye after telomere loss. In this background, I carried out a genetic misexpression screening to identify genes that help cells to survive better or incline them to die faster. My screen uncovered four suppressors and three enhancers of the cell death phenotype following telomere loss.

Materials and methods

Drosophila stock collections:

(1) *UAS-FLP* stocks used: *P{UAS-FLP1.1D}JD1* (BL 4539), *P{UAS-FLP1.1D}JD2* (BL 4540), *P{UAS-FLP.Exel}3* (BL 8209) and *P{UAS-FLP}2B* and *P{UAS-FLP, ry^{+}}SB3* were from our lab stock collection.

(2) *eyGal4* stocks used: *P{Gal4-ey.H}3-8* (BL 5534), *P{Gal4-ey.H}4-8* (BL 5535), *P{ey3.5Gal4.Exel}2* (BL 8220), and *P{ey3.5Gal4.Exel}3* (BL 8219).

(3) *P{EPgy2}*: All available *EPgy2* stocks on chromosome *X* (total # 600) were obtained from Bloomington *Drosophila* Stock Center. For a detailed list, refer to Appendix A.

(3) RNAi stocks used are as follows:

RNAi-*corp*: v102751, v16130

RNAi-*CG1632*: v106107, v5478

RNAi-*Pdcd4*: v16160, v16162, BL 38445

RNAi-*CG8924*: v48041, v48042, BL 35705

RNAi-*Med18*: v48490, v48491, v28265, v28264, v106760

RNAi-*CG2701*: v106635, v25433

RNAi-*fs(1)Yb*: BL 35181, BL35301

RNAi-*CG14814*: v41553

RNAi-*CrebB17A*: v6103

RNAi-*SmG*: BL 26617

RNAi-*mthl1*: v33136, BL 15318

(4) Other stocks used: *y w/DcY(H1)* or simply *H1* (Kurzhals et al., 2011), [>w+]89A (laboratory stock), *P{eyFLP.N}5* (BL5576).

Crosses: All crosses were maintained at 25°C on standard cornmeal food.

Results and discussion

Irreparable DNA damage is modeled in the form of a single telomere loss in the proliferating cells of the eye. To build a tractable model system where the fate of cells following irreparable DNA damage can be observed, we induced telomere loss on a single chromosome – a loss that cannot be repaired by the DNA repair machinery. The basic blueprint of this method is to induce recombination between inverted *FRT* sites on sister chromatids of the chromosome by FLP induction (Golic and Lindquist, 1989), so that a dicentric chromosome is produced. When this dicentric chromosome is pulled towards two opposite poles during the anaphase of the next mitotic cycle, it will break, delivering a chromosome with a broken end/ lost telomere to each of the daughter cells.

For our system, we used flies that carry *FRT*s on the *Y* chromosome. This chromosome is referred to as the *H1* chromosome (Figure 2A), after Heng Xie who constructed it. It has inverted *FRT*s inserted on its long arm, marked by w^{hs}. Distal to the *FRT*s is the dominant B^S mutation (Fristrom, 1969; Michinomae and Kaji, 1973). A y^+ gene is located at the tip of its short arm. FLP expression, for inducing recombination between the *FRT* sites, was produced specifically in proliferating cells of the eye by the *UAS-Gal4* system (Brand and Perrimon, 1993). On induction of FLP-mediated recombination between the inverted *FRT*s on the *H1* chromosome, a dicentric chromosome and a reciprocal acentric chromosome are formed and B^S is located on the acentric. This acentric fragment is frequently lost (Titen and Golic, 2008). Thus, the telomere loss is

marked by the loss of B^S mutation (Figure 3). Hence this method of inducing irreparable DNA damage in the form of a single telomere loss, marked by the loss of B^S, is called BARTL (*BAR*^{Stone} Telomere Loss) (Kurzhals et al., 2011).

We chose to induce telomere loss specifically in the eye because onset of severe apoptosis in the eye due to telomere loss may deplete the eye but should not affect the organismal viability, such that even the worst apoptotic phenotype can be reliably scored. As we shall see, this assumption is not entirely true, primarily because eyeless expression was not completely limited to the eye. We chose the *Y* chromosome for inducing the single telomere loss because it is dispensable for the viability of the fly only. Thus, if cells die *en masse* following telomere loss, it can be argued that the effect is solely in response to irreparable DNA damage, not due to aneuploidy.

Somatic cells can survive following irreparable DNA damage. Now that telomere loss is induced, the question is, what fate does this incur to the cells: do they all die or do some of them survive? If they all die, we would expect to see the ablation of the eye. If some survive in spite of the incurred telomere loss, we might see a larger eye owing to survival and proliferation of cells that have lost B^S.

I tested different combinations of *UAS-FLP* and *eyelessGal4* (*eyGal4*) transgenic insertion (on chromosome 2 or 3) lines from the Bloomington Stock Center in the BARTL assay to check which combination gives the strongest and most consistent phenotype. The outcome of each combination is presented in Figure 2C-T. The different combinations of *UAS-FLP* and *eyGal4* with *H1* gave a

variety of eye phenotypes, from no change to a wide range of eye sizes - from no eye or tiny eye to wildtype-like eyes, categorized from 1 to 5 (small to large) (Figure 2B). As a control, all the *UAS-FLP* and *eyGal4* transgenic lines were individually crossed to *H1* males to test if they can modify the B^S phenotype by themselves. They had no effect on B^S.

For our future experiments, we chose the two best combinations for generating telomere loss on *H1*: *P{UAS-FLP1.D}JD1, P{Gal4-ey.H}4-8* and *P{UAS-FLP}2B*, *P{Gal4-ey.H}4-8*. When tested for their ability to flip-out a *FRT*-flanked w^+ gene, they both produced maximum yellowish orange eye or mosaic eye phenotypes (yellowish orange base pigmentation due to the w^+ marker of the *FLP* transgene) with a few dark red ommatidia (Table 1). Besides, the *P{UAS-FLP1.D}JD1, P{Gal4-ey.H}4-8* combination mostly produces a consistent moderate-sized eye phenotype (Figure 2K), bigger than B^S, suggesting that some cells *do* survive following telomere loss and proliferate to reconstitute the eye, at least partially. This proved useful because the window of moderate-sized eye phenotype could be shifted either to be made worse, to produce tiny eyes as an inducer of cell-death phenotype, or to be made better, i.e., wildtype-like eyes as a suppressor of cell-death phenotype under different genetic misexpression conditions that would modify the cell fate to produce such shifted eye phenotypes. I recombined *P{UAS-FLP1.D}JD1* and *P{Gal4-ey.H}4-8* on chromosome 2 over the *SM1* balancer chromosome and abbreviated it as the *eGUF4.8JD1* recombinant. Similarly, I constructed the recombinant for the other combination and called it *eGUF4.82B*.

A genetic misexpression screen identifies novel genes that regulate somatic cell survival phenotype following irreparable DNA damage. In control *y w*/*H1; eGUF4.82B*/+ flies, the BARTL phenotype distribution was localized between eye size categories 2 and 3 (Figure 2D). To identify genes that regulate DNA damage-induced apoptosis, I carried out a genetic misexpression screen using *EP* elements (Rørth, 1996) in the *eGUF4.82B*/+-mediated BARTL background and screened for those *EP* lines that significantly modified this BARTL phenotype. For the screen, I crossed *y w/H1; eGUF4.82B/SM1, Cy* males individually to the females of each of the *EP* stocks in such a way that *eyGal4* drives telomere loss and *EP* element-induced misexpression of a random endogenous gene in all the proliferating cells of a developing eye (Figure 4). This allowed me to assess whether this alteration of gene expression had any effect on eye size. I screened ~600 X-chromosome *P{EPgy2}* lines available at Bloomington *Drosophila* Stock Center. The detailed screening datasheet is presented in Appendix I. From this screen, I identified seven elements that significantly altered eye size (Figures 5, 6; Table 2) when tested with *eGUF4.82B* and *eGUF4.8JD1*.

The identified *EP* lines' effects are limited to eyes with telomere loss. Next, we wanted to find out if these screened *EP* lines, induced or uninduced, have any modifying effect on B^S or wildtype eyes without telomere loss. In order to investigate this, I crossed the *EP* lines with (1) *y w/H1*; (2) *y w/H1 eyGal4-4.8/SM1, Cy*; (3) *y w/Y*; *eGUF4.8JD1*. None of the seven lines have a significant modifying effect on B^S or wildtype eyes in absence of telomere loss (Table 3).

Then, we wanted to determine if the modifying effect of *EP* on telomere loss requires *Gal4* (i.e., *EP/H1; eyFLP/+*). My results show that *EP* stock # 17674 produces large eyes after telomere loss without *Gal4* dependence (Table 3).

However, this does not exclude this line from consideration, but it possibly indicates that the change in phenotype is due to insertional mutagenesis. In support, some of the RNAi lines tested against the candidate gene of this stock, *MED18*, produced large eye phenotype too (Table 4).

RNAi-mediated knockdown confirms the efficacy of candidate genes as a potent modifier of BARTL phenotype. In order to verify that *EP* drives the BARTL phenotype, I tested RNAi-mediated knockdown of candidate genes for reversal of phenotype in the BARTL assay. Of the seven candidates, only knockdown of *corp* (the candidate gene of *EP* stock #15650) produced a phenotype radically opposite to that of *EP*-mediated overexpression and the knockdown of *fs(1)Yb* (the candidate gene of *EP* stock #15778) produced a somewhat opposite phenotype to that of *EP*-mediated overexpression (Table 4). *P{EPgy2}* insertion-induced overexpression of *corp*$^{+}$ (*EP-corp*$^{+}$) modifies the BARTL phenotype to produce wildtype eyes following telomere loss, while RNAi-mediated *corp* knockdown (RNAi-*corp*) eliminates the eyes entirely. One possibility was that *corp* might not be the effected gene in the *EP* line # 15650. *corp* is contained entirely in the intron of a gene, *CG1632*, which is transcribed in the opposite direction and the *EP* insertion might interfere with *CG1632* expression (Figure 7). However, since the RNAi-mediated knockdown of *CG1632*

did not modify the BARTL phenotype (Table 4), this indicated that *corp* is likely the affected gene in *EP* line # 15650.

The fact that RNAi against the rest of the candidate genes failed to produce an opposite effect to that of their *EP*-mediated overexpression, however, did not rule out their candidacy as enhancers or suppressors of cell-death phenotype following telomere loss. It is possible that the basal level of these genes is already quite low in normal conditions and that the knockdown could not take the levels down significantly lower beyond their basally low levels to produce any observably different phenotype in the BARTL assay. On the other hand, overexpression of these genes could increase their levels well above the threshold needed to produce a very significant modification of the BARTL phenotype.

An important implication of the uncovering of these candidate genes is that when cells survive irreparable DNA damage, it may not be only from deleterious mutations in the apoptotic pathway components, but it is also possible that there are some defined genetic pathways that control it.

Characterization of putative genes identified through our screen may shed more light into these pathways. Since *corp* and *fs(1)Yb* were identified as the two most interesting genes in the *EP* screen as modifiers of cell fate following irreparable DNA damage, we chose to further characterize these two genes.

Figure 2. BARTL phenotype produced by different combinations of *UAS-FLP* and *eyGal4*. (A) Graphical representation of the *DcY(H1)* chromosome used in the BARTL assay. The *DcY(H1)* chromosome is a *Y* chromosome that carries y^+ on the short arm and B^S on the long arm. Inverted *FRTs* are inserted proximal to B^S. The centromere is represented as a solid black circle, the telomeres as green rectangles, and the B^S gene as a red rectangle. The half-arrows indicate the inverted *FRTs*.
(B) The eye phenotype distribution observed in the BARTL assay. The B^S phenotype of *H1* control males is shown at the left. When FLP is expressed (*ey>FLP*), the phenotypes can either remain unchanged (B^S) or range from headless pharates (category 1) to adults with a fully developed wildtype eye (category 5).
(C-T) The distribution of BARTL eye phenotype produced by males carrying the *H1* chromosome and different combinations of various *UAS-FLP* and *eyGal4* stocks tested. N, number of fly eyes scored.

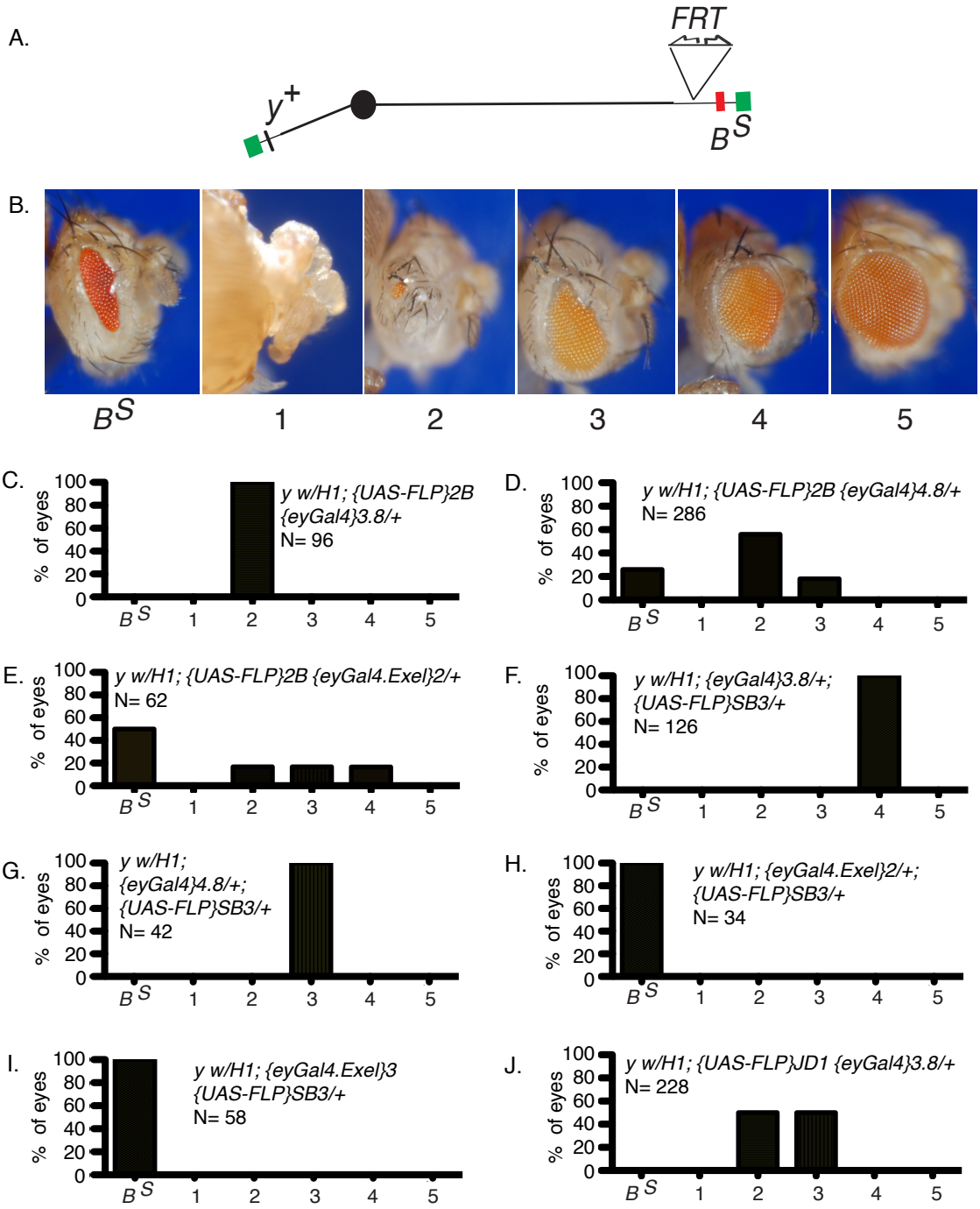
A.
FRT
y+
BS
B.
BS
1
2
3
4
5
C.
y w/H1; {UAS-FLP}2B
{eyGal4}3.8/+
N= 96
D.
y w/H1; {UAS-FLP}2B {eyGal4}4.8/+
N= 286
E.
y w/H1; {UAS-FLP}2B {eyGal4.Exel}2/+
N= 62
F.
y w/H1; {eyGal4}3.8/+;
{UAS-FLP}SB3/+
N= 126
G.
y w/H1;
{eyGal4}4.8/+;
{UAS-FLP}SB3/+
N= 42
H.
y w/H1; {eyGal4.Exel}2/+;
{UAS-FLP}SB3/+
N= 34
I.
y w/H1; {eyGal4.Exel}3
{UAS-FLP}SB3/+
N= 58
J.
y w/H1; {UAS-FLP}JD1 {eyGal4}3.8/+
N= 228
% of eyes
0
20
40
60
80
100

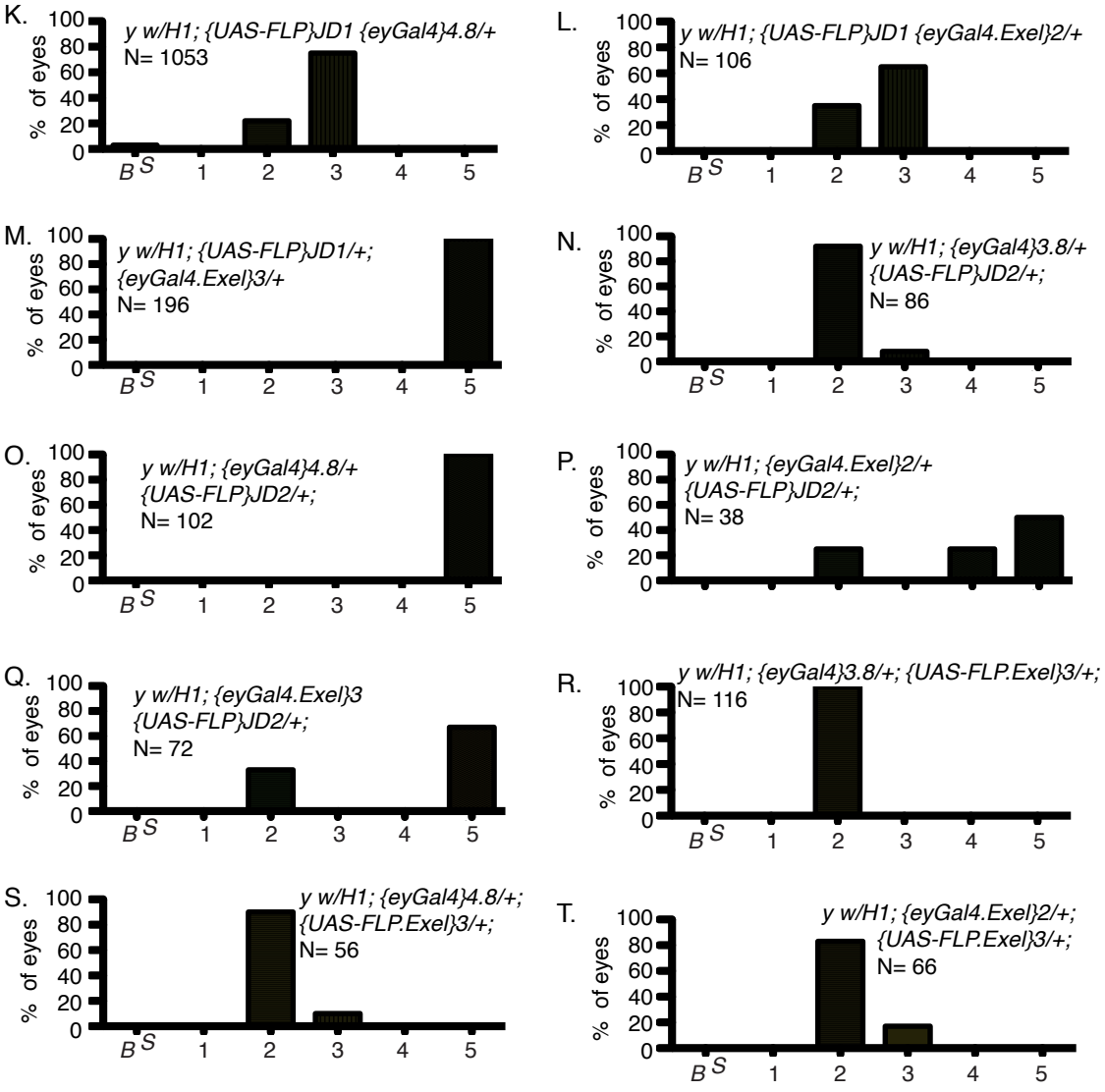

Figure 2 continued.

Figure 3. The *DcY(H1)* chromosome and BARTL assay.
Chromosome breakage and telomere loss in the BARTL assay. The *DcY(H1)* chromosome (drawn as sister chromatids in G2) is a *Y* chromosome that carries y^+ on the short arm and B^S on the long arm. Inverted *FRTs* are inserted proximal to B^S. The centromere is represented as a solid black circle, the telomeres as green rectangles, B^S gene as a red rectangle, and inverted *FRTs* as half-arrows. When FLP mediates unequal sister chromatid exchange between inverted *FRT*s, a dicentric and an acentric chromosome are produced. In the subsequent mitotic anaphase, the dicentric chromosome is pulled to opposite poles and usually breaks. Each daughter cell receives a chromosome with a single broken end and one or both daughter cells lose the B^S-containing acentric fragment.

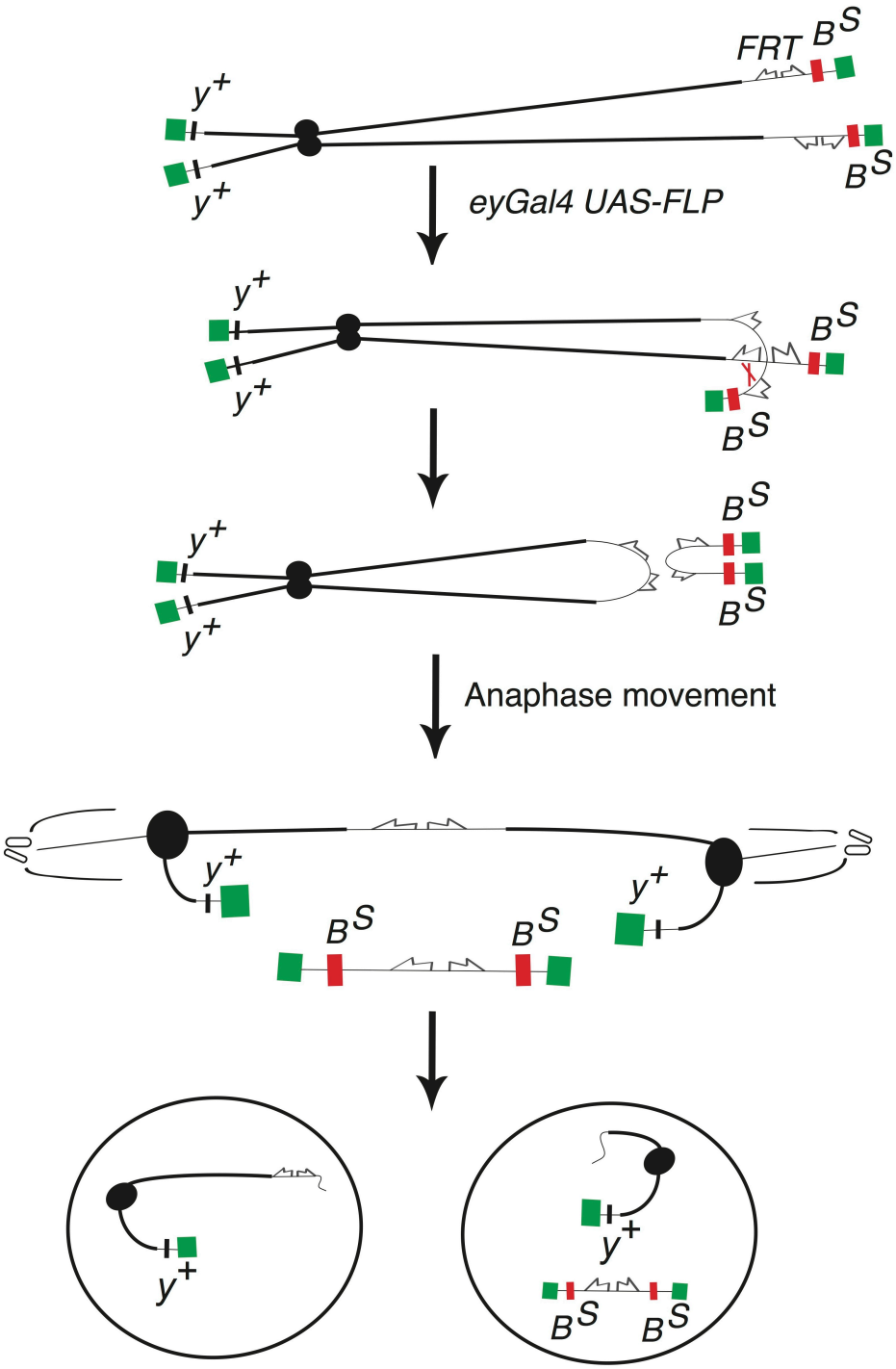
FRT
B^S
y+
eyGal4 UAS-FLP
Anaphase movement

Figure 4. Schematic of the *EP* screen. The *EP* screen is designed such that telomere loss and an endogenous gene is overexpressed at the same time in the developing eye. The *eyeless* promoter (yellow oval) drives *Gal4* (blue rectangle) expression specifically in the proliferating cells of the developing eye, where the Gal4 protein (blue oval) then binds to the *UAS* sequence (brown rectangle) upstream of *FLP* gene (red rectangle) and in the *EP*-element to simultaneously overexpress FLP and a random endogenous gene (magenta rectangle) at the downstream of the *EP* insertion. FLP (red oval) induces recombination of the *FRT*s and eventual telomere loss on the *H1* chromosome in these cells.

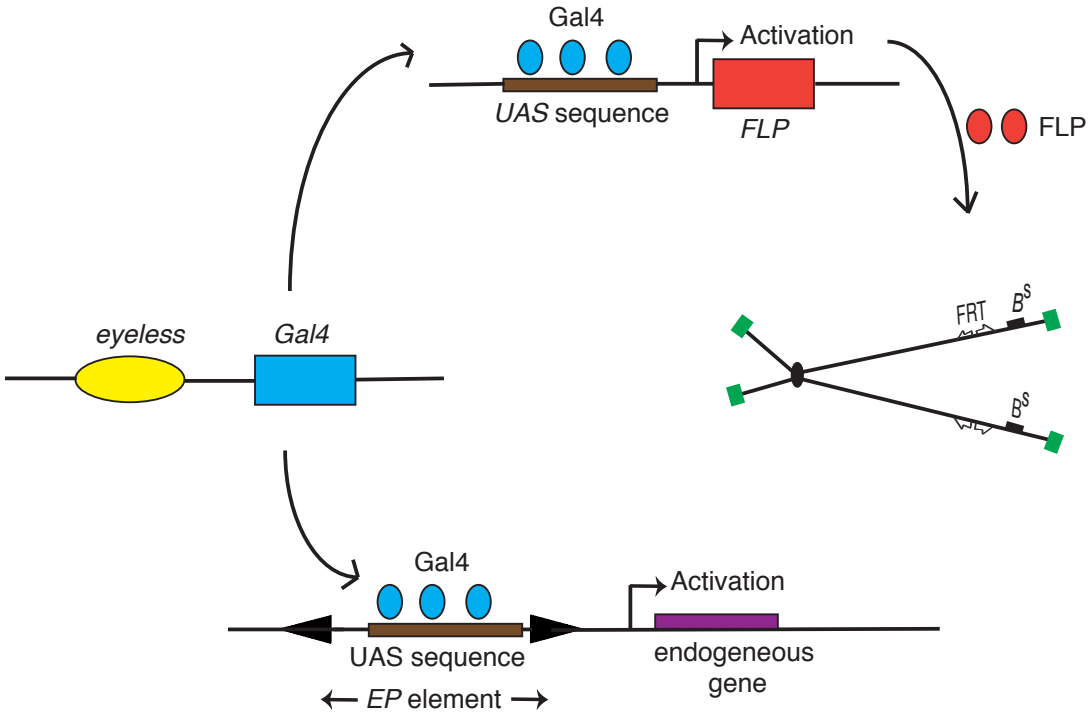
Gal4
Activation
UAS sequence
FLP
FLP
eyeless
Gal4
FRT
Bs
Bs
Gal4
Activation
UAS sequence
EP element
endogeneous
gene

Figure 5. *EP* screen identifies seven lines that suppresses or enhances the BARTL phenotype, produced by the *y w/H1; eGUF4.8JD1*.
The distribution of BARTL eye phenotype produced by males of (A) in control males following dicentric induction by *eGUF4.8JD1*; (B) in males carrying *P{EPgy2}EY03495* (BL 15650); (C) in males carrying *P{EPgy2}EY09634* (BL 16945); (D) in males carrying *P{EPgy2}EY00245* (BL 14821); (E) in males carrying *P{EPgy2}EY10359* (BL 17674); (F) in males carrying *P{EPgy2}EY04983* (BL 15778); (G) in males carrying *P{EPgy2}EY04780* (BL 16617); (H) in males carrying *P{EPgy2}EY16157* (BL 21192). For the eye phenotype distribution, refer to Figure 2B. N, number of fly eyes scored.

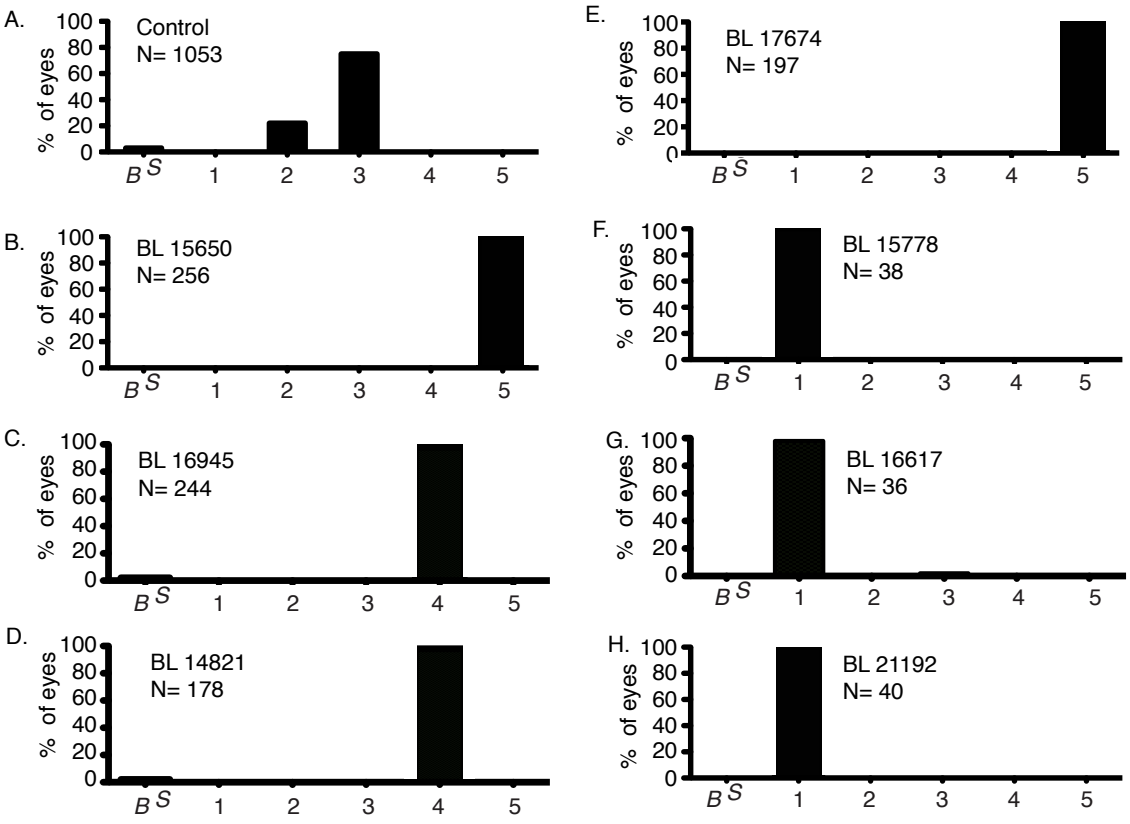
A.
Control
N= 1053
B.
BL 15650
N= 256
C.
BL 16945
N= 244
D.
BL 14821
N= 178
E.
BL 17674
N= 197
F.
BL 15778
N= 38
G.
BL 16617
N= 36
H.
BL 21192
N= 40
% of eyes
100
80
60
40
20
0
B S 1 2 3 4 5

Figure 6. The seven *EP* strains identified in the screen suppresses or enhances the BARTL phenotype, produced by the *y w/H1; eGUF4.82B*. The distribution of BARTL eye phenotype produced by males of (A) controls following dicentric induction by *eGUF4.82B*; (B) BL 15650; (C) BL 16945; (D) BL 14821; (E) BL 17674; (F) BL 15778; (G) BL 16617; (H) BL 21192. For the eye phenotype distribution, refer to Figure 2B. N, number of fly eyes scored.

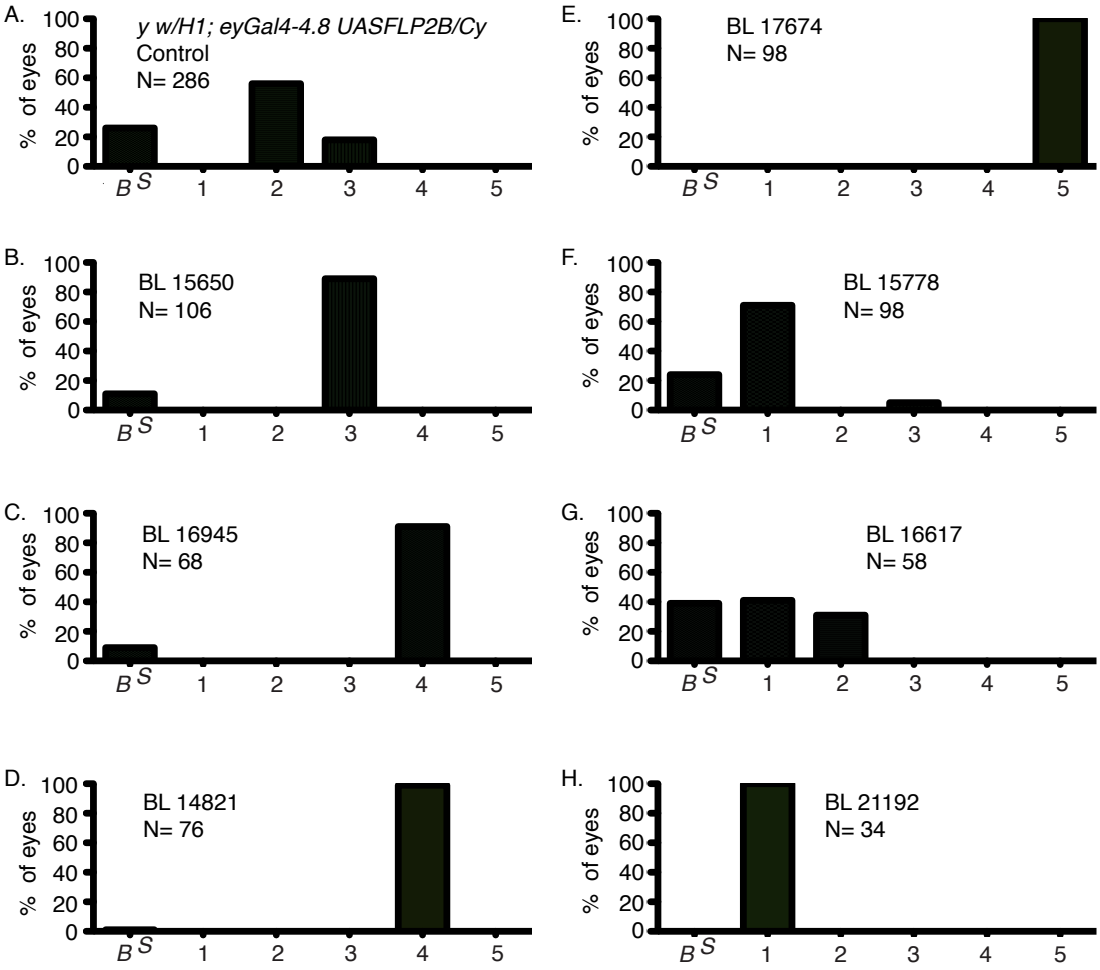
A.
y w/H1; eyGal4-4.8 UASFLP2B/Cy
Control
N= 286
B.
BL 15650
N= 106
C.
BL 16945
N= 68
D.
BL 14821
N= 76
E.
BL 17674
N= 98
F.
BL 15778
N= 98
G.
BL 16617
N= 58
H.
BL 21192
N= 34
% of eyes
0
20
40
60
80
100
B
S
1
2
3
4
5

Figure 7. *EP*-element insertion map at *corp* genomic region. The *corp* genomic region on the *X* chromosome (blue), *corp* transcripts (corp-RA), and *corp* cDNA sequence (CDS, color coded magenta); adapted from FlyBase: http://flybase.org/reports/FBgn0030028.html). Orange shading denotes the protein coding regions and grey shading denotes the 5' and 3' UTR regions on the *corp* transcript. The blue arrowhead indicates the site of the *EY03495 EPgy2* insertion, marked by a black empty rectangle. Directionality of *EP*-mediated induction: to the left if arrowhead points up, to the right if arrowhead points down.

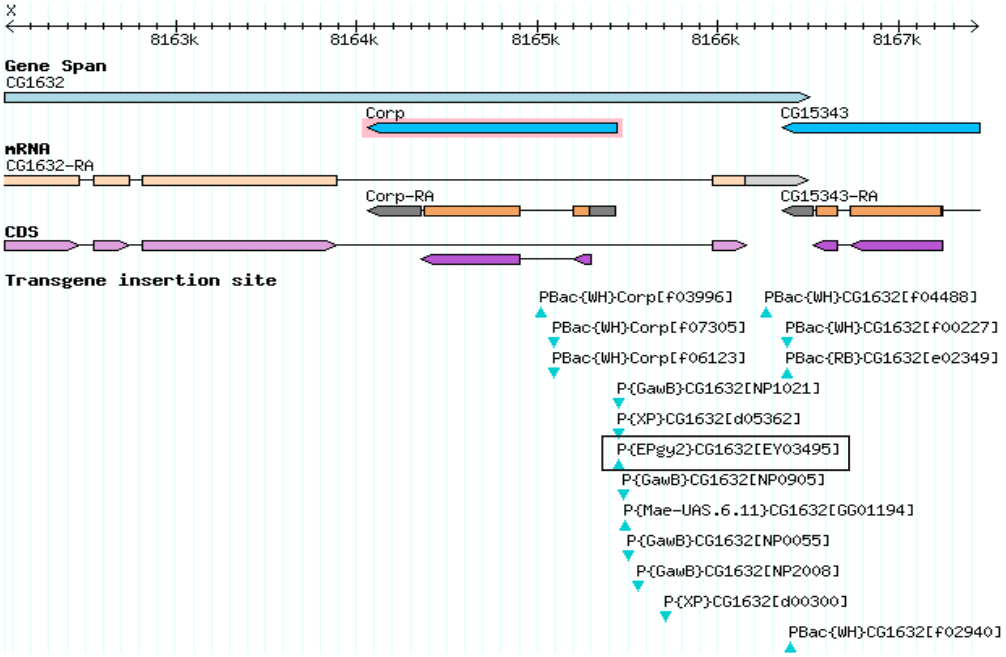
X
8163k
8164k
8165k
8166k
8167k
Gene Span
CG1632
Corp
CG15343
mRNA
CG1632-RA
Corp-RA
CG15343-RA
CDS
Transgene insertion site
PBac{WH}Corp[f03996]
PBac{WH}CG1632[f04488]
PBac{WH}Corp[f07305]
PBac{WH}CG1632[f00227]
PBac{WH}Corp[f06123]
PBac{RB}CG1632[e02349]
P{GawB}CG1632[NP1021]
P{XP}CG1632[d05362]
P{EPgy2}CG1632[EY03495]
P{GawB}CG1632[NP0905]
P{Mae-UAS.6.11}CG1632[GG01194]
P{GawB}CG1632[NP0055]
P{GawB}CG1632[NP2008]
P{XP}CG1632[d00300]
PBac{WH}CG1632[f02940]

Table 1. Strength of FLP expression tested by their ability to flip-out w^+ gene when crossed to *P[>w^+>]*.

Stocks tested	Eye phenotype of progenies
P{UAS-FLP2B} P(eyGal4}4.8	70% have orange eyes, 30% have mosaic eyes with a few w^+ (red) ommatidia.
P{UAS-FLP1.D}JD1 P(eyGal4}4.8	100% have yellowish orange eyes.
P(eyGal4}3.8; P{UAS-FLP }SB3	71% have orange eyes, 29% have mosaic eyes with a few w^+ (red) ommatidia.

Table 2. *EPgy2* lines identified as modifiers of BARTL phenotype induced by *y w/H1; eGUF4.8JD1/+*.

***P{EPgy2}* stocks[a]**	**Target gene**	**Cytogenetic map**	**N[b]**	**BARTL phenotype[c]**	**Functional annotation[d]**
15650	*corp*	7E1-7E1	256	100% cat. 5	*p53*-dependent, irradiation-induced, apoptosis-related
16945	*Pdcd4*	12B4-12B10	244	98% cat. 4, 2% B^S	stem cell differentiation
14821	*CG8924*	14A1-14A1	178	99% cat. 4, 1% cat. 2	transcriptional regulation during cell proliferation
17674	*Med18*	2B13-2B13	197	100% cat. 5	RNA pol II transcriptional mediator
15778	*fs(1)Yb*	3B3-3B3	38	100% cat. 1	germline stem cell maintenance
16617	*CrebB-17A*	17A7-17A8	36	98% cat. 1, 2% cat. 4	*cAMP*-regulated transcription
21192	*SmG/mthl1*	14F4-14F4	40	100% cat. 1	mitotic spindle organization

[a] *P{EPgy2}* stocks numbers mentioned are according to the Bloomington *Drosophila* Stock numbers.
[b] Numbers of flies scored.
[c] BARTL phenotypes are categorized according to that depicted in Figure 2B.
[d] Functional annotations are adapted from the information in FlyBase summary of individual genes.

Table 3. Control results for *EPgy2* lines on B^S or wildtype eyes.

P{EPgy2} stocks[a]	Eye phenotypes for genotypes tested[b]			
	y w /H1	***y w/H1; eyGal4-4.8***	***y w/Y; eGUF4.8JD1/SM1, Cy***	***y w/H1; {eyFLP.N}5/SM1, Cy***
15650	100% B^S	100% B^S	100% cat. 5	1% B^S, 1% cat. 2, 47% cat. 3, 45% cat. 4, 6% cat. 5
16945	100% B^S	100% B^S	100% cat. 5	5% B^S, 24% cat. 2, 71% cat. 3
14821	100% B^S	100% B^S	100% cat. 5	5% B^S, 24% cat. 2, 71% cat. 3
17674	100% B^S	100% B^S	100% cat. 5	22% cat. 4, 78% cat. 5
15778	100% B^S	98% B^S, 2% cat. 5	100% cat. 5	4% B^S, 17% cat. 2, 50% cat. 3, 29% cat. 4
16617	98% B^S, 2% cat. 5	90% B^S, 10% cat. 2	100% cat. 5	63% cat. 3, 37% cat. 5
21192	-	100% B^S	-	-

[a] *P{EPgy2}* stocks numbers mentioned are according to the Bloomington *Drosophila* Stock numbers.
[b] Eye phenotypes are categorized within the range BARTL eye phenotype, depicted in Figure 2B.

Table 4. Effect of candidate gene knockdowns or amorphic alleles on BARTL phenotype.

Candidate genes in *EP* stocks	RNAi lines[a]	N[b]	BARTL eye phenotype (%)[c]					
			B^S	1	2	3	4	5
corp	v102751	32	0	100	0	0	0	0
	v16130	48	0	88	12	0	0	0
CG1632	v106107	184	4	0	23	73	0	0
	v5478	42	5	0	24	71	0	0
Pdcd4	v16160	49	0	0	0	100	0	0
	v16162	114	4	0	23	73	0	0
	BL 38445	38	13	0	42	42	3	0
CG8924	v48041	96	4	0	28	68	0	0
	v48042	98	7	0	21	72	0	0
	BL 35705	32	0	0	25	53	11	11
MED18	v48490	126	0	0	18	29	52	1
	v48491	18	0	0	0	0	61	39
	v28265	28	7	0	29	25	39	0
	v28264	24	0	0	0	100	0	0
	v106760	30	10	0	13	77	0	0
CG2701	v106635	192	11	0	20	12	57	0
	v25433	162	0	0	14	62	23	1
fs(1)Yb	BL 35181	52	15	0	12	29	19	25
	BL 35301	38	5	0	21	39	11	24
CG14814	v41553	8	0	50	12	38	0	0
CrebB-17A	v6103	38	0	0	100	0	0	0
mthl1	v33136	46	4	0	39	57	0	0
	BL 15318	116	2	0	0	33	59	6
SmG	BL 26617	60	50	0	27	23	0	0

[a] RNAi lines are obtained from Bloomington Stock Center (BL) and Vienna *Drosophila* Resource Center (v).
[b] Numbers of flies scored.
[c] The range of BARTL phenotype is categorized according to that depicted in Figure 2B.

References

Ahmad, K.K., and Golic, K.G.K. (1999). Telomere loss in somatic cells of Drosophila causes cell cycle arrest and apoptosis. Genetics *151*, 1041–1051.

Al-Mulla, F.F., Keith, W.N.W., Pickford, I.R.I., Going, J.J.J., and Birnie, G.D.G. (1999). Comparative genomic hybridization analysis of primary colorectal carcinomas and their synchronous metastases. Genes Chromosomes Cancer *24*, 306–314.

Artandi, S.E., and DePinho, R.A. (2010). Telomeres and telomerase in cancer. Carcinogenesis.

Biessmann, H., and Mason, J.M. (2003). Telomerase-independent mechanisms of telomere elongation. *60*, 2325–2333.

Blackburn, E.H. (2001). Switching and Signaling at the Telomere. Cell *106*, 661–673.

Brand, A.H., and Perrimon, N. (1993). Targeted gene expression as a means of altering cell fates and generating dominant phenotypes. Development *118*, 401–415.

Cenci, G., Ciapponi, L., and Gatti, M. (2005). The mechanism of telomere protection: a comparison between Drosophila and humans. Chromosoma *114*, 135–145.

Fristrom, D. (1969). Cellular degeneration in the production of some mutant phenotypes in Drosophila melanogaster. Mol. Gen. Genet. *103*, 363–379.

Golic, K.G., and Lindquist, S. (1989). The FLP recombinase of yeast catalyzes site-specific recombination in the Drosophila genome. Cell *59*, 499–509.

Hackett, J.A., and Greider, C.W. (2003). End resection initiates genomic instability in the absence of telomerase. Molecular and Cellular Biology *23*, 8450–8461.

Kurzhals, R.L., Titen, S.W.A., Xie, H.B., and Golic, K.G. (2011). Chk2 and p53 are haploinsufficient with dependent and independent functions to eliminate cells after telomere loss. PLoS Genet *7*, e1002103–e1002103.

McClintock, B. (1939). The Behavior in Successive Nuclear Divisions of a Chromosome Broken at Meiosis. pp. 405–416.

Michinomae, M., and Kaji, S. (1973). Cell death during the development of the bar eye discs in Drosophila melanogaster. Jap J Genet *48*, 307–310.

Muller, H.J. (1940). An analysis of the process of structural change in

chromosomes of Drosophila. Journ. of Genetics *40*, 1–66.

Murnane, J.P. (2010). Telomere loss as a mechanism for chromosome instability in human cancer. Cancer Res. *70*, 4255–4259.

Ong, T.M.T., Song, B.B., Qian, H.W.H., Wu, Z.L.Z., and Whong, W.Z.W. (1998). Detection of genomic instability in lung cancer tissues by random amplified polymorphic DNA analysis. Carcinogenesis *19*, 233–235.

Rørth, P.P. (1996). A modular misexpression screen in Drosophila detecting tissue-specific phenotypes. Proc. Natl. Acad. Sci. U.S.a. *93*, 12418–12422.

Sabatier, L., Ricoul, M., Pottier, G., and Murnane, J.P. (2005). The Loss of a Single Telomere Can Result in Instability of Multiple Chromosomes in a Human Tumor Cell Line. Molecular Cancer Research.

Sandell, L. (1993). Loss of a yeast telomere: Arrest, recovery, and chromosome loss. Cell *75*, 729–739.

Schneider, B.L., and Kulesz-Martin, M. (2004). Destructive cycles: the role of genomic instability and adaptation in carcinogenesis. Carcinogenesis *25*, 2033–2044.

Titen, S.W.A., and Golic, K.G. (2008). Telomere Loss Provokes Multiple Pathways to Apoptosis and Produces Genomic Instability in Drosophila melanogaster. Genetics *180*, 1821–1832.

CHAPTER 3

IDENTIFICATION OF CORP AS A FUNCTIONAL ANALOG OF MDM2: NEGATIVE REGULATION OF P53 IN *DRSOPHILA MELANOGASTER*

Abstract

We identified the *corp* gene of *Drosophila melanogaster* as a negative regulator of P53. Its overexpression promotes survival of cells with DNA damage in the soma but eliminates such cells in the germline, similar to the effects of a *p53* null mutation in these tissues. *Corp* is also a transcriptional target of P53, thus constituting a negative feedback loop. We find that Corp shares conserved protein motifs with Mdm2, the major negative regulator of P53 in vertebrates, and physically interacts with *Drosophila* P53. Our findings show that *Drosophila* Corp is a functional analog of vertebrate Mdm2.

Introduction

Cells frequently encounter damage to their DNA as the result of intrinsic insults, such as replication stress, oxidative stress, and telomere shortening, or from exposure to environmental stressors such as mutagenic chemicals or radiation. In response to DNA double-strand breaks (DSBs), DNA damage response (DDR) pathways are triggered. The ensuing signaling cascades result in cell cycle arrest, induction of DNA repair genes, and in some cases, apoptosis. It is generally thought that if damage cannot be repaired, cells will undergo apoptosis rather than continue to divide and propagate a damaged genome. If cells with irreparable damage do survive and proliferate, it can result in widespread genomic instability, creating an early state in the progress towards cancer [1-3]. In *Drosophila melanogaster,* most cells undergo apoptosis in response to irreparable DNA damage, but a few cells escape, continue to divide and

exhibit genomic instability [4-6]. In our current study, we aimed to investigate the genetic mechanisms that allow cells to survive in the presence of irreparably damaged DNA.

One of the key players that controls the fate of a cell following DNA damage is the tumor-suppressor encoded by the *p53* gene*,* which has been found to be mutated in most forms of human cancers [7]. In response to DNA damage, the ATM kinase (encoded by *tefu* in *Drosophila*) phosphorylates Chk2 (encoded by *lok*), which in turn phosphorylates and activates P53 [8-10]. ATM may also phosphorylate P53 directly [11-14]. Activated P53 is primarily a transcriptional regulator that promotes or inhibits the expression of a large number of target genes [15-21]. These genes encode a variety of cellular functions such as DNA repair, cell cycle arrest, and apoptosis. A cell that detects damage and engages the P53 damage response pathway may either repair the damage or experience senescence or death [22]. Humans that lack one copy of *p53* are prone to develop cancers, and *p53* knockout mice develop cancers at an increased rate [1-3,23,24]. Similarly, *p53*-null *Drosophila* fail to eliminate cells with a DSB in their genome [5,24,25-27].

The *Mdm2* gene is a prominent target of P53 in mammals. It encodes a ubiquitin ligase that negatively regulates P53 and promotes its degradation, constituting a negative feedback loop [28,29]. Mediation of apoptosis by P53 is highly conserved throughout metazoa, including *Drosophila melanogaster* [21,22,25-27,30]. However, apart from DNA repair genes, targets of p53 that antagonize

apoptosis have yet to be reported in flies and no homolog of *Mdm2* has been identified.

Here, we report the identification of a gene, *companion of reaper* (*corp*), whose overexpression mimics the effects of *p53* mutants in the soma and the germline. Our experiments indicate that Corp is a negative regulator of P53. Furthermore, *corp* has been previously identified as a positively-regulated transcriptional target of P53 [18,19,31]. We also identified protein motif similarity between Corp and Mdm2, and found that Corp physically interacts with *Drosophila* P53. Although BLAST searches have failed to identify an Mdm2 homolog in *Drosophila*, our results indicate that *corp* encodes a functional equivalent. These findings further strengthen the functional conservation of the P53 pathways between *Drosophila* and mammals.

Results

Corp suppresses tissue ablation resulting from DNA damage. The previously described BARTL (*Bar* and Telomere Loss) assay [24] was used to screen for insertions of a *P*-element misexpression element [32] that modify the eye phenotype resulting from the production of an irreparable DNA DSB. In brief, a combination of *eyeless-Gal4* (*eyGal4*) and *UAS-FLP* is used to drive FLP recombinase expression in proliferating cells of the eye throughout development [33-35]. These flies also carry a *Y* chromosome with inverted *FRT* repeats (*DcY(H1)*, or simply *H1*). Recombination between *FRT*s in inverted orientation on sister chromatids produces dicentric chromosomes which break in the subsequent

mitotic division, delivering a chromosome with a single broken end to each of the two daughter cells (Figure 3). This results in substantial P53-mediated apoptosis and produces flies with characteristic small and rough eyes (Figure 8B). By introducing an *EP* transposon insertion, which carries *UAS* elements that can drive expression of a neighboring gene, the flies' eyes may become larger or smaller, indicating that the *EP* element in question modifies the fate of cells in these eyes. We identified one such *EP* insertion (*P{EPgy2}CG1632*^{EY03495}) that produced nearly wildtype eyes in the BARTL assay (Figure 8C). This insertion was ideally placed to drive expression of the *corp*$^{+}$ gene (*CG10965*). By qRT-PCR we confirmed that when Gal4 induces the *P{EPgy2}CG1632*^{EY03495} element (hereafter referred to as *EP-corp*$^{+}$), it drives overexpression of *corp*$^{+}$ (Figure 9). We also constructed a *UAS-corp*$^{+}$ transgene, and found that its effect was nearly identical to that produced by *EP-corp*$^{+}$ (Figure 8D).

When we tested RNAi-mediated knockdown of *corp* in the BARTL assay, the opposite result was obtained: the eye was completely ablated (Figure 8E; *n. b.*, *ey* expression extends beyond the eye proper, accounting for, in some cases, nearly complete ablation of the head). A *corp* mutant was also generated by imprecise excision of a *P* element located in the 5' region of the gene. This mutant, *corp*^{95B} (Figure 10), is viable in homozygous condition and without obvious phenotype on its own. However, like RNAi-mediated *corp* knockdown, *corp*^{95B} completely ablates the eye in the BARTL assay (Figure 8F). This effect can be rescued by the *UAS-corp*$^{+}$ transgene (Figure 8G).

If *EP-corp*$^{+}$ was not induced by Gal4, and *eyFLP* was instead used to

produce dicentric chromosomes in the eye, we found that the *EP-corp*$^{+}$ insertion, by itself, had no effect (Figure 11B). This further confirms that *corp*$^{+}$ overexpression is necessary to generate the large eye phenotype in the BARTL assay.

To determine whether *corp* has any influence in the absence of DNA, damage we examined wildtype or *B*^{S} flies carrying *EP-corp*$^{+}$, induced or uninduced, and flies carrying the *corp*^{95B} mutant, but without the induction of dicentric chromosomes. There was no change in eye phenotype in any of these cases, indicating that the effects of altered *corp*$^{+}$ expression are seen only after DNA damage (Figure 11C-G).

EP-corp^{+}-mediated rescue of the eye is not confined to males, or to effects produced by the *Y* chromosome. We generated *XXY* females carrying *eyGal4, UAS-FLP* and the *DcY(H1)* chromosome and found that *EP-corp*$^{+}$ produced almost wildtype eyes, similar to its effect in males (Figure 11H-I). Additionally, we found that *corp*$^{+}$ overexpression ameliorated the reduction in eye size produced by dicentric induction on chromosome *3* (Figure 11J-K). Therefore, the effect of *corp*$^{+}$ overexpression is independent of the sex of the fly or the particular chromosome experiencing damage.

Extant *corp* polymorphisms are functionally indistinguishable. We sequenced the *corp* genomic regions from five laboratory strains and found two allelic variants of *corp* that differed by 7 nucleotide changes. Four nucleotide changes were found in the second exon: two of them are silent mutations (C840T and C891T) and two (T725A and T873G) encode different amino acids (L96H

and L145M). These alternate amino acids are also present as polymorphisms in wildtype isolates of *D. melanogaster* and other *Drosophila* species (http://www.dpgp.org). There were also three single nucleotide differences (C277T, A398C, and A407T) in introns.

The *UAS-corp*$^{+}$ transgene that we constructed and tested (as mentioned previously) carries the canonical version, as found in *Canton*^{S}. The *EP-corp*$^{+}$*, y w*, and *w*^{1118} strains all carry the variant allele that differs from the reference *Canton*^{S} strain. Because the overexpression of either allele produces a similar large eye phenotype in the BARTL assay (Figure 2D), we conclude that both alleles function similarly, and that the two amino acid differences have, at most, minor effects.

***corp*$^{+}$ overexpression inhibits DNA damage-induced apoptosis in the soma.** Overexpression of *corp*$^{+}$ might produce larger eyes in the BARTL assay by blocking the apoptotic response, thereby allowing survival and proliferation of cells that would normally die. To test this, we examined wing imaginal discs for apoptotic cells in wildtype and *EP-corp*$^{+}$ larvae following exposure to ionizing radiation (IR). We induced *corp*$^{+}$ overexpression in the posterior compartment of wing discs using an *engrailed-Gal4* driver [36] and marked this compartment by co-induction of *UAS-GFP*. Apoptosis was significantly reduced by *corp*$^{+}$ overexpression (Figure 12A, C). We then found that IR-induced apoptosis was significantly enhanced in wing discs from *corp*^{95B} mutants relative to wildtype (Figure 12B, D). The results show that *corp*$^{+}$ is a potent negative regulator of apoptosis.

Overexpression of *corp*$^{+}$ restricts the transmission of healed chromosomes through the germline. In the male germline, broken dicentric chromosomes may be healed by *de novo* telomere addition [37,38]. With *DcY(H1)*, these healed chromosomes (denoted *FrY*) may be detected in testcrosses to *y w* females by the loss of the dominant B^{S} marker that lies distal to the inverted *FRT*s (*i.e.*, by the generation of *Bar*$^{+}$ sons). To assess the effect of *corp* on the transmission of broken-and-healed chromosomes, we induced expression of FLP by heat shock (*70FLP10*) during the first 24 hours of development and used *nanosGal4* to drive germ cell-specific overexpression of *corp*$^{+}$. Overexpression of *corp*$^{+}$ blocked transmission of *FrY* chromosomes (Table 5).

We also drove *corp*$^{+}$ and *FLP* expression specifically in the germline using *nanosGal4 (EP-corp*$^{+}$*; UAS-FLP nanosGal4)* and again observed a large decrease in *FrY* transmission relative to males with unaltered *corp* expression (Table 5), confirming that *corp*$^{+}$ inhibits transmission of broken-and-healed chromosomes through the male germline.

The relationship between *corp* and *p53*. Though it seems surprising that *corp*$^{+}$ overexpression produces dissimilar phenotypes in the soma (survival and proliferation of cells with broken chromosomes) vs. the germline (elimination of cells with broken chromosomes), there is precedent: the $p53^{5A\text{-}1\text{-}4}$ loss of function mutation acts similarly. The $p53^{5A\text{-}1\text{-}4}$ homozygotes have almost wildtype eyes in the BARTL assay [24], but strongly reduced transmission of broken-and-healed chromosomes through the male germline [39]. This similarity suggests a functional relationship between *corp* and *p53*.

To explore this relationship, we generated *corp*^{95B}*; p53*$^{5A-1-4}$ double mutants and examined them using the BARTL assay. We found that *p53* is epistatic to *corp*, with the double mutant producing almost wildtype eyes (Figure 13A). In a complementary experiment, we tested the effect of simultaneously overexpressing *corp*$^{+}$ and *p53*$^{+}$. When *GMR-Gal4* drives *p53*$^{+}$ overexpression in the developing eye, the adults that eclose have very small eyes, owing to an elevated frequency of cell death. We found that if *corp*$^{+}$ was simultaneously overexpressed, the eyes became significantly larger. Furthermore, when we combined the *corp*^{95B} mutant with *GMR>p53*$^{+}$, the eyes were much smaller than produced by *GMR>p53*$^{+}$ alone (Figure 13B). The mutant and overexpression results may both be accommodated under the hypothesis that Corp antagonizes P53, either by suppressing its apoptotic effects or by negatively regulating P53 itself.

P53 level is elevated in *corp* mutant or knockdown cells. To determine how Corp might affect P53, we examined P53 levels in eye discs by immunostaining. The *GMR* promoter was used to overexpress *p53*$^{+}$ behind the morphogenetic furrow, providing an easily detected level of expression. The *corp*^{95B} mutant eye discs exhibited a significantly higher level of P53 while *EP-corp*$^{+}$ overexpression driven by *GMR-Gal4* reduced the level of P53 (Figure 14A, B). To verify these results, we knocked down *corp* in S2 cells by treating with double-stranded RNA (dsRNA) against *corp* and measured P53 protein levels by Western blot. We found that the quantity of P53 was significantly elevated following *corp* knockdown (Figure 14C, D). Thus, we conclude that Corp is a

negative regulator of *p53*. Since it has been previously shown that *corp* is a transcriptional target of P53, our data indicate that Corp acts in a negative feedback loop on *p53*$^{+}$.

We used qRTPCR to measure *p53* transcript levels in *corp* mutant flies, or flies with *corp*$^{+}$ overexpression, to determine whether *corp* regulates the level of *p53* mRNA. We find that there are no significant or consistent changes in *p53* mRNA levels between these genotypes (Figure 15). We conclude that Corp regulation of P53 occurs primarily at the level of translation or protein stability.

Overexpression of *corp*$^{+}$ suppresses Hid- and Reaper- mediated cell death. P53 is well known as a positive regulator of the *hid* and *reaper* pro-apoptotic genes. Recently it was shown that these genes act recursively to increase *p53* expression and contribute to the apoptotic program [40]. Given that Corp overexpression results in downregulation of P53, we expect that it should also suppress the apoptotic phenotype caused by *hid* and *reaper* overexpression by attenuating this feedback loop. In order to test this prediction, we overexpressed *hid* or *reaper* in the eye under control of the *GMR-Gal4* driver. This produced adults with small eyes owing to cell death in the eye discs. When *corp*$^{+}$ was overexpressed at the same time, the eyes became significantly larger, confirming that Corp interferes with the *hid*- and *reaper*-mediated apoptotic programs (Figure 13C).

Corp shares protein motif similarity with the P53-interacting regions of Mdm2. Mdm2 is the major negative regulator of P53 in vertebrates. However, no homolog of Mdm2 has been found in *Drosophila*. Given that Corp acts in a

negative feedback loop on P53, we looked more closely at Corp to see whether any similarities to Mdm2 might be identified. We used the domain analysis tool MEME [41,42] to search for shared motifs. When the software was presented with four Mdm2 orthologs (*H. sapiens, M. musculus, G. gallus*, and *D. rerio*) and Corp from two *Drosophila* species (*D. melanogaster* and *D. virilis*) and was instructed that each protein sequence may or may not contain similar motifs, it identified seven similar motifs, with motifs 4 and 5 shared by Mdm2 and Corp (Figure 16A). Interestingly, motif 4 appears to correspond to the N-terminal region of Mdm2 that interacts with the transactivation domain of P53 and motif 5 appears to correspond to the central P53-binding site on Mdm2 [44,45].

Corp physically interacts with P53. Motivated by the finding of similarities between Corp and Mdm2 in regions of Mdm2 that bind P53, we asked whether *Drosophila* Corp and P53 physically interacted in cells. To probe whether Corp can directly interact with *Drosophila* P53 (DmP53), we purified GST-DmP53 using a bacterial expression system. C-terminal-tagged Corp-GFPFlag was then expressed via transient transfection of HeLa or 293 cells. Cell lysates extracted from these cells were incubated with either GST or GST-DmP53. Corp-GFPFlag was pulled-down specifically by GST-DmP53 but not by GST (Figure 17A), indicating that Corp expressed in mammalian cells interacts with DmP53. This result suggests either that Corp can interact directly with DmP53, or that the complex required for their interaction is conserved in mammalian cells. To further probe this, we tested the interaction between GST-DmP53 and *in vitro* synthesized Corp. We found that, similar to what we

observed with cellular lysates, GST-DmP53 strongly interacts with *in vitro* synthesized Corp (Figure 17B). Together, these results strongly suggest that Corp can interact directly with DmP53.

Discussion

Several studies have identified transcriptional targets of P53 in *Drosophila*. Some of these play important roles in DNA damage repair or in triggering apoptosis [18-21,46,47]. However, the functions of most P53 target genes have yet to be determined. Our discovery that *corp*$^{+}$ antagonizes apoptosis by negatively regulating P53 is the first demonstration in *Drosophila* that a P53-regulated gene (apart from DNA repair genes) is not solely devoted to apoptosis, and shows that P53 target genes act in competing pathways: the *hid*- and *reaper*-mediated pro-apoptotic pathway, and the *corp*-mediated anti-apoptotic pathway (Figure 16B). By increasing or decreasing the expression of *corp*$^{+}$*,* the balance is shifted in favor of survival or death, respectively.

In vertebrates, the major negative regulator of P53 is Mdm2. It binds to P53 and ubiquitinates it, leading to its degradation, and is responsible for restraining P53 activity in unstressed cells. Furthermore, *Mdm2* is also a transcriptional target of P53, and is utilized to turn down the P53 response so that cells that have recovered from the initiating stress, for instance DNA damage, may survive. Though no strict Mdm2 homolog is known in *Drosophila*, our experiments indicate that Corp provides that function. Similar to *Mdm2,* the *corp* gene is a transcriptional target of P53, Corp antagonizes the P53-mediated

apoptotic program, P53 levels are inversely correlated with *corp*$^{+}$ expression, and Corp physically interacts with P53. Additionally, Corp shares protein motifs with vertebrate Mdm2 and these correspond to regions of Mdm2 that physically interact with P53. These similarities lead us to propose that Corp is the functional analog of mammalian Mdm2.

There are, nonetheless, significant differences between Corp and Mdm2. Mdm2 is an E3 ubiquitin ligase containing a RING domain [48]. Corp shows no evidence of such a domain. But, recent work [49] established that subunits of the proteasome are the predominant physical interactors of Corp (Figure 18). We suggest that Corp, like Mdm2, promotes degradation of P53. In contrast to Mdm2, Corp may achieve this by recruiting P53 to the proteasome, rather than by ubiquitination.

In the mouse, many *Mdm2* mutations cause recessive lethality, though they can be rescued by the additional mutation of *p53* [50], indicating that lethality results from unrestrained P53 activity. In contrast, the *corp*^{95B} null mutation is not lethal and exhibits no obvious phenotype in the unstressed condition. Corp appears to function only when DNA damage is detected. The normal level of P53 expression is insufficient to cause lethality in the absence of Corp, unless P53 is activated by upstream kinases.

However, these differences between Corp and Mdm2 may not be as significant as they appear. First, recent findings in mice indicate that the constitutive and induced levels of Mdm2 can be functionally separated. When the P53 Response Element was mutated in the promoter of *Mdm2*, so that Mdm2

was still expressed at a basal level but could no longer be induced to high levels by P53, the resulting mice were viable [51]. Furthermore, when the RING domain of Mdm2 was mutated, so that it no longer functioned as a ubiquitin ligase, but could still interact with its partner Mdmx, the mice were also viable [52]. In both cases, the mice were still highly sensitive to induced DNA damage, indicating that higher levels of Mdm2 activity are required to recover from DNA damage. Moreover, the latter experiments show that Mdm2 is capable of repressing P53 function without its ubiquitin ligase activity [52]. This may indicate that P53-Mdm2 binding is a more ancient mode of regulation, with the ubiquitin ligase activity acquired as a later adaptation in vertebrates.

There is still room for alternative or additional explanations for Corp's phenotypes. If Corp targeted downstream components of the apoptotic pathway for degradation, it might also lead to the phenotypes we observed. Given the existence of a positive feedback loop between downstream pro-apoptotic genes and *p53* [40], Corp might indirectly affect P53 levels by promoting degradation of components of the pro-apoptotic pathway. However, detection of a physical interaction between Corp and P53 strongly suggests that Corp directly regulates P53, regardless of whether it may also regulate downstream apoptotic components.

Corp is the first reported negative regulator of P53 in *Drosophila* that is also a transcriptional target of P53. Although Bonus and Rad6 have been identified as negative regulators of P53 in *Drosophila* [53,54], neither of them are transcriptional targets of P53, and are thus less similar to Mdm2 than is Corp.

Recent experimental findings from others [19,30,40,55], and as reported here, indicate that regulation of P53 is complex, involving activation by upstream factors, with both positive and negative feedback loops affecting its activity. Further investigation of how these pathways are regulated and how they affect these outcomes should greatly improve our understanding of the many functions of P53.

It remains to be understood what benefit might be provided by Corp. If it is normally beneficial to eliminate a cell with unrepaired DNA damage, preventing its proliferation, then what purpose could be served by saving such cells from death? Previous experiments have shown that in wildtype larvae, many cells with damaged genomes are not eliminated by apoptosis immediately, but rather over a period of a few days [5]. Since *corp* mutants show increased cell death after irradiation, Corp is clearly one factor that restrains the immediate death of cells with damaged genomes. We have often thought it surprising that flies can survive when dicentric chromosomes are formed, and break, in >90% of their cells during development [5,6]. Perhaps if all cells with broken chromosomes immediately succumbed to apoptosis, such flies would not survive. In fact, *corp* mutants survive very poorly after widespread induction of *Y* chromosome dicentrics. Corp, then, may be advantageous to modulate the rate at which cells are eliminated following DNA damage. If >90% of cells in a developing imaginal disc were eliminated at the same time, it is easy to imagine that the few remaining survivors, adrift in a sea of dead cells, might not be capable of regenerating a complete disc. If, instead, the cells with damaged genomes could be eliminated gradually, it might give the surviving cells a suitable matrix to regenerate an entire disc. This

could be the vital function fulfilled by Corp. Bilak *et al.*, (2014) [56] recently showed that dying cells signal their neighbors to become resistant to damage-induced death. We would not be surprised to find that this pathway acts through Corp.

Material and methods

***Drosophila* stocks.** All flies were maintained at 25°C on standard cornmeal food. Construction of the *DcY(H1)* and *Dc3(FrTr61A5)1A* chromosomes have been described previously by Kurzhals e*t al*. (2011) [24] and $p53^{5\text{-}A\text{-}1\text{-}4}$ by Xie *et al*. (2004) [57]. We obtained the following stocks from the Bloomington, IN (USA) *Drosophila* Stock Center: *P{UAS-FLP1.D}JD1* (BL 4539), *P{Gal4-ey.H}4-8* (BL 5535), $P\{EPgy2\}CG1632^{EY03495}$ (BL 15650), *P{eyFLP.N}5* (BL5576), *M{3xP3-RFP.attP}ZH-86Fb; M{vas-int.B}ZH-102D* (BL 23648), *P{UAS-2xeGFP}AH2* (BL 6874), *nanos-Gal4* [58], *P{GMR-p53.Ex}3/TM3, Sb, Ser* (BL 8417), *GMR-Gal4* [59], *P{GMR-hid}G1/CyO* (BL 5771), *P{GMR-rpr.H}S/TM6B, Tb* (BL 5773), and *P{Act5C-Gal4}17F01/TM6B, Tb* (BL 3954). Two *corp*-RNA*i* stocks were obtained from VDRC: v102751 and v16130. The following stocks were obtained from Golic lab collections: heat-shock inducible *FLP*, *P{70FLP}10*, *P{UAS-GFP} P{Act-Gal4}/CyO*, and *y w; Sp/CyO; nanosGal4 UAS-FLP(95%).* The *engrailed-Gal4* stock was kindly gifted by Mark Metzstein.

Plasmids and transgenic constructions. The coding region of *corp* from $Canton^{S}$ flies was amplified by PCR with 5' *NotI* and 3' *XbaI* overhangs (primers used: Fwd-5'CATATTCGCGGCCGCATGGCCGATATCAGGAGCAG3' and Rev- 5'CCGCGGGTCTAGACTAGATGCGAATCGAGCGCA3') and cloned

into the pUAST-w^+-attB transgenic fly vector [60]. Vector plasmid was injected in embryos carrying *attP* docking sites on chromosome *3* and vasa-ΦC31 integrase on chromosome *4* (BL 23648). w^+ flies were selected for establishing stable transgenic stocks.

The $corp^{95B}$ deletion mutation was generated via imprecise excision of the EY03495 P-element insertion (Baylor College of Medicine Genome Disruption Project). The DNA break points were identified by PCR amplification (primer sets used: Fwd 1: 5'CCAAGCGAACGCATCGCTG3', Fwd 2: 5'GAAGAGGTCATCTCCCAAGG3', Rev1: 5'CTTAGGAACAATGGTTCAACC3', and Rev2: 5'GCAGCCGAGGTATGGAAATC3' and sequencing of genomic DNA obtained from the homozygous mutant.

DNA sequencing. Sequencing of $corp^+$ from the genomic region in five different genotypes, *y w*, w^{1118}, *EP-*$corp^+$, $Canton^S$, and *v; Sco/Cy; ry*, was carried out by the Core Facilities, University of Utah.

Eye photographs. Eye photographs were taken using a Nikon D200 digital camera and processed in Adobe Photoshop.

Quantitative reverse transcriptase PCR. Total RNA was extracted from 12-15 adults or third instar larvae using Trizol Reagent (Sigma Aldrich, MO), treated with DNaseI (Fermentas, PA), and cDNA was synthesized using RevertAid™ First Strand cDNA synthesis kit (Thermo Scientific, PA) according to manufacturer's protocol. 1µl of cDNA was used per reaction in triplicates for performing qRT-PCR experiment using Maxima™ SYBR green/Fluorescein qPCR Master Mix (Fermentas, PA) or PerfeCTa SYBR Green FastMix (Quanta

Biosciences, MD) in an iQ-PCR machine (Bio-Rad, CA). Relative quantification of mRNA levels was calculated using the standard curve method. Relative copy numbers of each gene of interest (X) was calculated by normalizing cDNA levels of X over cDNA levels of Ribosomal Protein L32. Primers that were used are: Fwd-corp: 5' GCAGCCGAGGTATGGAAATC 3'; Rev-corp: 5'AAGCCGAGGGTCAGAAGG 3'; Fwd-p53: 5' GCCGCCTCCTTAATCATGCC 3'; Rev-p53: 5' GCCGAGACTGCGACGACTC 3'; Fwd-rpl: 5' CCGCTTCAAGGGACAGTATC3'; Fwd-rpl: 5' ATCTCGCCGCAGTAAACG 3'.

Irradiation. 15-18 wandering third instar larvae were collected in clean 10 mm petri plates and irradiated at 4000 rads in a TORREX120D X-ray generator (Astrophysics Research Corp, CA), set at 110kV and 5mA. These larvae were returned to fresh food and incubated at 25°C until further experimental treatments.

Eye size measurement. For determining eye sizes, the left eye of each fly was measured along the anterio-posterior axis (A) and the dorso-ventral axis (B), using a digital filar micrometer (Lasico, CA). Then these two measurements were used to calculate the area of an ellipse (i.e., Π x A/2 x B/2), as the area of the eye. Then this area was normalized over mean of the area of wildtype (w^{1118} or *y w*) eyes and was represented as a fraction of wildtype eye size.

Germline fragment chromosome transmission assay. Flies were allowed to lay eggs and transferred to fresh vials every day. Embryos were collected for 24 hrs, heat-shocked at 38°C for 1 hour in a circulating water bath

and then immediately returned to 25°C. After eclosion, the males were collected and singly mated to 2-3 *y w* females and their progeny were scored. Alternatively, *nosGal4* was used to drive *UASFLP* in the male germline.

Imaginal disc staining procedures and fluorescence microscopy. Wing and eye imaginal discs were dissected from third instar larvae and stained with TUNEL, acridine orange, or P53 antibody.

TUNEL staining: TUNEL staining was performed using Apoptag Red *In Situ* Apoptosis Detection Kit (#S7165, Chemicon International). Briefly, dissected imaginal discs were fixed in 4% paraformaldehyde, rinsed twice in PBT_W (0.3% Tween-20 in 1X PBS) for 5 minutes/rinse, post-fixed in 2:1 EtOH/1X PBS, rinsed again as before, and then incubated with equilibration buffer, TdT enzyme, and anti-digoxigenin Rhodamine congujate antibody in subsequent steps, according to manufacturer's protocol. Finally, the discs were mounted in Vectashield (Vector Laboratories Inc., CA) and photographed. All images were at taken at 500 ms shutter speed and at neutral density 3. The minimum and maximum intensity ranges for TUNEL staining were set at 200 and 2000, respectively, for all captured images. TUNEL fluorescence intensity was measured individually in the posterior and anterior compartments of each disc, normalized to the area of that compartment and expressed as integrated density of fluorescence intensity/area (InDen/area) in posterior compartment to that in the anterior compartment.

Acridine orange staining: Acridine orange staining was performed on freshly dissected imaginal discs. The discs were then incubated in a 1.6×10^{-6} M

solution of acridine orange (1.6 µl of 1mM solution of AO in 1 ml. Ringer's solution) for 5 minutes, then mounted in Ringer's solution and photographed immediately. All images were taken at 100 ms shutter speed and at neutral density 4. Minimum and maximum intensity range: 200-600. AO intensity is expressed as InD/area of the whole disc.

P53 immunostaining: Third instar larvae were dissected in 1X PBS and fixed in 4% paraformaldehyde for 15 minutes at room temperature. They were washed in PBT_X (0.3% Triton-X in 1X PBS) twice for 30 minutes each, followed by 1 hour blocking in 5% BSA in PBT_X. Next, they were incubated overnight at 4°C in primary antibody, p53-7A4 (DSHB, University of Iowa, IA) at 1:10 concentration in 5% BSA. The discs were then rinsed twice with PBT_X, 30 minutes each and once in blocking buffer for 1 hour and finally incubated with Alexa Fluor® 568 goat anti-mouse secondary antibody (Invitrogen, OR) at 1: 1000 concentration for 2 hours. Finally, they were washed twice with PBT_X as before and mounted in Vectashield (Vector Laboratories Inc., CA). All images were taken at 100 ms shutter speed and at neutral density 3. Minimum and maximum intensity range: 200-550. P53 staining intensity is expressed as InD/area where the area of only the region behind the morphogenetic furrow is considered.

All fluorescent images were z stacks taken using an inverted Olympus IX2-DSU spinning disc confocal microscope, a Hamamatsu Orca-ER digital camera, and SLIDEBOOK software (Intelligent Imaging Innovations, CA).

dsRNA synthesis. To synthesize double-stranded RNA for RNA interference experiments with cultured cells, PCR products not more than 700 base pairs were made of the cDNA of interest flanked by T7 RNA polymerase sites at both ends. After gel purification of the PCR product, it was used as template for *in vitro* transcription for 6 hours at 37°C in a circulating water bath in 5-6 replicates of 20 µl reaction each for better yield using Ambion Megascript® T7 Transcription Kit (Life Technologies), according to manufacturer's protocol. Then, the reactions were pooled together in a microcentrifuge tube and extracted with phenol-chloroform and chloroform. Finally, dsRNA was precipitated with ispropanol, dissolved in DEPC-treated H_2O, and quantified in a Nanodrop 1000 spectrophotometer (Thermo Scientific).

Primers used for obtaining PCR products were: Fwd_T7corp: 5'TTAATACGACTCACTATAGGGAGAATGGCCGATATCAGGAGCAG3'; Rev_T7corp: 5'TTAATACGACTCACTATAGGGAGACTAGATGCGAATCGAGCGCA3'; Fwd_T7p53: 5'TTAATACGACTCACTATAGGGAGAAGATCCAGGCGAACACGCTG3'; Rev_T7p53: 5'TTAATACGACTCACTATAGGGAGAGGCTTCCGGCACGGACTTG3'; Fwd_T7Pav: 5'TTAATACGACTCACTATAGGGAGAACAACTGCTCTTGGCAGATACC3'; Rev_T7Pav: 5'TTAATACGACTCACTATAGGGAGAAAATCCGTAACGAAACTAACCG3'.

Detection of P53 levels in S2 cells.

Cell culture and dsRNA treatment. S2 cells were cultured at 25°C in Schneider's *Drosophila* Medium (Invitrogen) with 10% heat inactivated fetal bovine serum (HyClone) and 1X Antibiotic-Antimycotic (Invitrogen). Cells were passaged into fresh medium every 3-4 days and were discarded after passage 25 (P25).

The dsRNA treatment protocol was performed as described [61]. Cells were passaged on day 0 at the rate of 2 x 10^6 cells/ml. On day 1, they were washed and seeded in 24-well plates at 800 µl/well. 15 µg of dsRNA was added to each well. The plates were then returned to the 25°C incubator. On day 4-5, cells were re-seeded in 6-well plates at 2 ml/well and retreated with 30 µg of dsRNA. As a control of dsRNA uptake rate, cells were treated with Pavarotti dsRNA, which makes them large and multinucleate [62,63]. On day 6-7, cells were collected, lysed, and processed for Western blot.

S2 cells, with or without dsRNA treatment, were irradiated at 4000 rads to observe any elevation/change in P53 levels from unirradiated cells, with or without dsRNA treatment. No significant changes in P53 levels were observed following irradiation, so treated cells were grouped and categorized as (I) no dsRNA control group and (II) + dsRNA experimental group for quantification.

Western blotting. Cells were collected and lysed in RIPA buffer containing protease inhibitor (Thermo Scientific, IL) to a final concentration of 1X. Protein concentration was measured by BCA assay (Thermo Scientific, IL) and cell lysates were mixed with sample buffer and β–mercaptoethanol to a final

concentration of 1X before loading onto a 10% SDS gel at equal concentrations. Western blotting was carried out following standard procedure. Antibodies used: mouse monoclonal anti-*Drosophila* P53 (# sc-74573, Santa Cruz Biotechnology; as used by Chen *et al.*[54]) at 1:1000 concentration and mouse monoclonal anti-*Drosophila* β–tubulin (E7, Developmental Studies Hybridoma Bank, University of Iowa, IA) at 1:10,000 concentration. After incubation with fluorescent goat anti-mouse secondary antibody (# 926-68020, Li-COR Biosciences) at 1:10,000, the membranes were scanned on an infrared Odyssey scanner (LI-COR Biosciences). The Western signals were quantified on the Li-COR scanner and the results from 6 independent experiments were averaged. Of these 6 experiments, 2 were following irradiation at 4000 rads and allowing 4 hours recovery before cell lysis. Relative P53 levels in each experiment were calculated by normalizing total P53 protein level to total β–tubulin level.

Protein interaction assays.

Purification of GST and GST-DmP53. The open reading frame of DmP53 was cloned into pGEX and transformed to BL21 DE3 cells. The expression was induced by addition of IPTG to a final concentration of 0.1mM in LB/Ampicillin media. Bacterial cells were harvested 4 hours following the induction and resuspended in ice-cold STE buffer (10mM Tris-HCl pH8.0, 150mM NaCl, 1mM EDTA, and protease inhibitors) with 1.5% Sarcosyl. Cells were then lysed with sonication and subsequently incubated with STE containing 1% Triton X-100 for 30 minutes. Insoluble proteins were removed by centrifugation at 16,000g for 5 minutes. Supernatant was then incubated

overnight with 50% slurry of glutathione-agarose beads at 4°C. The beads were pelleted by centrifuge at 100g and washed 4 more times with 10 ml of ice-cold PBTP (PBS with 0.1% Triton X-100 and protease inhibitors). Washed beads were then resuspended in PBTP with 0.01% sodium azide.

Expression of Corp-GFPFlag in HeLa cells. 15ug of pRK5-*corp-gfp-flag* plasmid DNA was transfected to 2 million HeLa cells with calcium phosphate. Cells were lysed on plate with 1ml RIPA buffer at 48 hours following transfection.

***In vitro* synthesis of Corp-HA6His.** Corp-HA6His was cloned into pCDNA3. *In vitro* synthesis were carried out using the TnT® Coupled Reticulocyte Lysate Systems (Promega, Catalog number L4611) following manufacturer's instructions.

GST pull-down assays. For *in vitro* synthesized protein, 1 ug GST or GST-DmP53 bound to Glutathione-agarose beads was incubated with 5 ul of synthesized protein in 500ul Binding buffer (50mM Tris-HCl, pH 8.0; 2mM EDTA; 150mM NaCl; 0.1% NP40; 20uM $ZnCl_2$; 10mM $MgCl_2$; protease inhibitors) containing BSA (0.2ug/ul). Following 1 hour incubation at RT and 1 hour incubation at 4^{o}C, the beads were washed 4 times with Binding buffer. Beads were then pelleted at 100g, re-suspended and boiled in 30 ul sampling buffer, and resolved on SDS-PAGE gel. Following electrophoresis, the gel was fixed in (Isopropenol:dH_2O:Acitic acid=25:65:10) for 30 minutes and incubated in the Amplify Fluorographic Reagent (GE Healthcare, NAMP100) for 1 hour. The gel was then vacuum dried and processed for autoradiography with an intensify screen at -80^{o}C.

For cellular extract, 1 ug GST or GST-DmP53 bound to Glutathione-agarose beads was first incubated for 30 minutes in 500ul binding buffer with 0.2ug/ul BSA. 500 ul cell lysate was then added and incubated at 4^{o}C for overnight. Following incubation, the beads were washed 4 times with 1 ml of RIPA buffer and pelleted by centrifugation at 100g for 5 minutes. Beads were then resuspended in 30ul sampling buffer and resolved on SDS-PAGE gel. Western analysis was performed with anti-Flag M2 antibody (Sigma, F1804).

Co-immunoprecipitation. 10ug of pRK5-*corp-gfp-flag* plasmid DNA and 10ug of pEX-3B-*hsp53-ha* was transfected to 2 million HeLa cells with calcium phosphate. At 48 hours post transfection, cells were lysed with RIPA buffer, precleared with protein G–Sepharose beads, and then incubated with anti-Flag(M2) mouse monoclonal antibody for overnight at 4^{o}C. The immunocomplex was then precipitated with protein G- Sepharose beads, followed by SDS-PAGE and Western blot analysis.

Graphical methods and statistical analyses. Construction of graphs and calculations of statistical significance were performed using Prism 5.0 (Graphpad). In box-and-whisker plots, the ends of whiskers represent 5th and 95th percentiles, top and bottom of the boxes represent 25th and 75th percentile, and the horizontal line in the box represents the median, i.e., 50th percentile. The Mann-Whitney test was used in all cases except for Figure 5D, where a paired t-test was used.

Software. The MEME tool used for searching motif similarity is publicly available software (http://meme.nbcr.net/meme/). Images were quantitatively

analyzed using IMAGE J software from National Institutes of Health (http://imagej.nih.gov/ij/index.html) and images were processed using Adobe Photoshop. All line diagrams were composed using Adobe Illustrator.

Acknowledgements

A part of this work is done in the laboratory of our collaborator, Dr. Lei Zhou, Department of Molecular Genetics and Microbiology, College of Medicine, University of Florida. The *corp*^{95B} mutant was constructed by Dr. Zhou's lab. The Corp-P53 interaction assays were performed by a postdoc, Dr. Ying Li at the Zhou lab.

We thank Mark Metzstein for fly stocks, Colin Dale for qRT-PCR facilities, Markus Babst and Julie Hollien for Western blot and cell culture facilities, and Changwang Deng and Suming Huang of Zhou lab for technical assistance. Two of our antibodies were obtained from Developmental Studies Hybridoma Bank, University of Iowa, Iowa City, IA. We thank Tin Tin Su and Andreas Bergmann for sharing unpublished results. R.C. was partially supported by University of Utah Graduate School Research Fellowship. The project was supported by NIH grant R01-GM065604 to K.G.G. and R01-GM106174 to L.Z.

Figure 8. Overexpression of *corp*$^{+}$ suppresses the BARTL phenotype. (A) The range of eye phenotypes observed in the assay. The B^{S} phenotype of *H1* control males is shown at the left. When FLP is expressed (*ey>FLP*), the phenotypes can range from headless pharates (category 1) to adults with a fully developed wildtype eye (category 5). The distribution produced (B) in control males; (C) in males carrying *P{EPgy2}EY03495*, referred to as *EP-corp*$^{+}$; (D) by inclusion of a *UAS-corp*$^{+}$ transgene; (E) with RNAi-mediated knockdown of *corp*; (F) in *corp*^{95B} mutants; and, (G) with rescue of the *corp*^{95B} phenotype by expression from the *UAS-corp*$^{+}$ transgene. N represents number of eyes scored for each genotype. Genotypes used are as follows: (B) *y w/H1; eyGal4 UAS-FLP/+*; (C) *y w EP-corp*$^{+}$*/H1; eyGal4 UAS-FLP/+*; (D) *y w/H1; eyGal4 UAS-FLP/+; UAS-corp*$^{+}$*/+*; (E) *y w/H1; eyGal4 UAS-FLP/RNAi-corp*; (F) *y w corp*^{95B}*/H1; eyGal4 UAS-FLP/+*; (G) *y w corp*^{95B}*/H1; eyGal4 UAS-FLP/+; UAS-corp*$^{+}$*/+*.

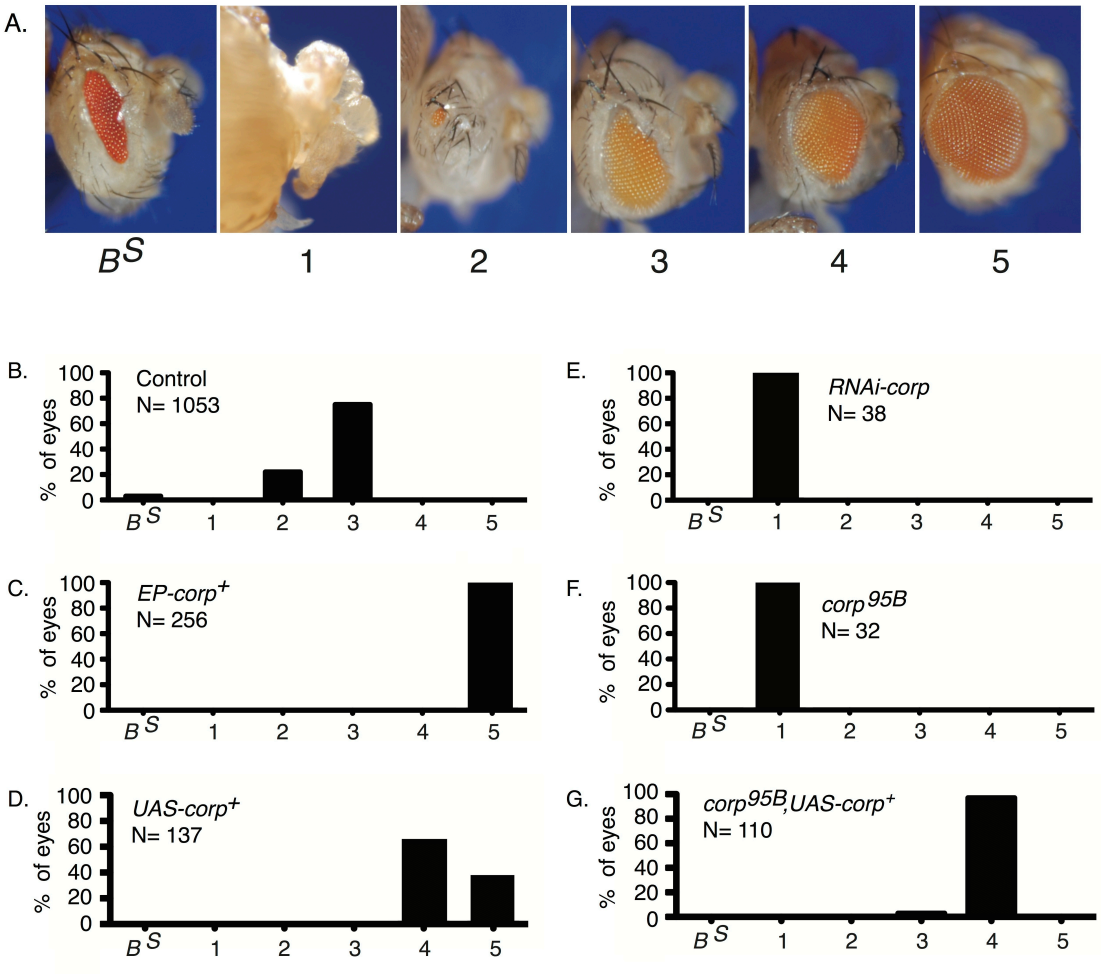
A.
BS
1
2
3
4
5
B.
Control
N= 1053
C.
EP-corp+
N= 256
D.
UAS-corp+
N= 137
E.
RNAi-corp
N= 38
F.
corp95B
N= 32
G.
corp95B,UAS-corp+
N= 110
% of eyes
100
80
60
40
20
0

Figure 9. *EP-corp*$^{+}$ induces *corp*$^{+}$ overexpression.
corp mRNA levels were measured by qRTPCR on total cDNA extracts from *Actin-Gal4 EP-corp*$^{+}$ or *y w* control adults. The Y-axis indicates *corp* transcript levels normalized to the *Rpl32* transcript. Data are represented as mean +SEM. N represents the number of biological replicates of each experiment. Statistical significance was calculated by the Mann-Whitney test. Although *corp* expression was ~15X higher when the *EP-corp*$^{+}$ was driven, the difference was not significant at the 5% level.

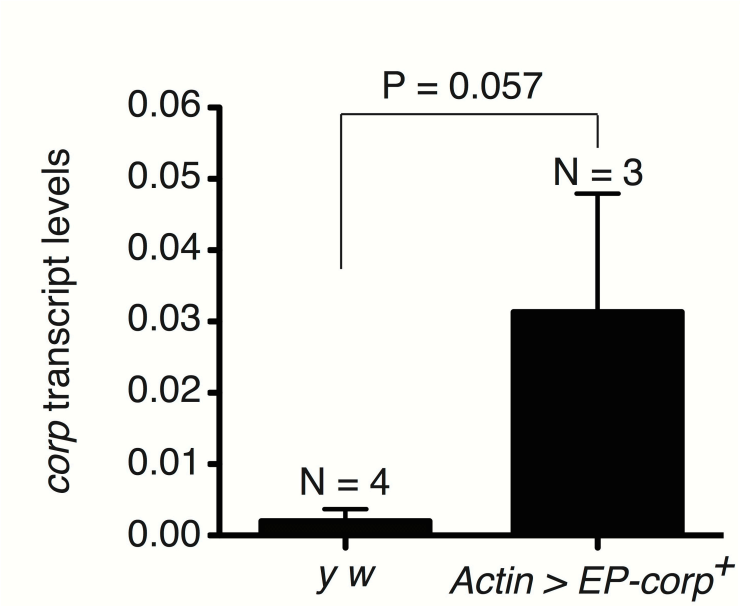
P = 0.057
0.06
0.05
0.04
0.03
0.02
0.01
0.00
corp transcript levels
N = 3
N = 4
y w
Actin > EP-corp+

Figure 10. Deletion mapping in the *corp*^{95B} mutant.
(A) The *corp* genomic region on the *X* chromosome and *corp* transcripts (RA and RB; adapted from FlyBase: http://flybase.org/reports/FBgn0030028.html). Orange shading denotes the protein coding regions. The blue arrowhead indicates the site of the *EY03495 EPgy2*. Imprecise excision of the *EY03495* element produced the *corp*^{95B} allele. The black line indicates the region of the genome that is deleted in *corp*^{95B} mutant. Two sets of primers, Fwd1, Rev1 and Fwd2, Rev2 were used for PCR amplification of *corp* genomic region.
(B,C) Visualization of PCR results. The *corp* genomic region was amplified either by Fwd1, Rev1 or by Fwd 2, Rev2 primer pairs in four different genotypes, run in the four lanes on the gel, marked 1 through 4: (1) *y w*; (2) *corp* mutant 1; (3) *corp*^{95B}; and (4) *corp* mutant 2. M1 is a 1 kb ladder and M2 is the 100 bp ladder. The vertical red arrow indicates the lane 3, which lacks any PCR product and corresponds to the *corp*^{95B} template. The horizontal red arrowhead points to the size expected in the *y w* control. Only the *corp*^{95B} mutant was used in this work. The extent of the *corp*^{95B} deletion allele was determined by DNA sequencing of genomic DNA.

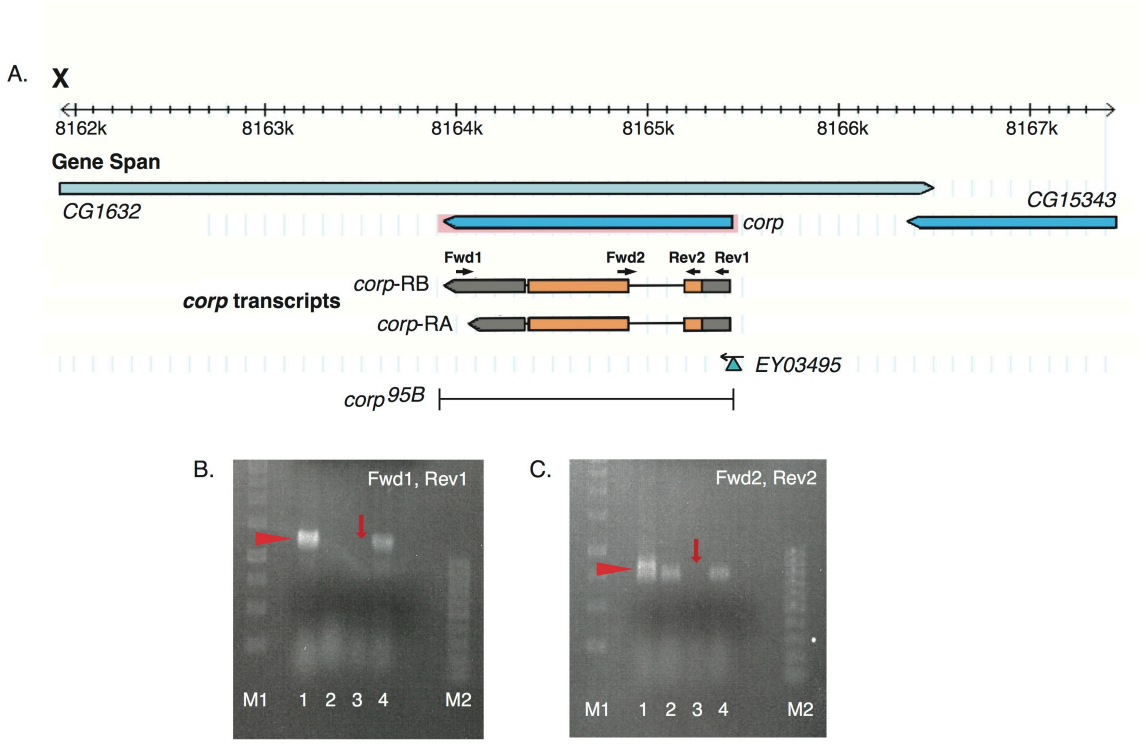
A.
X
8162k
8163k
8164k
8165k
8166k
8167k
Gene Span
CG1632
CG15343
corp
Fwd1
Fwd2
Rev2
Rev1
corp transcripts
corp-RB
corp-RA
EY03495
corp 95B
B.
Fwd1, Rev1
M1 1 2 3 4 M2
C.
Fwd2, Rev2
M1 1 2 3 4 M2

Figure 11. Altered *corp* function only affects eyes after dicentric chromosome induction.
The distribution of eye sizes when (B) *H1* dicentrics are produced in the presence of uninduced *EP-corp*$^{+}$; (C) *EP-corp*$^{+}$ is induced in B^{+} flies without dicentric induction; (D, E) *EP-corp*$^{+}$ is introduced, uninduced (D), and induced (E) into B^{S} flies without dicentric induction; (F) *corp*^{95B} is introduced into B^{S} background without dicentric induction; (G) *corp*^{95B} is introduced into B^{+} flies without dicentric induction; (H) *H1* dicentrics are produced in *XXY(H1)* females; (I) *EP-corp*$^{+}$ is overexpressed following dicentric induction in *XXY(H1)* females; (J) dicentric chromosome formation is induced on chromosome 3 (*Dc3*); and (K) *EP-corp*$^{+}$ is overexpressed with chromosome *3* dicentric induction (K). *N* represents the number of fly eyes scored for each genotype.

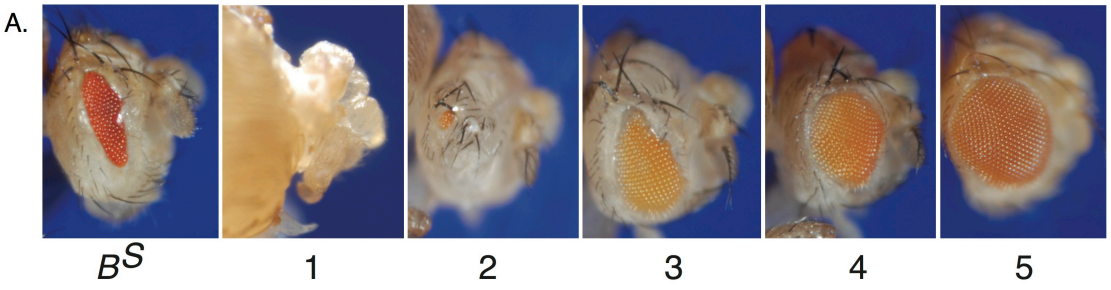
A.
BS
1
2
3
4
5

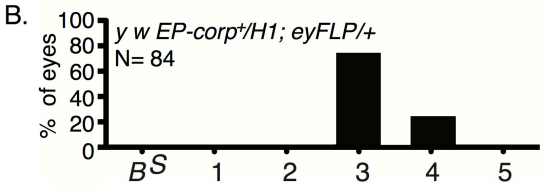
B.
y w EP-corp+/H1; eyFLP/+
N= 84
% of eyes
BS 1 2 3 4 5

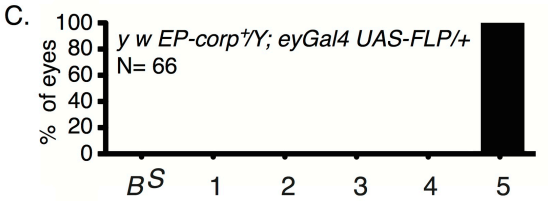
C.
y w EP-corp+/Y; eyGal4 UAS-FLP/+
N= 66
% of eyes
BS 1 2 3 4 5

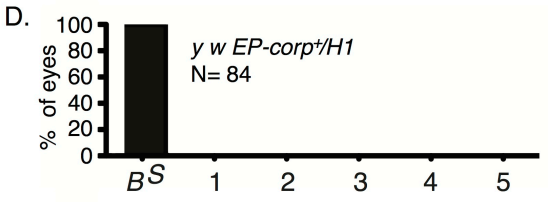
D.
y w EP-corp+/H1
N= 84
% of eyes
BS 1 2 3 4 5

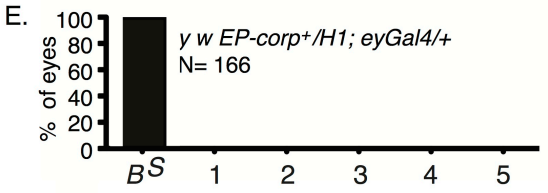
E.
y w EP-corp+/H1; eyGal4/+
N= 166
% of eyes
BS 1 2 3 4 5

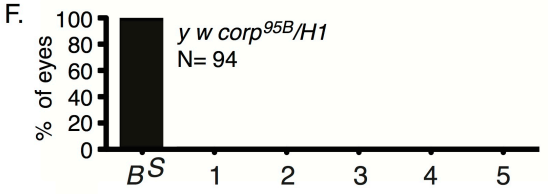
F.
y w corp95B/H1
N= 94
% of eyes
BS 1 2 3 4 5

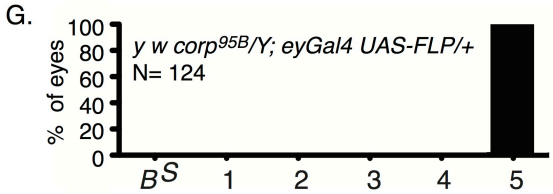
G.
y w corp95B/Y; eyGal4 UAS-FLP/+
N= 124
% of eyes
BS 1 2 3 4 5

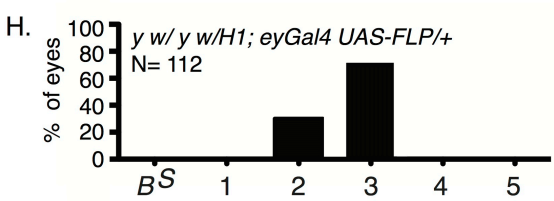
H.
y w/ y w/H1; eyGal4 UAS-FLP/+
N= 112
% of eyes
BS 1 2 3 4 5

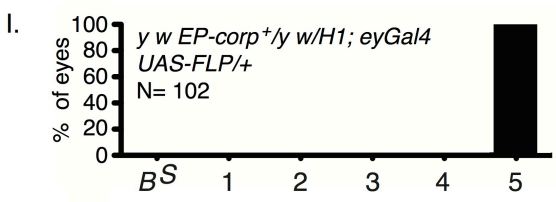
I.
y w EP-corp+/y w/H1; eyGal4
UAS-FLP/+
N= 102
% of eyes
BS 1 2 3 4 5

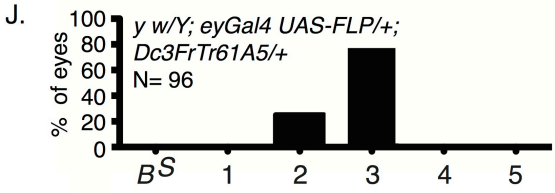
J.
y w/Y; eyGal4 UAS-FLP/+;
Dc3FrTr61A5/+
N= 96
% of eyes
BS 1 2 3 4 5

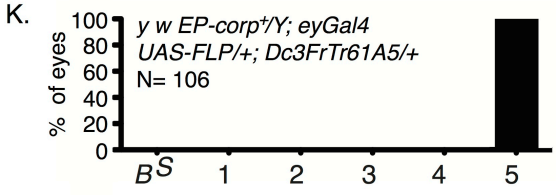
K.
y w EP-corp+/Y; eyGal4
UAS-FLP/+; Dc3FrTr61A5/+
N= 106
% of eyes
BS 1 2 3 4 5

Figure 12. *corp*$^{+}$ inhibits DNA damage-induced apoptosis in somatic tissue.

(A) The effect of *corp*$^{+}$ overexpression assayed by TUNEL staining of third instar wing discs 3 hours after exposure to 4000 rads of IR. The white broken line marks the boundary between the anterior (ant) and posterior (post) compartments of the disc, based on *engrailed*-driven GFP fluorescence that marks the posterior compartment (i and iii). (i, ii) The staining pattern in wildtype control. (iii, iv) Staining in discs where *engrailed* is driving *EP-corp*$^{+}$ overexpression in posterior compartment. TUNEL staining is very dense in wildtype larvae in the posterior segment (ii), but is greatly reduced with *corp*$^{+}$ overexpression (iv). All images were taken with a 20X objective.

(B) The effect of the *corp*^{95B} mutant assayed by acridine orange (AO) staining of wing discs from irradiated third instar larvae. Larvae were exposed to 4000 rads of X-ray and dissected 5-6 hours later. Staining is greatly increased in *corp*^{95B} mutants compared to the *y w* control. Images were captured with a 10X objective. Representative discs are shown here as negative images for ease of visualization.

(C) Quantitation of TUNEL staining. The ratio of posterior:anterior fluorescence intensity in each disc was used as a measure of how *corp*$^{+}$ overexpression alters apoptosis. Genotypes tested are indicated on the X-axis. N represents total number of discs used for quantification.

(D) Quantitation of AO staining. Staining intensity per unit area for *y w* control and *corp*^{95B} mutant. N represents total number of discs used for quantification.

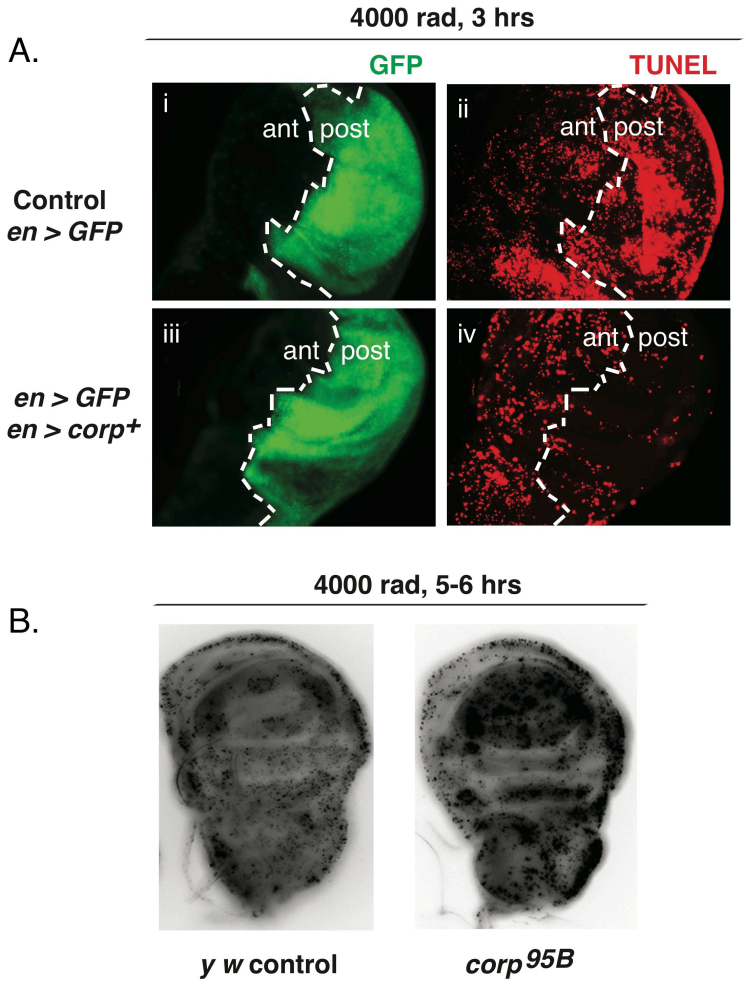
A.
4000 rad, 3 hrs
GFP
TUNEL
i
ii
iii
iv
ant
post
Control
en > GFP
en > GFP
en > corp+
B.
4000 rad, 5-6 hrs
y w control
corp95B

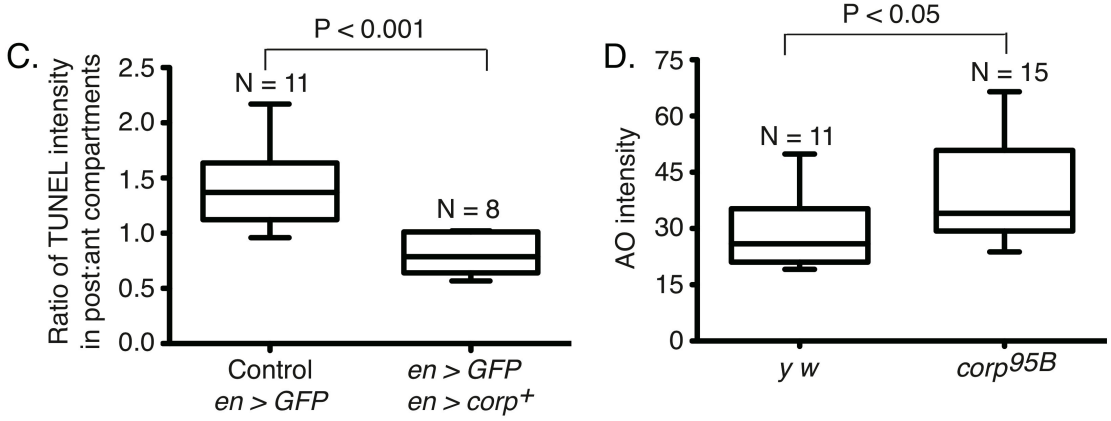
C.
P < 0.001
N = 11
N = 8
Ratio of TUNEL intensity in post:ant compartments
2.5
2.0
1.5
1.0
0.5
0.0
Control
en > GFP
en > GFP
en > corp+
D.
P < 0.05
N = 11
N = 15
AO intensity
75
60
45
30
15
0
y w
corp95B

Figure 13. Interaction of *corp* and *p53*.
(A) The $p53^{5A\text{-}1\text{-}4}$ mutation is epistatic to *corp* in the BARTL assay. The $corp^{95B}$ mutation produces headless flies in the BARTL assay (reproduced from Figure 2), while $p53^{5A\text{-}1\text{-}4}$ has the opposite effect, producing flies with wildtype eyes. The double mutant is indistinguishable from the $p53^{5A\text{-}1\text{-}4}$ single mutant. N represents the number of eyes or headless pharates scored. Genotypes used were *y w* $corp^{95B}$*/H1; eyGal4 UAS-FLP*; *y w/H1; eyGal4 UAS-FLP/+;* $p53^{5A\text{-}1\text{-}4}$; *y w* $corp^{95B}$*/H1; eyGal4 UAS-FLP/+;* $p53^{5A\text{-}1\text{-}}$*.*
(B) Overexpression of $corp^{+}$ suppresses the apoptotic phenotype caused by overexpression of $p53^{+}$. Eye sizes were measured from flies that overexpressed $p53^{+}$, and that also overexpressed $corp^{+}$ or were $corp^{95B}$ mutants. The Y-axis represents fraction of wildtype eye size. N is the number of eyes measured.
(C) $corp^{+}$ overexpression suppresses the cell-death phenotypes mediated by hid^{+} or $reaper^{+}$ overexpression. *GMR* drives $corp^{+}$, hid^{+}, and $reaper^{+}$ overexpression. The Y-axis represents eye size, normalized to wildtype, for each genotype. N is the number of eyes.

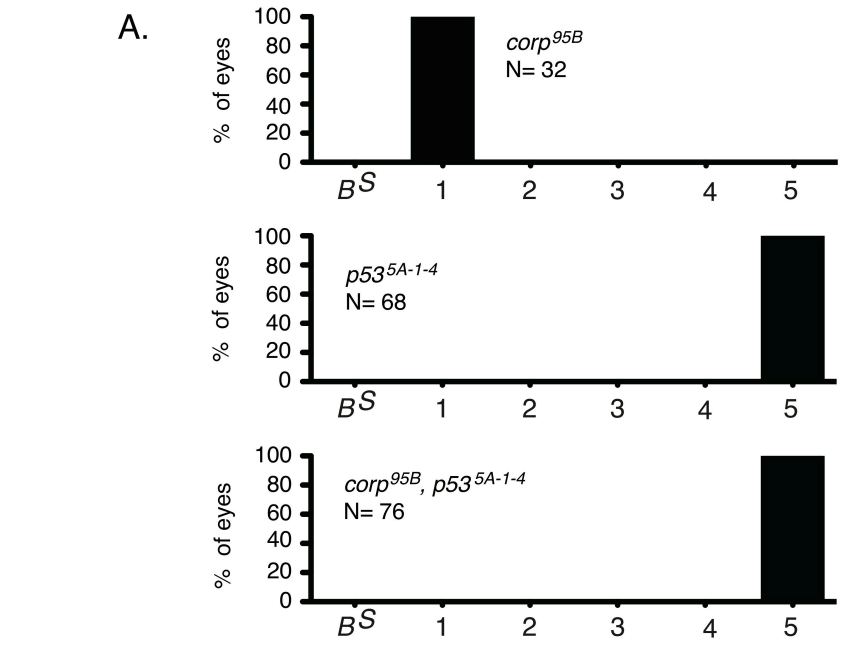
A.
% of eyes
100
80
60
40
20
0
B S 1 2 3 4 5
corp95B
N= 32
p535A-1-4
N= 68
corp95B, p535A-1-4
N= 76

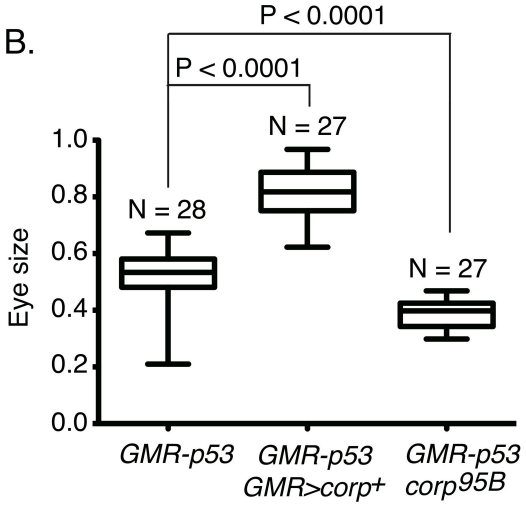
B.
P < 0.0001
P < 0.0001
N = 28
N = 27
N = 27
Eye size
1.0
0.8
0.6
0.4
0.2
0.0
GMR-p53
GMR-p53
GMR>corp+
GMR-p53
corp95B

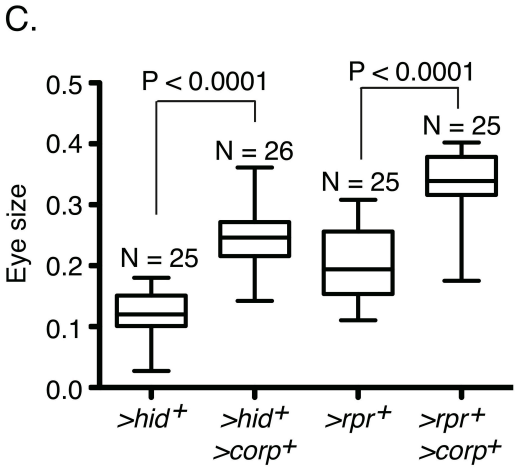
C.
P < 0.0001
P < 0.0001
N = 25
N = 26
N = 25
N = 25
Eye size
0.5
0.4
0.3
0.2
0.1
0.0
>hid+
>hid+
>corp+
>rpr+
>rpr+
>corp+

Figure 14. Corp negatively regulates P53 protein levels.
(A) Immunostaining of eye discs of flies expressing *p53*$^{+}$ under control of the *GMR* promoter (shown here as negative images). Red arrowheads indicate approximate position of the morphogenetic furrow. Posterior is to the right. Genotypes are as indicated. All images were taken with a 40X objective.
(B) Quantitation of P53 immunostaining. N represents the number of eye discs scored.
(C, D) P53 protein level increases in *corp* knockdown cells.
(C) Western blot of protein extracts from S2 cells. The first lane represents untreated cells (WT), and the second lane after treatment with dsRNA directed against *corp*. β–tubulin is the loading control. Blots are cropped to display only the desired sizes for clarity and conciseness of data presentation.
(D) Quantitation of P53 protein levels. P53 protein levels are represented as the P53 protein level normalized to β–tubulin. *N* represents the number of experimental repetitions. Data are represented as mean +SEM.

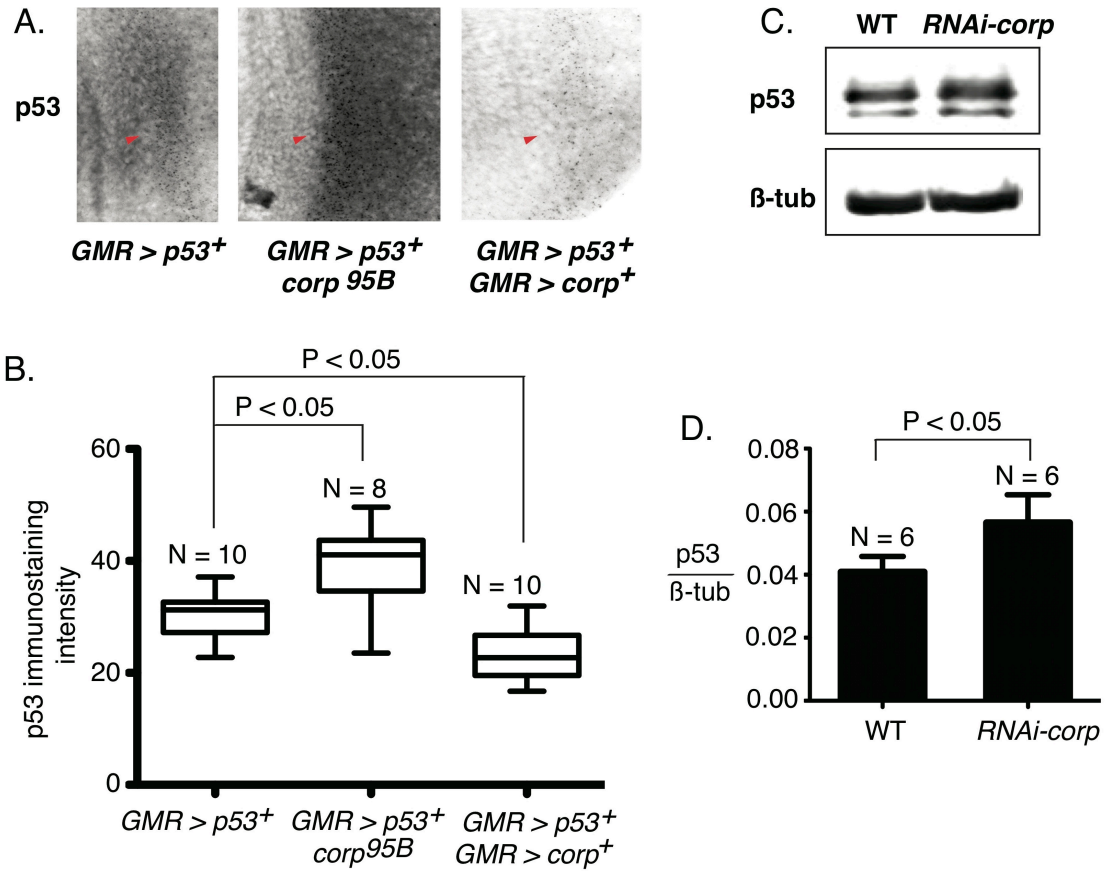
A.
p53
GMR > p53+
GMR > p53+ corp 95B
GMR > p53+ GMR > corp+
C.
WT
RNAi-corp
p53
ß-tub
B.
P < 0.05
P < 0.05
N = 10
N = 8
N = 10
p53 immunostaining intensity
60
40
20
0
GMR > p53+
GMR > p53+ corp95B
GMR > p53+ GMR > corp+
D.
P < 0.05
N = 6
N = 6
p53 / ß-tub
0.08
0.06
0.04
0.02
0.00
WT
RNAi-corp

Figure 15. *corp*$^{+}$ does not affect *p53* transcript levels.
p53 mRNA levels were measured by qRTPCR on total cDNA extracts of irradiated and nonirradiated third instar larvae. The graphs represent *p53* mRNA levels with no irradiation and at different time points after irradiation, in control (light blue bars) *corp*$^{+}$ overexpressing (yellow bars) and *corp*^{95B} mutant (pink bars) larvae (as indicated). The larvae were irradiated at 4000 rads and allowed to recover for 1, 2, and 3 hours before cDNA extraction. Three biological replicates were carried out for each experiment. Data are represented as mean +/- SEM.

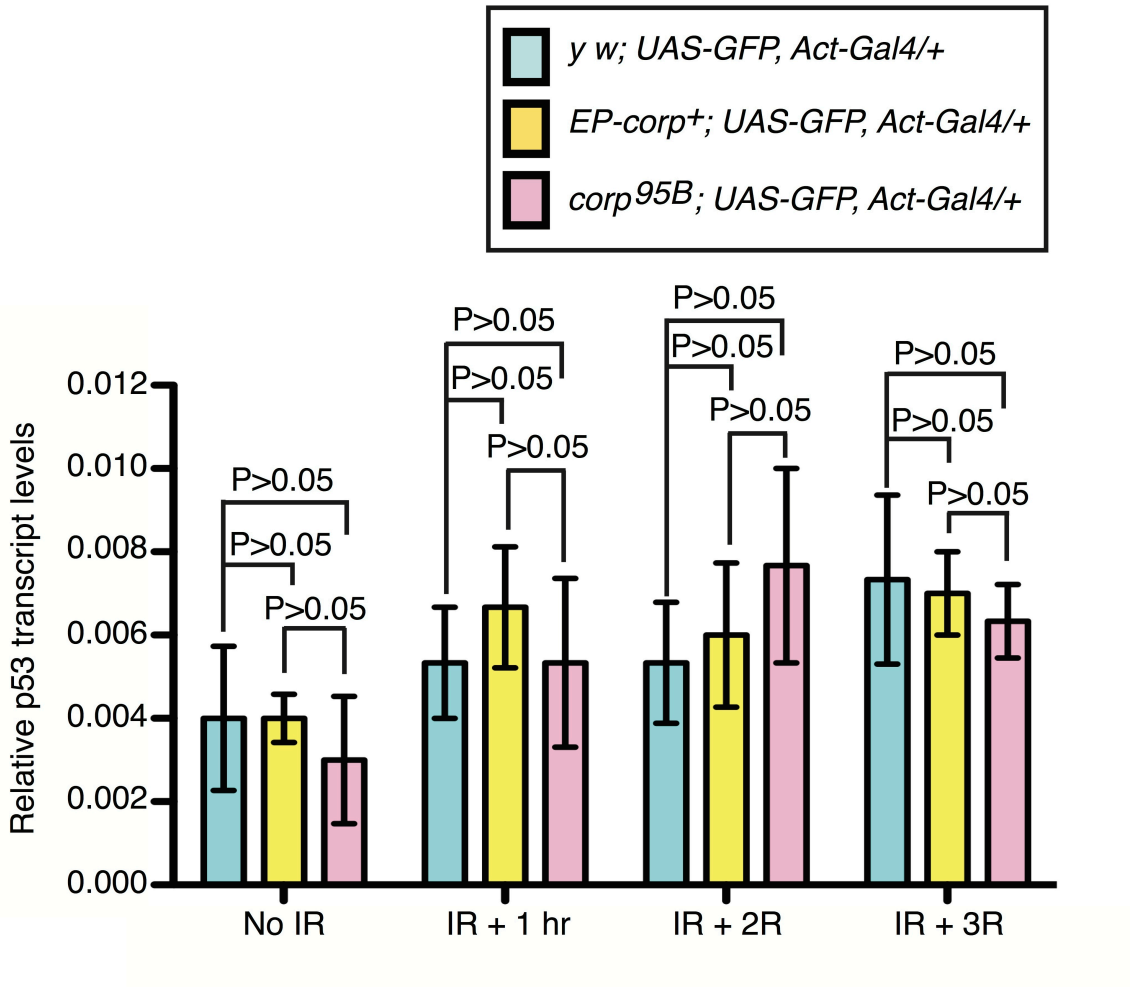
y w; UAS-GFP, Act-Gal4/+
EP-corp+; UAS-GFP, Act-Gal4/+
corp95B; UAS-GFP, Act-Gal4/+
Relative p53 transcript levels
0.012
0.010
0.008
0.006
0.004
0.002
0.000
P>0.05
P>0.05
P>0.05
P>0.05
P>0.05
P>0.05
P>0.05
P>0.05
P>0.05
P>0.05
P>0.05
P>0.05
No IR
IR + 1 hr
IR + 2R
IR + 3R

Figure 16. Relationships between Corp, Mdm2, and P53.
(A) Conserved protein motifs between Mdm2 and Corp identified by MEME. Seven similar protein motifs between 4 vertebrate Mdm2 orthologs (*H. sapiens*, *M. musculus*, *D. rerio*, *G. gallus*) and 2 Corp orthologs (*D. melanogaster*, *D. virlis*). Two motifs are conserved between Mdm2 and Corp in all six species. (i) A complete map of the 6 proteins indicating 7 shared motifs, represented by colored rectangles. A scale below indicates length of the individual proteins. Motifs 4 and 5 are found in Corp. (ii) The amino acid sequence of motif 4. Start site indicates the first amino acid residue in that motif. Amino acids of conserved motifs are color-coded [64]. *P*-values that indicate the significance of conservation of each motif were produced by MEME. (iii) The amino acid sequence of the motif 5 region.
(B) A model of the pro-apoptotic and anti-apoptotic pathways under P53 control in *Drosophila melanogaster*. A DNA double-strand break activates the DNA damage response leading to P53 activation. The well-known pro-apoptotic genes *hid* and *reaper* are indicated in one pathway downstream from P53, while the anti-apoptotic gene *corp* is diagrammed in a second branch of the pathway. Hid and Reaper inhibit the inhibitor of apoptosis Diap1, thus triggering the downstream initiator and effector caspases, Dronc and Drice, respectively, to induce apoptosis. A positive feedback loop acting on *p53* exists downstream of *hid* and *reaper*. Corp constitutes a second feedback loop, in this case acting negatively on P53.

A. (i)

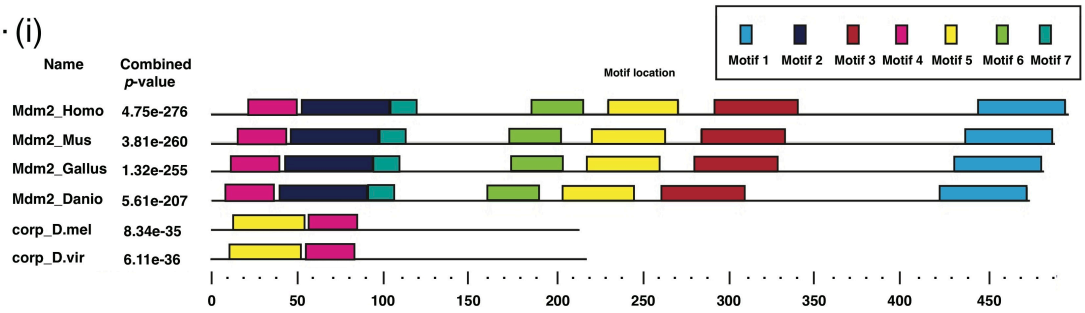

(ii)

Name	Start	p-value	
Mdm2_Mus	17	1.26e-29	SVSTEGAAST SQIPASEQETLVRPKPLLLKLLKSVGA QNDTYTMKEI
Mdm2_Homo	23	1.26e-29	SVPTDGAVTT SQIPASEQETLVRPKPLLLKLLKSVGA QKDTYTMKEV
Mdm2_Gallus	13	2.76e-25	NTEMTSLTDG SPVSASEQEALVKPKPLLLKLLKLAGA EKDTFTMKEV
corp_D.vir	56	3.16e-21	LVLTNGQGYV FEQQLLEYFLLLFPCPELLFYLRLDWQ KLRRALIEPV
corp_D.mel	58	4.01e-20	LILTNGKDYV FEAPLLEYFLLLFPCPEITFHLRFDWS KMRRSLGQTE
Mdm2_Danio	10	5.66e-19	MATESCLSS SQISKVDNEKLVRPKVQLKSLLEDAGA DKDVFTMKEV

(iii)

Name	Start	p-value	
Mdm2_Homo	231	1.08e-40	STGTPSNPDL DAGVSEHSGDWLDQDSVSDQFSVEFEVESLDSEDYSLSEEG QELSDEDDEV
Mdm2_Mus	223	2.13e-38	STETPSHQDL DDGVSEHSGDCLDQDSVSDQFSVEFEVESLDSEDYSLSDEG HELSDEDDEV
Mdm2_Gallus	219	1.70e-34	STDSVSIPDL DASSLSENSDWFDHGSVSDQFSVEFEVESIYSEDYSHNEEG QELTDEDDEV
Mdm2_Danio	205	2.65e-26	SSDANSNSDV GISRSEGSEESEDSDSDSDNFSVEFEVESINSDAYSENDVD SVPGENEIYE
corp_D.mel	14	7.75e-26	IRSSLKVLFQ GETNLITCGSSNTYEEVISQAMTRFAIPETQRKALILTNGK DYVFEAHLLE
corp_D.vir	12	4.76e-24	MKSCLKISFR GEVSFVICEAGSSYEQIIAQACARFHIPETQRAGLVLTNGQ GYVFEQQLLE

B.

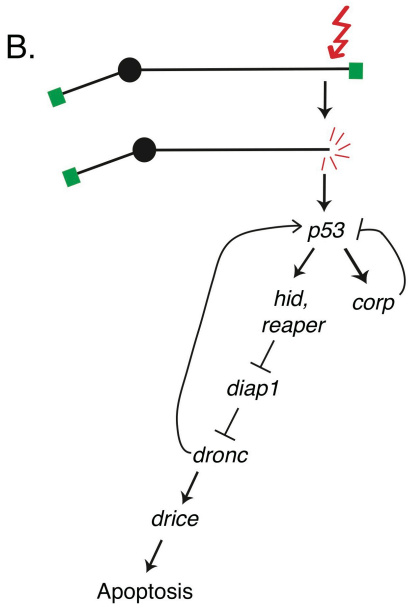

Figure 17. Corp physically interacts with *Drosophila* P53.
(A) The results of pull-down from HeLa cells expressing Corp-GFPFlag. Cell lysate was incubated with GST or GST-DmP53 bound to glutathione-agarose beads. Captured proteins were resolved with SDS-PAGE and probed with anti-Flag antibody. The predicted molecular weight of Corp-GFPFlag is about 55 KDa. The smaller (~33KDa) band on the input lane likely reflects the C-terminal fragment of the fusion protein, which does not interact with GST-DmP53.
(B) *In vitro* synthesized Corp-HA6His (~28KDa) interacts with GST-DmP53. The smaller band likely reflects an N-terminal ^{35}S-Methionine containing fragment of Corp, which does interact with DmP53.

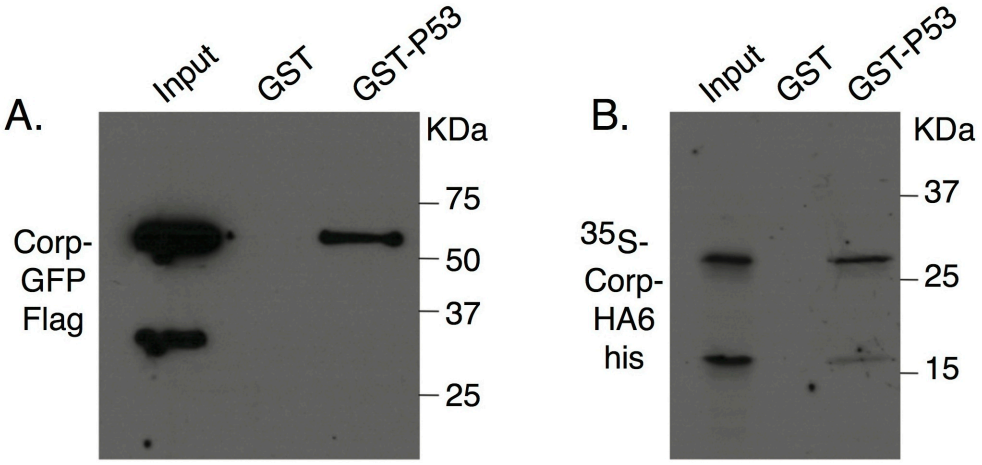
A.
Input
GST
GST-P53
KDa
75
50
37
25
Corp-
GFP
Flag
B.
Input
GST
GST-P53
KDa
37
25
15
35S-
Corp-
HA6
his

Figure 18. Protein interactions of Corp in *Drosophila melanogaster*.
This figure, taken from FlyBase (http://flybase.org/cgi-bin/get_interactions.html?items=FBgn0030028&mode=ppi), shows proteins that have been identified as physically interacting with Corp [1]. Nine of these 19 interactors are proteasome subunits.

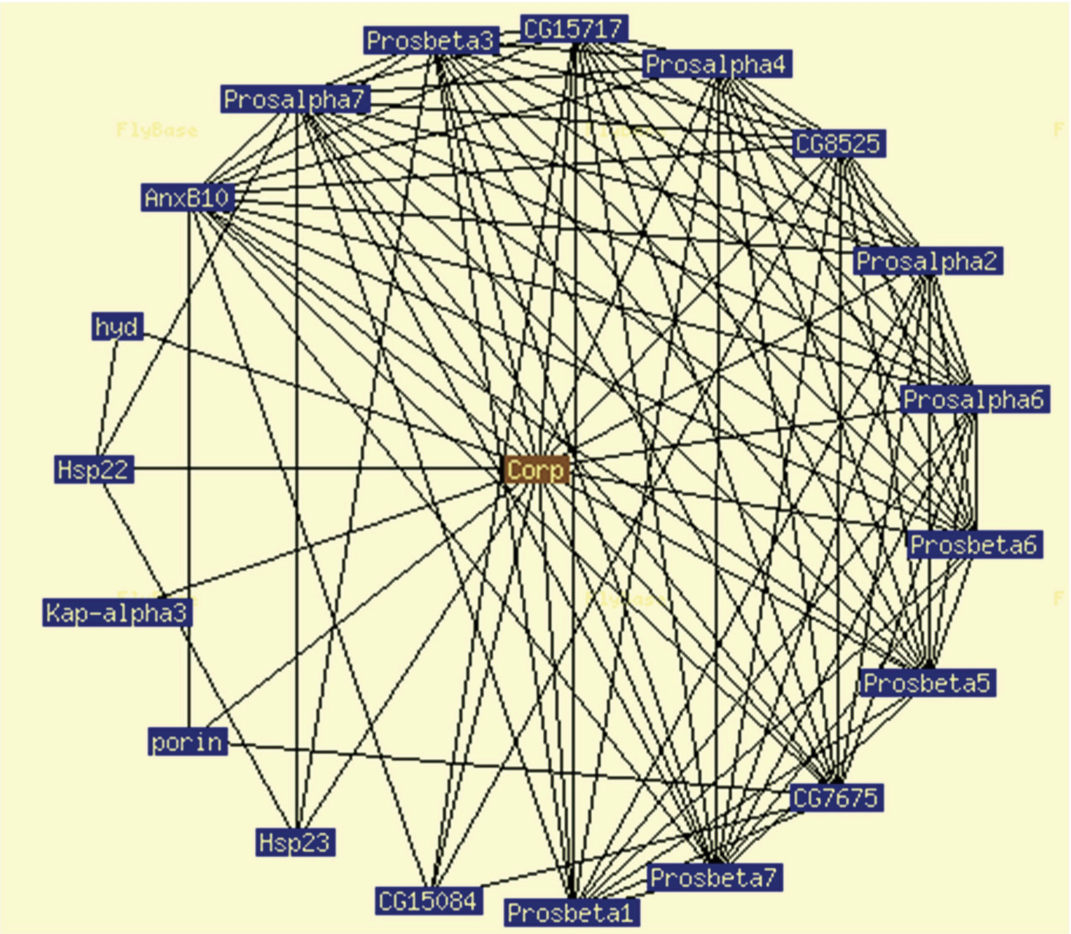
Prosbeta3
CG15717
Prosalpha4
Prosalpha7
CG8525
AnxB10
Prosalpha2
hyd
Prosalpha6
Hsp22
Corp
Prosbeta6
Kap-alpha3
Prosbeta5
porin
CG7675
Hsp23
Prosbeta7
CG15084
Prosbeta1

Table 5. Effect of *corp* on transmission of broken-and-healed chromosomes through the male germline.

Genotype	N[a]	Sterility (%)[b]	*FrY* sons	*Y* sons	Fragment Ratio[c] (P value)	Daughters
y w/H1; 70FLP10/+	317	55	6401	14411	0.31	25011
y w EP-corp^{+}/H1; 70FLP10/+; nosGal4/+	247	51	7	9801	0.001 (P<0.0001)	11611
y w/H1; UAS-FLP nosGal4/+	247	14	11998	2425	0.83	16675
y w EP-corp^{+}/H1; UAS-FLP nosGal4/+	174	30	2180	7573	0.22 (P<0.0001)	11386

[a] N, number of males testcrossed.

[b] Percentage of tested males that were sterile.

[c] Fragment ratio is calculated as *FrY* sons/total sons. *P* values were determined with the Mann-Whitney test using Fragment Ratios of individual males. Each *P* value represents comparison with the row immediately above in this table.

References

1. Elledge, S. J. & Zhou, B.-B. S. The DNA damage response: putting checkpoints in perspective. *Nature* **408,** 433–439 (2000).

2. Sancar, A. A., Lindsey-Boltz, L. A. L., Unsal-Kaçmaz, K. K. & Linn, S. S. Molecular mechanisms of mammalian DNA repair and the DNA damage checkpoints. *Biochemistry* **73,** 39–85 (2004).

3. Jackson, S. P. & Bartek, J. The DNA-damage response in human biology and disease. *Nature* **461,** 1071–1078 (2009).

4. Ahmad, K. K. & Golic, K. G. K. Telomere loss in somatic cells of Drosophila causes cell cycle arrest and apoptosis. *Genetics* **151,** 1041–1051 (1999).

5. Titen, S. W. A. & Golic, K. G. Telomere Loss Provokes Multiple Pathways to Apoptosis and Produces Genomic Instability in Drosophila melanogaster. *Genetics* **180,** 1821–1832 (2008).

6. Golic, K. G. Local Transposition of P Elements in Drosophila Melanogaster and Recombination between Duplicated Elements Using a Site-Specific Recombinase. *Genetics* **137,** 551 (1994).

7. Hollstein, M., Sidransky, D., Vogelstein, B. & Harris, C. C. p53 mutations in human cancers. *Science* **253,** 49–53 (1991).

8. Hirao, A. DNA Damage-Induced Activation of p53 by the Checkpoint Kinase Chk2. *Science* **287,** 1824–1827 (2000).

9. Matsuoka, S., Huang, M. & Elledge, S. J. Linkage of ATM to cell cycle regulation by the Chk2 protein kinase. *Science* **282,** 1893–1897 (1998).

10. Chaturvedi, P. P. *et al.* Mammalian Chk2 is a downstream effector of the ATM-dependent DNA damage checkpoint pathway. *Oncogene* **18,** 4047–4054 (1999).

11. Saito, S. *et al.* ATM Mediates Phosphorylation at Multiple p53 Sites, Including Ser46, in Response to Ionizing Radiation. *Journal of Biological Chemistry* **277,** 12491–12494 (2002).

12. Banin, S. *et al.* Enhanced Phosphorylation of p53 by ATM in Response to DNA Damage. *Science* **281,** 1674–1677 (1998).

13. Khanna, K. K. *et al.* ATM associates with and phosphorylates p53: mapping the region of interaction. *Nat Genet* **20,** 398–400 (1998).

14. Kodama, M. *et al.* Requirement of ATM for rapid p53 phosphorylation at Ser46 without Ser/Thr-Gln sequences. *Molecular and Cellular Biology* **30,** 1620–1633 (2010).

15. Chehab, N. H. N., Malikzay, A. A., Appel, M. M. & Halazonetis, T. D. T. Chk2/hCds1 functions as a DNA damage checkpoint in G(1) by stabilizing p53. *Genes & Development* **14,** 278–288 (2000).

16. Wahl, G. M. & Carr, A. M. The evolution of diverse biological responses to DNA damage: insights from yeast and p53. *Nat Cell Biol* **3,** E277–E286 (2001).

17. Liu, Y. p53 protein at the hub of cellular DNA damage response pathways through sequence-specific and non-sequence-specific DNA binding. *Carcinogenesis* **22,** 851–860 (2001).

18. Akdemir, F., Christich, A., Sogame, N., Chapo, J. & Abrams, J. M. p53 directs focused genomic responses in Drosophila. *Oncogene* **26,** 5184–5193 (2007).

19. Brodsky, M. H. *et al.* Drosophila melanogaster MNK/Chk2 and p53 Regulate Multiple DNA Repair and Apoptotic Pathways following DNA Damage. *Molecular and Cellular Biology* **24,** 1219–1231 (2004).

20. Colombani, J., Polesello, C., Josué, F. & Tapon, N. Dmp53 activates the Hippo pathway to promote cell death in response to DNA damage. *Curr. Biol.* **16,** 1453–1458 (2006).

21. Lee, J. H. *et al.* In vivo p53 function is indispensable for DNA damage-induced apoptotic signaling in Drosophila. *FEBS Letters* **550,** 5–10 (2003).

22. Vousden, K. H. & Lu, X. Live or let die: the cell's response to p53. *Nat. Rev. Cancer.* **2,** 594–604 (2002).

23. Donehower, L. A. L. *et al.* Mice deficient for p53 are developmentally normal but susceptible to spontaneous tumours. *Nature* **356,** 215–221 (1992).

24. Kurzhals, R. L., Titen, S. W. A., Xie, H. B. & Golic, K. G. Chk2 and p53 are haploinsufficient with dependent and independent functions to eliminate cells after telomere loss. *PLoS Genet* **7,** e1002103–e1002103 (2011).

25. Brodsky, M. H. *et al.* Drosophila p53 Binds a Damage Response Element at the reaper Locus. *Cell* **101,** 103–113 (2000).

26. Ollmann, M. *et al.* Drosophila p53 is a structural and functional homolog of

the tumor suppressor p53. *Cell* **101,** 91–101 (2000).

27. Jin, S. *et al.* Identification and characterization of a p53 homologue in Drosophila melanogaster. *Proc. Natl. Acad. Sci. U.S.A.* **97,** 7301–7306 (2000).

28. Kubbutat, M. H. G., Jones, S. & Vousden, K. H. Regulation of p53 stability by Mdm2. *Proc. Natl. Acad. Sci. U.S.A.* **387,** 299–303 (1997).

29. Momand, J., Zambetti, G. P., Olson, D. C., George, D. & Levine, A. J. The mdm-2 oncogene product forms a complex with the p53 protein and inhibits p53-mediated transactivation. *Cell* **69,** 1237–1245 (1992).

30. Peters, M. *et al.* Chk2 regulates irradiation-induced, p53-mediated apoptosis in Drosophila. *proc Natl Acad Sci USA* **99,** 11305–11310 (2002).

31. Zhang, Y. *et al.* Epigenetic Blocking of an Enhancer Region Controls Irradiation-Induced Proapoptotic Gene Expression in Drosophila Embryos. *Developmental Cell* **14,** 481–493 (2008).

32. Rørth, P. P. A modular misexpression screen in Drosophila detecting tissue-specific phenotypes. *Proc. Natl. Acad. Sci. U.S.A.* **93,** 12418–12422 (1996).

33. Hauck, B. B., Gehring, W. J. W. & Walldorf, U. U. Functional analysis of an eye specific enhancer of the eyeless gene in Drosophila. *Proc. Natl. Acad. Sci. U.S.A.* **96,** 564–569 (1999).

34. Fan, Y. & Bergmann, A. Distinct Mechanisms of Apoptosis-Induced Compensatory Proliferation in Proliferating and Differentiating Tissues in the Drosophila Eye. *Developmental Cell* **14,** 399–410 (2008).

35. Brand, A. H. & Perrimon, N. Targeted gene expression as a means of altering cell fates and generating dominant phenotypes. *Development* **118,** 401–415 (1993).

36. Tabata, T., Schwartz, C., Gustavson, E., Ali, Z. & Kornberg, T. B. Creating a Drosophila wing de novo, the role of engrailed, and the compartment border hypothesis. *Development* **121,** 3359–3369 (1995).

37. Ahmad, K. & Golic, K. G. The transmission of fragmented chromosomes in Drosophila melanogaster. *Genetics* **148,** 775–792 (1998).

38. Titen, S. W. A. & Golic, K. G. Healing of euchromatic chromosome breaks by efficient de novo telomere addition in Drosophila melanogaster. *Genetics* **184,** 309–312 (2010).

39. Titen, S. W. A., Lin, H.-C., Bhandari, J. & Golic, K. G. Chk2 and p53 regulate the transmission of healed chromosomes in the Drosophila male germline. *PLoS Genet* **10,** e1004130–e1004130 (2014).

40. Shlevkov, E. & Morata, G. A dp53/JNK-dependant feedback amplification loop is essential for the apoptotic response to stress in Drosophila. *Cell Death Differ* **19,** 451–460 (2012).

41. Bailey, T. L. T. & Elkan, C. C. Fitting a mixture model by expectation maximization to discover motifs in biopolymers. *Proc Int Conf Intell Syst Mol Biol* **2,** 28–36 (1994).

42. Bailey, T. L. T., Williams, N. N., Misleh, C. C. & Li, W. W. W. MEME: discovering and analyzing DNA and protein sequence motifs. *Nucleic Acids Research* **34,** W369–W373 (2006).

43. Chen, J., Marechal, V. & Levine, A. J. Mapping of the p53 and mdm-2 interaction domains. *Mol. Cell. Biol.* **13,** 4107–4114 (1993).

44. Kussie, P. H. *et al.* Structure of the MDM2 oncoprotein bound to the p53 tumor suppressor transactivation domain. *Science* **274,** 948–953 (1996).

45. Kulikov, R., Winter, M. & Blattner, C. Binding of p53 to the central domain of Mdm2 is regulated by phosphorylation. *J. Biol. Chem.* **281,** 28575–28583 (2006).

46. Sogame, N., Kim, M. & Abrams, J. M. Drosophila p53 preserves genomic stability by regulating cell death. *Proc. Natl. Acad. Sci. U.S.A.* **100,** 4696–4701 (2003).

47. Nordstrom, W. & Abrams, J. M. Guardian ancestry: fly p53 and damage-inducible apoptosis. *Cell Death Differ* **7,** 1035–1038 (2000).

48. Manfredi, J. J. The Mdm2-p53 relationship evolves: Mdm2 swings both ways as an oncogene and a tumor suppressor. *Genes & Development* **24,** 1580–1589 (2010).

49. Guruharsha, K. G. *et al.* A protein complex network of Drosophila melanogaster. *Cell* **147,** 690–703 (2011).

50. Jones, S. N., Roe, A. E., Donehower, L. A. & Bradley, A. Rescue of embryonic lethality in Mdm2-deficient mice by absence of p53. *Nature* **378,** 206–208 (1995).

51. Pant, V. *et al.* The p53-Mdm2 feedback loop protects against DNA damage by inhibiting p53 activity but is dispensable for p53 stability, development,

and longevity. *Genes & Development* **27,** 1857–1867 (2013).

52. Tollini, L. A., Jin, A., Park, J. & Zhang, Y. Regulation of p53 by Mdm2 E3 Ligase Function Is Dispensable in Embryogenesis and Development, but Essential in Response to DNA Damage. *Cancer Cell* **26,** 235–247 (2014).

53. Allton, K. *et al.* Trim24 targets endogenous p53 for degradation. *Proc. Natl. Acad. Sci. U.S.A.* **106,** 11612–11616 (2009).

54. Chen, S., Wei, H.-M., Lv, W.-W., Wang, D.-L. & Sun, F.-L. E2 ligase dRad6 regulates DMP53 turnover in Drosophila. *Journal of Biological Chemistry* **286,** 9020–9030 (2011).

55. Oikemus, S. R. Drosophila atm/telomere fusion is required for telomeric localization of HP1 and telomere position effect. *Genes & Development* **18,** 1850–1861 (2004).

56. Bilak, A., Uyetake, L. & Su, T. T. Dying cells protect survivors from radiation-induced cell death in Drosophila. *PLoS Genet* **10,** e1004220 (2014).

57. Xie, H. B. & Golic, K. G. Gene Deletions by Ends-In Targeting in Drosophila melanogaster. *Genetics* **168,** 1477–1489 (2004).

58. Rørth, P. Gal4 in the *Drosophila* female germline. *Mechanisms of Development* **78,** 113–118 (1998).

59. Freeman, M. Reiterative use of the EGF receptor triggers differentiation of all cell types in the Drosophila eye. *Cell* **87,** 651–660 (1996).

60. Bischof, J. J., Maeda, R. K. R., Hediger, M. M., Karch, F. F. & Basler, K. K. An optimized transgenesis system for Drosophila using germ-line-specific phiC31 integrases. *Proc. Natl. Acad. Sci. U.S.A.* **104,** 3312–3317 (2007).

61. Clemens, J. C. *et al.* Use of double-stranded RNA interference in Drosophila cell lines to dissect signal transduction pathways. *Proc. Natl. Acad. Sci. U.S.A.* **97,** 6499–6503 (2000).

62. Somma, M. P., Fasulo, B., Cenci, G., Cundari, E. & Gatti, M. Molecular dissection of cytokinesis by RNA interference in Drosophila cultured cells. *Mol Biol Cell* **13,** 2448–2460 (2002).

63. Goshima, G. & Vale, R. D. The roles of microtubule-based motor proteins in mitosis: comprehensive RNAi analysis in the Drosophila S2 cell line. *The Journal of Cell Biology* **162,** 1003–1016 (2003).

64. Kyte, J. & Doolittle, R. F. A simple method for displaying the hydropathic character of a protein. *J Mol Biol* **157,** 105–132 (1982).

CHAPTER 4

ROLE OF *FS(1)YB* AS AN INDUCER OF CELL DEATH FOLLOWING IRREPARABLE DNA DAMAGE

Abstract

The *EP* misexpression screen in the BARTL background identified a gene, *fs(1)Yb*, that severely reduces cell survival following irreparable DNA damage in the form of a telomere loss, leading to the ablation of the whole tissue. *fs(1)Yb* knockdown, on the other hand, reduces the severity of apoptotic phenotype. *fs(1)Yb* is an upstream component in the piwi/piRNA pathway that plays an essential role in germline stem cell maintenance by inducing piRNA generation and transposon silencing through the downstream components, *armi* and *piwi*. Though the function of *armi* in suppression of DNA damage response and that of both *armi* and *piwi* in maintenance of telomere integrity have been previous reported, the role of *fs(1)Yb* in response to DNA damage has not been studied. Our results indicate a possible role of *fs(1)Yb* in the induction of DDR pathway following telomere loss.

Introduction

The *fs(1)Yb* gene was originally uncovered by mutations that caused semi-sterility in females of *Drosophila melanogaster* (Young and Judd, 1978). Later, it was determined that *fs(1)Yb* plays an essential role in germline stem cell maintenance, particularly during differentiation of ovarian follicle cells. *Yb* mutants produce few or no eggs (Johnson et al., 1995; King and Lin, 1999; Szakmary et al., 2009). The female sterility caused by *fs(1)Yb* was partially suppressed by increasing the *Notch* dosage, while reduction of *Notch* dosage produced a more severe phenotype, suggesting a possible functional or

regulatory interplay between *fs(1)Yb* and *Notch* signaling during oogenesis (Johnson et al., 1995).

Later, *Yb* was characterized as a major upstream component of the *piwi*/piRNA pathway (King et al., 2001; Qi et al., 2011). The complex class of small noncoding RNAs, called piRNAs, that interact with Piwi proteins have been widely implicated for their germline-specific roles in stem cell maintenance, spermiogenesis, and transposon silencing (Cox et al., 1998; Megosh et al., 2006; Szakmary et al., 2009; Thomson and Lin, 2009). Structural analysis revealed that Fs(1)Yb contains a TUDOR domain, which is present in most piRNA pathway proteins (King and Lin, 1999; Shoji et al., 2009). Fs(1)Yb localizes to dense cytoplasmic regions called Yb bodies where it recruits armitage (Armi), a putative RNA helicase involved in the piRNA pathway, and recruits Piwi, another piRNA component, into the nucleus of somatic and germ cells, where Piwi then silences genes by piRNA generation. In *Yb* mutants, the co-immunoprecipitation of Armi with Yb is disrupted, Piwi fails to enter the nucleus and is freed from piRNAs, which then get drastically diminished, and somatic transposons are desilenced (Qi et al., 2011; Saito et al., 2010). Thus, *fs(1)Yb* poses to be an upstream piRNA pathway component and plays a crucial role in monitoring the Piwi-piRNA binding and eventual transposon silencing. There are two parallel pathways downstream of *fs(1)Yb*: the *piwi*-mediated germline stem cell self-renewal and the *hedgehog* (*hh*)-mediated somatic stem cell proliferation. Via these pathways, *fs(1)Yb* maintains both the germline and somatic stem cell populations. *Yb* mutants

eliminate and *Yb*$^{+}$ overexpression overproliferates both stem cell populations (King et al., 2001).

Piwi-pathway proteins have been shown to play an important role in maintenance of telomere integrity. This is achieved by silencing the transcription of telomeric repeat sequences and maintaining the telomeric capping complex. In fact, *armi* mutants have been shown to disrupt HOAP binding to telomere, reduce expression of a subpopulation of telomere-specific piRNAs, and enhance *HeT-A* copy numbers. *armi* mutants also lead to extensive fragmentation of the zygotic genome (Khurana et al., 2010), probably due to DNA damage signaling from genome-wide over-transcription. Furthermore, mutations of piRNA pathway proteins, like *armi* and *aub*, have developmental implications in the context of DNA damage response. They result in disruption of asymmetric RNA localization along the axes of the oocyte, which is rescued by *chk2* mutants (Chen et al., 2007; Klattenhoff et al., 2007), implying that mutation of piRNA pathway proteins triggers DNA damage response at their downstream, which is suppressed by mutating damage response pathway proteins, for example, *chk2*. All these evidences point to the fact that disruption of piRNA pathway proteins can be the causative agent of DNA damage, which induces the responses downstream to it.

However, there has been no report so far on the role of *fs(1)Yb* in DNA damage response. Here, we demonstrate that *fs(1)Yb*$^{+}$ acts as an enhancer of cell-death phenotype in the soma following telomere loss, probably through elimination of cells with telomere loss in a P53-dependent manner. It also

eliminates germline cells that have been induced with telomere loss and inhibits transmission of broken-and-healed chromosome through the germline.

Results

***EP* misexpression screen identifies *fs(1)Yb* as an enhancer of apoptosis phenotype following irreparable DNA damage.** Through the *EP* misexpression screen in the BARTL background (Kurzhals et al., 2011), we identified an *EP* insertion, *P{EPgy2}CG2701*^{EY04983}, that produced headless pharates in the BARTL assay (Figure 19C). This insertion was ideally placed to drive expression of the *fs(1)Yb*$^{+}$ gene (*CG2706*) (Figure 20A). When we tested RNAi-mediated knockdown of *fs(1)Yb* in the BARTL assay, an opposite result was obtained: the eyes were significantly larger, though not fully wildtype-like (Figure 19E,F). Similarly, a *fs(1)Yb* null mutant gave mostly large eyes when tested in the BARTL background (Figure 19D). If *EP-fs(1)Yb*$^{+}$ was not induced by Gal4, and *eyFLP* was instead used to produce dicentric chromosomes in the eye, we found that the *EP-fs(1)Yb*$^{+}$ insertion, by itself, had no effect (Figure 19J). This further confirms that *fs(1)Yb*$^{+}$ overexpression is necessary to generate the large eye phenotype in the BARTL assay.

To determine whether *fs(1)Yb* has any influence in the absence of DNA damage, we examined wildtype or *B*^{S} flies carrying *EP-fs(1)Yb*$^{+}$, induced or uninduced, but without the induction of dicentric chromosomes. There was mostly no change in eye phenotype in any of these cases, indicating that the effects of altered *fs(1)Yb* expression are seen only after DNA damage (Figure

19G-I).

***EP-corp*$^{+}$ suppresses the apoptotic phenotype of *EP-fs(1)Yb*$^{+}$ following telomere loss.** We have previously identified *corp* as one of the genes in the *EP* screen that displayed a suppressor effect in the BARTL assay and have demonstrated that *corp* acts as a negative regulator of the tumor suppressor P53 (Chapter 2 and 3). We wanted to find out if *corp* and *fs(1)Yb* act in the same or in a complementary pathway in response to DNA damage. So, we overexpressed both *fs(1)Yb*$^{+}$ and *corp*$^{+}$, mediated by *EP*, in the BARTL background. This recovered adults with wildtype-like eyes (Figure 20B-D), suggesting that *corp* acts downstream of *fs(1)Yb* following DNA damage to rescue the cell-death phenotype produced by *fs(1)Yb*. This further implies that it functions upstream of p53, therefore in the DDR pathway.

***EP*-induced *fs(1)Yb* overexpression inhibits germline transmission of broken and healed chromosomes.** Since *EP-fs(1)Yb*$^{+}$ produced an apoptotic phenotype in the somatic tissue following telomere loss, we wanted to investigate if it also eliminates cells after telomere loss in the germline. We have previously seen that if a germline cell suffers a telomere loss, that chromosome may be healed by addition of a telomere cap, and then transmitted to progeny (Ahmad and Golic, 1998; Titen and Golic, 2010). In order to find out if *EP-fs(1)Yb*$^{+}$ affects the transmission of broken-and-healed chromosome, we induced expression of FLP by heat shock (*70FLP10*) during the first 24 hours of development and used *nanosGal4* to drive germ cell-specific overexpression of *EP-fs(1)Yb*$^{+}$. We found

that *EP-fs(1)Yb*$^{+}$ significantly reduced transmission of broken-and-healed chromosomes (Table 6).

Overexpression of telomere cap component, *hiphop*, rescues the cell-death phenotype produced by *EP*-induced *fs(1)Yb* overexpression. Since *EP-fs(1)Yb*$^{+}$ reduced transmission of broken-and-healed chromosomes, there is a possibility that it plays a role to inhibit the addition of *de-novo* telomeres at broken ends of chromosomes. If this holds true, then *fs(1)Yb*$^{+}$ would likely disrupt the phenotype produced telomere capping components. In order to test this, we co-overexpressed *EP-fs(1)Yb*$^{+}$ with a component of the telomere cap complex, *hiphop*. We found, as previously seen (R. Kurzhals, personal communication), that induction of UAS-*hiphop*$^{+}$ produces near-wildtype eyes following telomere loss (Figure 20E). However, co-expression of *fs(1)Yb*$^{+}$ produced no change in the phenotype (Figure 20F). This fails to demonstrate a role of *fs(1)Yb*$^{+}$ in inhibition of *de novo* telomere addition.

Knockdown of *piwi* pathway components induce an apoptotic phenotype independent of DNA damage induction. Since *fs(1)Yb* is a component of the piRNA pathway, we wanted to test the *piwi* and *armi* genes for their role on cell survival following telomere loss. Interestingly, we found that knockdown of *piwi* and *armi* induced a cell-death phenotype, as opposed to *fs(1)Yb* knockdown (Table 7). To determine whether they have a general effect on eye development, we induced *piwi* and *armi* knockdown in a wildtype background without induction of telomere loss. We found that knockdown of *piwi* or *armi* reduced cell survival in the eye even without any DNA damage induction,

implying that their loss hinders normal eye development and that this effect is aggravated after induction of DNA damage to the cells of the eye.

Discussion and future directions

In the BARTL assay, *fs(1)Yb* overexpression and knockdown produced drastically opposite phenotypes: *fs(1)Yb* overexpression ablated the eye completely following telomere loss while the *Yb* mutant and knockdowns produced significantly enlarged eyes. This suggests that *fs(1)Yb* normally makes only a small contribution to the elimination of cells with DNA damage, or that the RNA interference is not highly effective; however, its overexpression in the somatic cells is clearly capable of mediating the death of virtually all cells with irreparable DNA damage. Similar to the effect in soma, *fs(1)Yb* overexpression increases the elimination of cells with broken chromosomes in the germline, seen as reduced transmission of broken-and-healed chromosomes through the germline. This could have suggested a possible role of *fs(1)Yb*$^{+}$ in inhibition of *de novo* telomere addition. However, our finding, that *fs(1)Yb*$^{+}$ overexpression does not alter the large eye phenotype produced by *hiphop*$^{+}$ overexpression in the BARTL assay, indicates a declined probability of its role in inhibition of *de novo* telomere capping. The fact that *fs(1)Yb*$^{+}$ inhibits broken-and-healed chromosome transmission but not a significant change in sex ratio, compared to the wildtypes carrying a broken chromosome, suggests that *fs(1)Yb*$^{+}$ plays a role in controlling the survival of germline cells with a broken chromosome: it aids the elimination of primary spermatocytes with an unhealed damaged chromosome at the 16 cell-

stage, but not of the post-meiotic *FrY* spermatids - that results in the decrease in fragment transmission but not a significant difference in the sex ratio. It was also interesting to note a sharp drop in the average number of progenies produced by each fertile male carrying a broken chromosome and with *fs(1)Yb*$^{+}$ overexpression in its germline. This may be due to the fact a large number of primary spermatocytes are eliminated by *fs(1)Yb*$^{+}$. However, since the experiment was carried out in different ways (total number of progenies were scored from two vials for each wildtype tester male and the progenies scored for *fs(1)Yb*$^{+}$ overexpressing tester males were obtained from one vial), prediction cannot be made based on these numbers. Still, if we halve the average number of progenies produced by the wildtype (that is, 145 progenies on an average), it is still about three folds more than those produced by the *fs(1)Yb*$^{+}$ overexpressing testers (50 progenies on an average). Nevertheless, this is not reliable and so, this experiment would be carried out in a similar setup, using *UAS-FLP nanosGal4*-mediated dicentric formation in the germline. The hypothesis, that *fs(1)Yb*$^{+}$ is eliminating cells with broken chromosome at a pre-meiotic stage, can be tested by dissecting out testes from newly eclosed adult tester males with *fs(1)Yb*$^{+}$ overexpression and scoring the population of primary spermatocytes within single cysts over a time course after dicentric induction. I predict to find a decrease in the number of primary spermatocytes in *fs(1)Yb*$^{+}$ overexpressing males, compared to wildtype.

One way by which *fs(1)Yb*$^{+}$ may act is by inducing the DDR pathway at its downstream. In support, we found that *corp*$^{+}$ overexpression alleviates the

BARTL phenotype produced by *fs(1)Yb*$^{+}$ overexpression. This can be interpreted as, *fs(1)Yb*$^{+}$ overexpression induces a P53-dependent cell death following DNA damage, which is rescued through *corp*$^{+}$ overexpression. Alternatively, it may also suggest that *corp* acts through a pathway independent of *fs(1)Yb*, yet interferes, somewhere downstream, with *fs(1)Yb*-mediated induction of apoptotic phenotype. In order to find out if *fs(1)Yb*$^{+}$ induces apoptotic phenotype in a P53-dependent manner, a BARTL assay of *EP-fs(1)Yb*$^{+}$ in a *p53*$^{5A\text{-}1\text{-}4}$ background can be carried out. Here, I would expect to observe a rescue of eye phenotype, producing large to wildtype-like eyes. To further investigate where exactly does *fs(1)Yb*$^{+}$ fits in the DDR pathway, a BARTL assay of *EP-fs(1)Yb*$^{+}$ can be carried out in a *chk2*$^{-/-}$ background. Further, to study if *EP-fs(1)Yb*$^{+}$-mediated overexpression induces apoptosis, TUNEL or acridine orange staining of imaginal discs of irradiated *fs(1)Yb*$^{+}$ overexpressing larvae can be performed.

Methods and materials

***Drosophila* stock collections.** The Bloomington stocks obtained were: *P{EPgy2}CG2701*^{EY04983} (BL15778), RNAi-*fs(1)Yb* (BL 35301 and BL 35181), RNAi-*piwi* (BL 34866 and BL 33724), RNAi-armi (BL 34789), *P{Gal4-ey.H}4-8* (BL 5535), *P{eyFLP.N}5* (BL5576), *P{EPgy2}CG1632*^{EY03495} (BL 15650). *DcY(H1)* (Kurzhals et al., 2011), *eGUF4.8JD1*, *w; 70FLP10*, and UAS-*hiphop(HRH008H*) were obtained from our laboratory stock collection. The *Yb*^{72} stock was kindly gifted by Dr. Haifan Lin.

Germline fragment chromosome transmission assay. Flies were allowed to lay eggs and transferred to fresh vials every day. Embryos were collected for 24 hrs, heat-shocked at 38°C for 1 hour in a circulating water bath, and then immediately returned to 25°C. After eclosion, the males were collected and singly mated to 2-3 *y w* females and their progeny were scored.

Graphical methods and statistical analyses. Construction of graphs and calculations of statistical significance were performed using Prism 5.0 (Graphpad). The Mann-Whitney test was used.

Figure 19. Overexpression of *fs(1)Yb*$^{+}$ suppresses the BARTL phenotype only after telomere loss. (A) The eye phenotype distribution observed in the BARTL assay. The B^{S} phenotype of *H1* control males is shown at the left. When FLP is expressed (*ey>FLP*), the phenotypes can range from headless pharates (category 1) to adults with a fully developed wildtype eye (category 5). The distribution produced (B) in control males following dicentric induction by *eGUF4.8JD1*; (C) in males carrying *P{EPgy2}EY04983* (BL 15778); (D) in *fs(1)Yb*^{72} mutants; (E, F) RNAi-mediated knockdowns of *fs(1)Yb*; (G, H) when *EP-fs(1)Yb*$^{+}$ is introduced, uninduced (G) and induced (H) into B^{S} flies without dicentric induction; (I) when *EP-fs(1)Yb*$^{+}$ is induced in B^{+} flies without dicentric induction; (J) when *H1* dicentrics are produced in the presence of uninduced *EP-fs(1)Yb*$^{+}$. N represents number of eyes or headless pharates scored for each genotype.

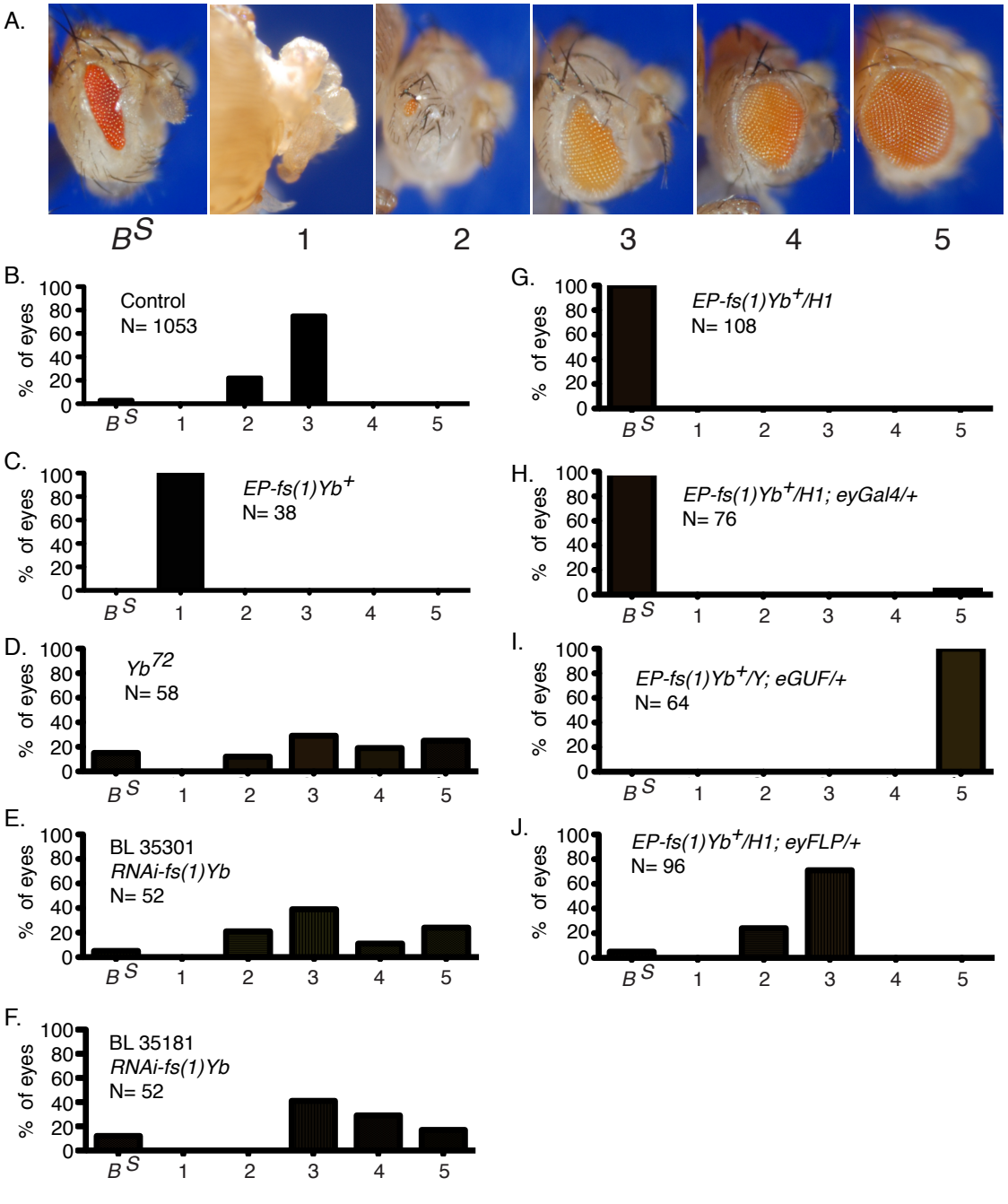
A.
BS
1
2
3
4
5
B.
Control
N= 1053
C.
EP-fs(1)Yb+
N= 38
D.
Yb72
N= 58
E.
BL 35301
RNAi-fs(1)Yb
N= 52
F.
BL 35181
RNAi-fs(1)Yb
N= 52
G.
EP-fs(1)Yb+/H1
N= 108
H.
EP-fs(1)Yb+/H1; eyGal4/+
N= 76
I.
EP-fs(1)Yb+/Y; eGUF/+
N= 64
J.
EP-fs(1)Yb+/H1; eyFLP/+
N= 96
% of eyes
0
20
40
60
80
100

Figure 20. Effect of *corp*$^{+}$ and *hiphop*$^{+}$ overexpression on *fs(1)Yb*$^{+}$-mediated apoptotic phenotype in the BARTL assay. (A) The *fs(1)Yb* genomic region on the *X* chromosome and *fs(1)Yb* transcripts, fs(1)Yb-RA (adapted from FlyBase: http://flybase.org/cgibin/gbrowse2/dmel/?Search=1;name=FBgn0000928). Orange shading denotes the protein coding regions and grey shading denotes the 5' and 3' UTR regions on the *fs(1)Yb* transcript. The blue arrowhead, highlighted by an orange rectangle, indicates the site of the *EY04983 EPgy2* insertion. (B) The *EP-fs(1)Yb*$^{+}$ produces headless pharates in the BARTL assay (reproduced from Figure 14), while (C) *EP-corp*$^{+}$ has the opposite effect, producing flies with wildtype eyes. (D) Co-induction of both is indistinguishable from the *EP-corp*$^{+}$-mediated overexpression. (E) *hiphop*$^{+}$ overexpression produces and wildtype eyes and (F) co-induction of both *fs(1)Yb*$^{+}$ and *hiphop*$^{+}$ is indistinguishable from the *hiphop*$^{+}$ overexpression alone. N represents the number of eyes or headless pharates scored.

A.

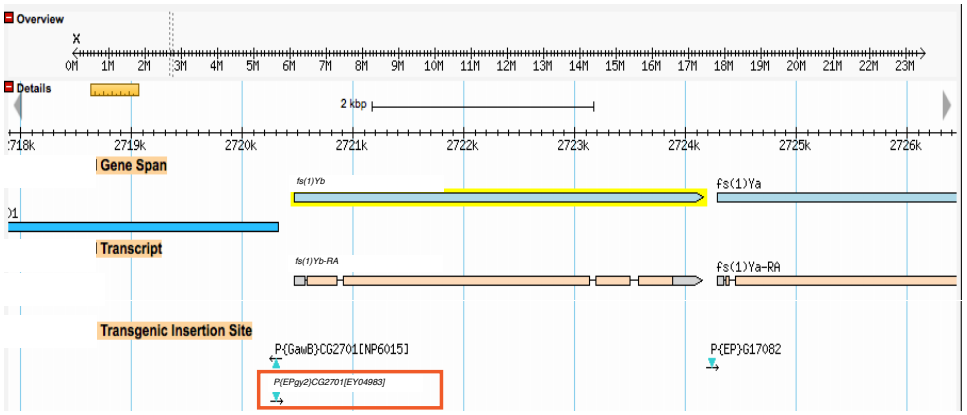
Overview
X
Details
2 kbp
Gene Span
fs(1)Yb
fs(1)Ya
Transcript
fs(1)Yb-RA
fs(1)Ya-RA
Transgenic Insertion Site
P{GawB}CG2701[NP6015]
P{EP}G17082
P{EPgy2}CG2701[EY04983]

B.

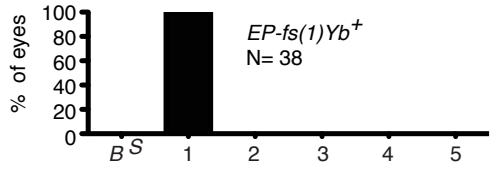
% of eyes
EP-fs(1)Yb+
N= 38
B S 1 2 3 4 5

C.

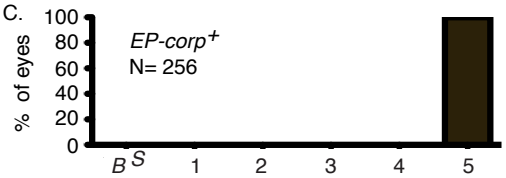
% of eyes
EP-corp+
N= 256
B S 1 2 3 4 5

D.

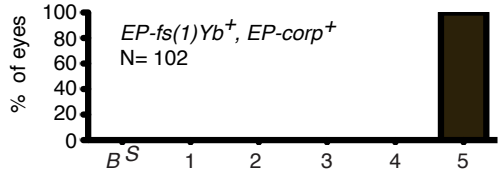
% of eyes
EP-fs(1)Yb+, EP-corp+
N= 102
B S 1 2 3 4 5

E.

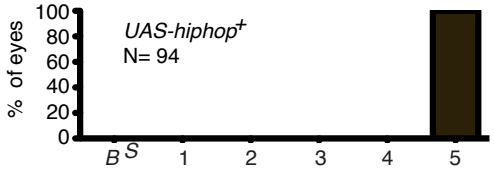
% of eyes
UAS-hiphop+
N= 94
B S 1 2 3 4 5

F.

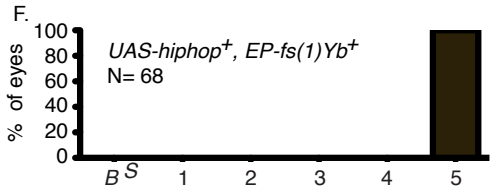
% of eyes
UAS-hiphop+, EP-fs(1)Yb+
N= 68
B S 1 2 3 4 5

Table 6. Effect of *fs(1)Yb*$^{+}$ on transmission of broken-and-healed chromosomes through the male germline.

Genotype	N[a]	Sterility (%)[b]	*FrY* sons	*Y* sons	Fragment Ratio[c] (P value)	Daughters	Sex ratio	Progeny$_{avg}$[d]
y w/H1; 70FLP10/+	341	53	6470	14727	0.31	25476	0.83	291
y w EP-fs(1)Yb^{+}/H1; 70FLP10/+; nosGal4/+	363	26	901	5540	0.14 (P<0.0001)	7208	0.89	50
hjky w EP-fs(1)Yb^{+}/H1; 70FLP10/+; nosGal4/+ (no heat-shock control)	15	20	0	476	0.0	528	0.90	84

[a] N, number of males testcrossed.

[b] Percentage of tested males that were sterile.

[c] Fragment ratio is calculated as *FrY* sons/total sons. *P* values were determined with the Mann-Whitney test using Fragment Ratios of individual males. The *P* value represents comparison with the row immediately above in this table.

[d] Average number of progenies (male+female) produced by each fertile tester male.

Table 7. Effect of *piwi* and *armi* knockdowns/amorphic alleles on BARTL phenotype and on B^S eye phenotype without telomere loss.

Effected gene	RNAi/ amorphic allele[a]	N[b]	BARTL phenotype (%)[c]					
			B^S	1	2	3	4	5
Crossed to *y w/H1; eGUF4.8JD1* (telomere loss)								
piwi	BL 34866	40	0	100	0	0	0	0
	BL 33724	42	0	92	0	0	4	4
armi	BL 34789	55	0	50	7	7	2	34
Crossed to *y w/Y; eyGal4-4.8* (without telomere loss)								
piwi	BL 34866	36	0	100	0	0	0	0
	BL 33724	52	0	0	0	0	50	50
armi	BL 34789	42	0	0	10	10	2	78

[a] RNAi and amorphic stocks are obtained from Bloomington Stock Center (BL).
[b] Numbers of flies scored.
[c] The range of BARTL eye phenotypes are categorized as either B^S or from no eye (category 1) to full grown eye (category 5), as depicted in Figure 14A.

References

Ahmad, K., and Golic, K.G. (1998). The transmission of fragmented chromosomes in Drosophila melanogaster. Genetics *148*, 775–792.

Chen, Y.Y., Pane, A.A., and Schüpbach, T.T. (2007). cutoff and aubergine Mutations Result in Retrotransposon Upregulation and Checkpoint Activation in Drosophila. Curr. Biol. *17*, 6–6.

Cox, D.N., Chao, A., Baker, J., Chang, L., Qiao, D., and Lin, H. (1998). A novel class of evolutionarily conserved genes defined by piwi are essential for stem cell self-renewal. Genes & Development *12*, 3715–3727.

Johnson, E., Wayne, S., and Nagoshi, R. (1995). fs(I) Yb is Required for Ovary Follicle Cell Differentiation in Drosophila melanogaster and Has Genetic Interactions With the Notch Group of Neurogenic Genes. Genetics *140*, 207–217.

Khurana, J.S., Xu, J., Weng, Z., and Theurkauf, W.E. (2010). Distinct functions for the Drosophila piRNA pathway in genome maintenance and telomere protection. PLoS Genet *6*, e1001246–e1001246.

King, F.J.F., and Lin, H.H. (1999). Somatic signaling mediated by fs(1)Yb is essential for germline stem cell maintenance during Drosophila oogenesis. Development *126*, 1833–1844.

King, F.J., Szakmary, A., Cox, D.N., and Lin, H. (2001). *Yb* Modulates the Divisions of Both Germline and Somatic Stem Cells Through *Piwi*- And *Hh*-Mediated Mechanisms in the *Drosophila* Ovary. Mol. Cell *7*, 497–508.

Klattenhoff, C.C., Bratu, D.P.D., McGinnis-Schultz, N.N., Koppetsch, B.S.B., Cook, H.A.H., and Theurkauf, W.E.W. (2007). Drosophila rasiRNA Pathway Mutations Disrupt Embryonic Axis Specification through Activation of an ATR/Chk2 DNA Damage Response. Developmental Cell *12*, 11–11.

Kurzhals, R.L., Titen, S.W.A., Xie, H.B., and Golic, K.G. (2011). Chk2 and p53 are haploinsufficient with dependent and independent functions to eliminate cells after telomere loss. PLoS Genet *7*, e1002103–e1002103.

Megosh, H.B., Cox, D.N., Campbell, C., and Lin, H. (2006). The role of PIWI and the miRNA machinery in Drosophila germline determination. Curr. Biol. *16*, 1884–1894.

Qi, H., Watanabe, T., Ku, H.-Y., Liu, N., Zhong, M., and Lin, H. (2011). The Yb body, a major site for Piwi-associated RNA biogenesis and a gateway for Piwi expression and transport to the nucleus in somatic cells. Journal of Biological Chemistry *286*, 3789–3797.

Saito, K., Ishizu, H., Komai, M., Kotani, H., Kawamura, Y., Nishida, K.M., Siomi,

H., and Siomi, M.C. (2010). Roles for the Yb body components Armitage and Yb in primary piRNA biogenesis in Drosophila. Genes & Development *24*, 2493–2498.

Shoji, M., Tanaka, T., Hosokawa, M., Reuter, M., Stark, A., Kato, Y., Kondoh, G., Okawa, K., Chujo, T., Suzuki, T., et al. (2009). The TDRD9-MIWI2 complex is essential for piRNA-mediated retrotransposon silencing in the mouse male germline. Developmental Cell *17*, 775–787.

Szakmary, A., Reedy, M., Qi, H., and Lin, H. (2009). The Yb protein defines a novel organelle and regulates male germline stem cell self-renewal in Drosophila melanogaster. The Journal of Cell Biology *185*, 613–627.

Thomson, T., and Lin, H. (2009). The biogenesis and function of PIWI proteins and piRNAs: progress and prospect. Annu. Rev. Cell Dev. Biol. *25*, 355–376.

Titen, S.W.A., and Golic, K.G. (2010). Healing of euchromatic chromosome breaks by efficient de novo telomere addition in Drosophila melanogaster. Genetics *184*, 309–312.

Titen, S.W.A., Lin, H.-C., Bhandari, J., and Golic, K.G. (2014). Chk2 and p53 regulate the transmission of healed chromosomes in the Drosophila male germline. PLoS Genet *10*, e1004130–e1004130.

Young, M.W., and Judd, B.H. (1978). Nonessential Sequences, Genes, and the Polytene Chromosome Bands of DROSOPHILA MELANOGASTER. Genetics *88*, 723–742.

CHAPTER 5

MODULATORS OF IRRADIATION SURVIVAL IN *DROSOPHILA MELANOGASTER*

Abstract

Viability to high doses of ionizing radiation was investigated In *Drosophila melanogaster*. Stocks with comparatively clearer genetic backgrounds, derived from the original wildtype laboratory strain showed variable sensitivity to X-ray dose. Females survived better than males following irradiation. The viability of the organisms decreased significantly in a *p53* mutant. Interestingly, a *corp* mutant exhibited a similar effect to the *p53* mutant, that is, decreased organismal viability following irradiation. *corp*$^{+}$ overexpression significantly increased their survival rate, particularly in males.

Introduction

Ionizing irradiation is a widely used method for inducing DNA damage to cells and as a leading anticancer therapy. Organisms are regularly exposed to radiation naturally and thus have evolved mechanisms to survive its detrimental effects. Irradiation causes DNA damage and genomic instability primarily by inducing double-strand breaks, and cells respond to it by activating checkpoints to induce cell cycle arrest and DNA repair, and to trigger apoptosis if the damage is beyond repair (Jackson and Bartek, 2009; Morgan et al., 1996; Sancar et al., 2004; Zhou and Elledge, 2000). These response pathways serve the critical function of maintaining genomic integrity, since widespread genetic instability and abnormality can lead to development of cancer in mammals.

It has been reported that DNA repair is extremely essential for surviving irradiation; cell cycle regulation and apoptosis are neither indispensable nor

sufficient (Jaklevic et al., 2006; Jaklevic and Su, 2004). *mei-41* (*DmATR*) and *okra* (*DmRad54*) mutants that are deficient in DNA repair die as pupae following irradiation, whereas a *grp* (*DmChk1*) mutant that can repair DNA damage but cannot regulate the cell cycle does not. This is possibly because, if cells continue to survive and proliferate with unrepaired DNA, the aberrations spread to the daughter cells and is unhealthy for the organism as a whole. To ensure organismal survival following radiation exposure, cell cycle progression is delayed and repair of DNA breaks commences. Unrepaired cells are removed by apoptosis and compensatory proliferation produces additional cells to maintain tissue integrity and organismal viability (Jaklevic and Su, 2004).

The *p53* tumor suppressor gene is one of the central players that govern adaptive responses to stress and is found to be mutated in most forms of human cancers (Hollstein et al., 1991; Vousden and Lu, 2002). It mediates transcriptional activation of genes that function in DNA repair and apoptosis. *p53* mutants have been found to be sensitive to doses of irradiation (Jaklevic et al., 2006; Jaklevic and Su, 2004; Sogame et al., 2003). This may be because, even though cells are escaping apoptosis in a *p53* mutant following DNA damage, they ultimately die through other stress pathway activation (McNamee and Brodsky, 2009; Titen and Golic, 2008; van Bergeijk et al., 2012; Wichmann et al., 2006) due to a heavy load of unrepaired DNA damage in these cells. As a result, the tissue integrity is lost and the organisms fail to survive.

Here we report that, when tested for their ability to survive a high irradiation dose, stocks with a lesser degree of background genetic variability,

derived from original wildtype laboratory strain, exhibited variable rates of sensitivity between themselves. We found that a *corp* mutant becomes sensitive, similar to the *p53* mutant, and that *corp*$^{+}$ overexpression induces resistance to irradiation in males.

Results and discussion

The original wildtype laboratory strain, *y w*, is extremely sensitive to irradiation. When individuals from our control laboratory strain, *y w*, were irradiated with 4000 rad of X-ray as third instar larvae and scored for rate of eclosure as adults, we found that they are extremely sensitive to irradiation: only 8% eclose (Figure 21). This outcome was surprisingly different from previous reports on irradiation survival of wildtype laboratory strains: survival rates of wildtype strains are significantly better than our result, nearing 60% survival on an average (Jaklevic et al., 2006; Jaklevic and Su, 2004; Sogame et al., 2003). Moreover, we found that *p53*$^{5A\text{-}1\text{-}4}$ mutants exhibited 44% irradiation survival, higher than the *y w* control (Figure 21). This was again in contrast to that reported before: *p53* mutants make flies sensitive to irradiation (Jaklevic and Su, 2004; Sogame et al., 2003). We speculated that these vast differences in the results could be due to unrecognized background mutations that have accumulated over time in the stock. The best way to approach this conflict was to diminish any genetic variability between the individuals of a single stock by building stocks with a genetically uniform background, or at least one closer to uniformity, except for the introduction of desired mutations or transgenes.

Background-reduced stocks, built from the original laboratory strain, *y w*, show significant variation in sensitivity to irradiation. To investigate the high sensitivity of our *y w*, I generated several lines with reduced background variation, by setting up several single male to single female crosses and maintaining them over generations. These derivative lines were called *y* w_{BR}, where BR stands for background reduced. I tested the *y* w_{BR} lines individually for survival rates following exposure to irradiation. Interestingly, I found that the irradiation survival rates of all the tested *y* w_{BR} lines improved over that of the original *y w* stock, and also vary significantly between themselves (Figure 22). Of these, *y* w_{BR3} line showed a median effect and so, I chose *y* w_{BR3} line for further experimental procedures. Males were found to be more sensitive than females to irradiation in all *y* w_{BR3} lines, a well-known phenomenon that can be accounted for by the hemizygosity of the *X* chromosome in males.

Background-reduced *p53*$^{5A-1-4}$ is more sensitive to irradiation. We next introgressed *p53*$^{5A-1-4}$ mutant strain into the *y* w_{BR3} background in order to give it a genetic background equivalent to that of *y* $w_{BR3,}$ except for the deletion of the *p53* gene region (henceforth referred to as *y* w_{BR3}; *p53*$^{5A-1-4}$). When tested for irradiation survival, we found that *y* w_{BR3}; *p53*$^{5A-1-4}$ homozygous mutants become sensitive to irradiation, similar to previous reports (Figure 23). However, the rate of survival of *y* w_{BR3}; *p53*$^{5A-1-4}$/+ heterozygotes is not significantly different from that of *y* w_{BR3} wildtype controls, suggesting that losing a single copy of the *p53* gene does not sensitize them to irradiation (Figure 23). Since ubiquitous *p53*

overexpression by *Actin-Gal4* or heat-shock inducible *Gal4* kills the organism, they could not be used for testing irradiation survival.

Thus, by reducing unrecognized background effects, our results of irradiation survival of wildtype and *p53* mutant strains become comparable with previously reported data.

***corp*$^{+}$ promotes survival of males after exposure to irradiation.** We next tested whether *corp* alters survival rates following irradiation. Since we have previously shown that *corp* is a negative regulator of *p53*, we thought that the *corp* mutant might produce an opposite effect to that of *p53* on organismal viability following irradiation. Interestingly, we found that the *corp*^{95B} mutant, like the *p53* mutant, is sensitive to irradiation (Figure 24A,B). However, another *corp* mutant, *corp*^{1A}, failed to reproduce the result produced by *corp*^{95B}: it did not change survival rate, compared to wildtype (Figure 24B). This can be explained by the possibility that *corp*^{1A} may not be a mutant at all, as verified by mapping for deletion of the genomic region in *corp*^{1A} by PCR. My PCR results indicate that virtually no part of *corp* is missing in *corp*^{1A} (Figure 24C-E). So, the *corp*^{1A} irradiation survival result cannot be trusted with regard to accounting for how a *corp* null allele behaves. Further, it is to be noted that the two *corp* mutants were not introgressed into the *y* w_{BR3} background. So, the possible effect of background variability between the control and the mutants on irradiation survival cannot be overlooked. One way to address this problem is to construct a *corp* mutant in a *y* w_{BR3} background. This project is currently underway by others in the lab.

In order to verify the effects of *corp*^{95B} on irradiation survival, I next wanted to see if *corp*$^{+}$ overexpression produces an opposite effect to that produced by *corp*^{95B}. I ubiquitously overexpressed *EP-corp*$^{+}$ by the *Actin-Gal4* driver and tested for organismal viability following irradiation. The *EP-corp*$^{+}$ and the *Actin-Gal4* lines were introgressed into the *y* w_{BR3} background to maintain the homogeneity of the genetic background of all the lines that were being tested. I found that *corp* overexpression makes the males significantly more resistant to irradiation and enhances their survival rate, compared to the controls (Figure 25, Table 8). In females, however, it does not show any effect (Figure 25, Table 8). This leads to the question of why *corp*$^{+}$ helps only the males to survive better to irradiation. Is there a possibility of background suppressors that are playing a role here affecting female survival? Or, does it unveil an unknown characteristic feature of *corp*? These questions necessitate the generation of an isogenic background where all the genes would have a single allele and no variation, unless otherwise introduced.

Nevertheless, the disparate effects of *p53* and *corp*$^{+}$, at least in males, on survival rate following irradiation-induced DNA damage may be explained in a number of ways. *p53* mutants are sensitive to irradiation because the DNA repair pathway is blocked in them and the DNA repair pathway genes have been reported to be essential for irradiation survival (Jaklevic et al., 2006; Jaklevic and Su, 2004). Interestingly, it has been found in mammalian cells that UV-radiation exposure induces P53 expression in a dose-dependent manner and a lower P53 expression level correlates with transcription of DNA damage repair genes while

a higher dose of P53 is required for transcription of pro-apoptotic genes (Latonen et al., 2001; Li and Ho, 1998). In this vein, it can be reasoned that *corp*$^{+}$ overexpression-mediated downregulation of P53 significantly reduces its levels so that it cannot induce apoptosis; however, the residual level of P53 that still persists may be adequate to induce DNA repair. That may lead to an increased survival rate. Another possible explanation of the *corp*$^{+}$- mediated increased organismal viability is that the *corp*$^{+}$- mediated P53 downregulation delays apoptosis that gives the DNA repair machinery extra time to repair the damaged genome and save the cells, thus enhancing adult eclosure rate. Alternatively, it can also be hypothesized that *corp* has other targets besides *p53* and that the role of *corp* in irradiation survival may be mediated through these targets, for example, through downregulation of inhibitors of the DNA repair pathway.

Future experiments

1. Generate an isogenic *y w* stock, introgress all transgenes and mutants tested in that background, and recheck irradiation survival data.

2. If *corp*$^{+}$-induced irradiation resistance result still holds true, then test if *corp*$^{+}$ overexpression can still enhance organismal survival in a *p53* mutant background: *EP-corp*$^{+}$*; UAS-GFP Actin-Gal4; p53*$^{5A\text{-}1\text{-}4}$.

3. Test if *corp*$^{+}$ induces DNA repair: Irradiate *EP-corp*$^{+}$ overexpressing larvae at 200 rads, dissect their wing and eye imaginal discs over a time-course after irradiation, and stain with H2AγX, marker of DNA damage. I would expect to find a decrease in H2AγX staining in *corp*$^{+}$ overexpressing discs. Verify if a

decrease in staining is displayed by the *corp*^{95B} mutant. Next, this experiment can be performed in a *p53* mutant background, to check if *corp*$^{+}$ induces DNA repair in a P53-independent way.

4. To find out genes that are upregulated or downregulated by *corp* induction without and after DNA damage: Generate a RNAseq data of *corp*$^{+}$ overexpressing and *corp*^{95B} lines with and without irradiation treatment. I would expect to find many targets of *corp* other than *p53*.

Materials and methods

***Drosophila* stock collections.** Construction of *p53*$^{5A\text{-}1\text{-}4}$ has been described previously (Xie and Golic, 2004).The Bloomington stock used was *P{EPgy2}CG1632*^{EY03495} (BL 15650). The following lines were obtained from our laboratory collection: *y w*, *y w; UAS-GFP Actin-Gal4/CyO* and *y w; Sb/TM6, Ubx*.

Constructing lines with lesser background variability. 11 batches of single male to single female crosses from the original *y w* laboratory stock were carried out to build up *y w* lines with lesser degree of background variability (referred to as *y* $w_{BR1\text{-}11}$) and were maintained thereafter. Then, *y w EP-corp*$^{+}$, *y w; UAS-GFP Actin-Gal4/CyO*, and *y w; p53*$^{5A\text{-}1\text{-}4}$ strains were introgressed into the *y* w_{BR3} reduced background strain in a manner similar to making recombinant inbred lines. Briefly, *y w EP-corp*$^{+}$, *y w; UAS-GFP Actin-Gal4/CyO* females were crossed to *y* w_{BR3}*/Y* males; from the progenies, *y w EP-corp*$^{+}$*/ y* w_{BR3}, *y w/ y* w_{BR3}*; UAS-GFP Actin-Gal4/+*, and *y w/ y* w_{BR3}*; +/CyO* virgins were collected and were crossed to *y* w_{BR3}*/Y* males repeatedly for 5 generations. The undisrupted

presence of the transgenes in successive generations was verified by the w^+ eye color marker for *EP-corp*$^+$ and the GFP fluorescence for *UAS-GFP Actin-Gal4*. The transgenic lines, introgressed into the isogenic background, were henceforth referred to as *y* w_{BR3} *EP-corp*$^+$ and *y* w_{BR3}*; UAS-GFP Actin-Gal4/CyO*. Since *y w;* $p53^{5A\text{-}1\text{-}4}$ is not phenotypically marked, it could be directly introgressed into *y* w_{BR3}. So, *y w; Sb/TM6, Ubx* was first introgressed into *y* w_{BR3} line for 3 generations in the same way as described above, and then *y w;* $p53^{5A\text{-}1\text{-}4}$ was further introgressed into *y* w_{BR3}*; Sb/TM6, Ubx* for another three generations. In each generation, *y w/y* w_{BR3}*;* $p53^{5A\text{-}1\text{-}4}$*/TM6, Ubx* virgins, marked by *Sb*$^+$ *Ubx* were collected and then crossed to *y* w_{BR3}*/Y; Sb/TM6, Ubx* males.

Irradiation. 15-18 wandering third instar larvae were collected in clean 10 mm petri plates and irradiated at 4000 rads in a TORREX120D X-ray generator (Astrophysics Research Corp, CA), set at 110kV and 5mA. The base of the petri plates was either covered with a moistened Whatmann or construction paper (to ensure that the larvae are not drying up quickly) or was without a cover. These larvae were returned to fresh food and incubated at 25°C until further experimental treatments.

Calculating irradiation viability. Irradiated larvae were returned to food and incubated at 25°C and allowed to eclose. All the eclosed individuals were counted, including the ones that got stuck to the food and died. Since the flies had spread-out wings as a result of irradiation exposure and could not fly well, getting stuck to the food was a commonly observed phenomenon. Rate of irradiation viability and sex ratios were calculated.

PCR. Deletions of the genomic region in the corp mutants were mapped by PCR amplification of genomic DNA isolated from the adult flies of homozygous mutants. Primer sets used: FW 1: 5'CCAAGCGAACGCATCGCTG3', FW 2: 5'GAAGAGGTCATCTCCCAAGG3', RV1: 5'CTTAGGAACAATGGTTCAACC3' and RV2: 5'GCAGCCGAGGTATGGAAATC3'.

Graphical methods and statistical analyses. Construction of graphs and calculations of statistical significance were performed using Prism 5.0 (Graphpad). The contingency test was used in all cases.

Figure 21. *p53*$^{5A-1-4}$ null mutant survives better than original laboratory *y w* strain following irradiation. Rate of irradiation survival was measured as the ratio of eclosed adults to total number of irradiated larvae. The graph represents percentage of viability of *y w* laboratory strain and *p53*$^{5A-1-4}$, with (pink) and without (yellow) irradiation (IR). The larvae were irradiated at 4000 rads. L3, number of larvae irradiated. Irradiation was performed in empty petriplates without a moistened paper.

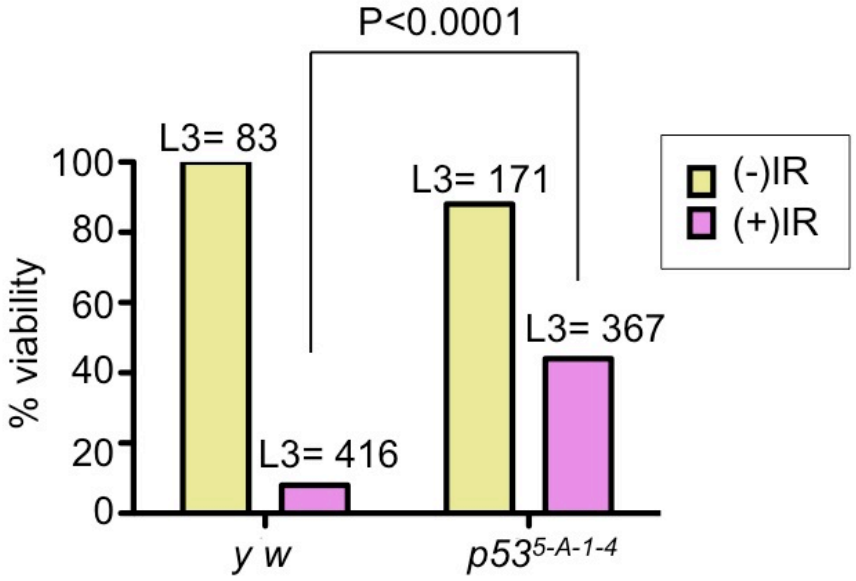
P<0.0001
L3= 83
L3= 416
L3= 171
L3= 367
100
80
60
40
20
0
% viability
(-)IR
(+)IR
y w
p53 5-A-1-4

Figure 22. *y* w_{BR} stocks differ in irradiation sensitivity. The graph represents the percent viability of five background-reduced (BR) stocks in males to females, with and without irradiation exposure. Color-coding for individual categories are shown in the inset. L3, total number of larvae irradiated; N, total number of adults eclosed. *P* values are presented for variability of viability rates between the irradiated *y* w_{BR} stocks, only where statistically significant. Larval irradiation was performed in petriplates coated with a moistened Whatmann paper.

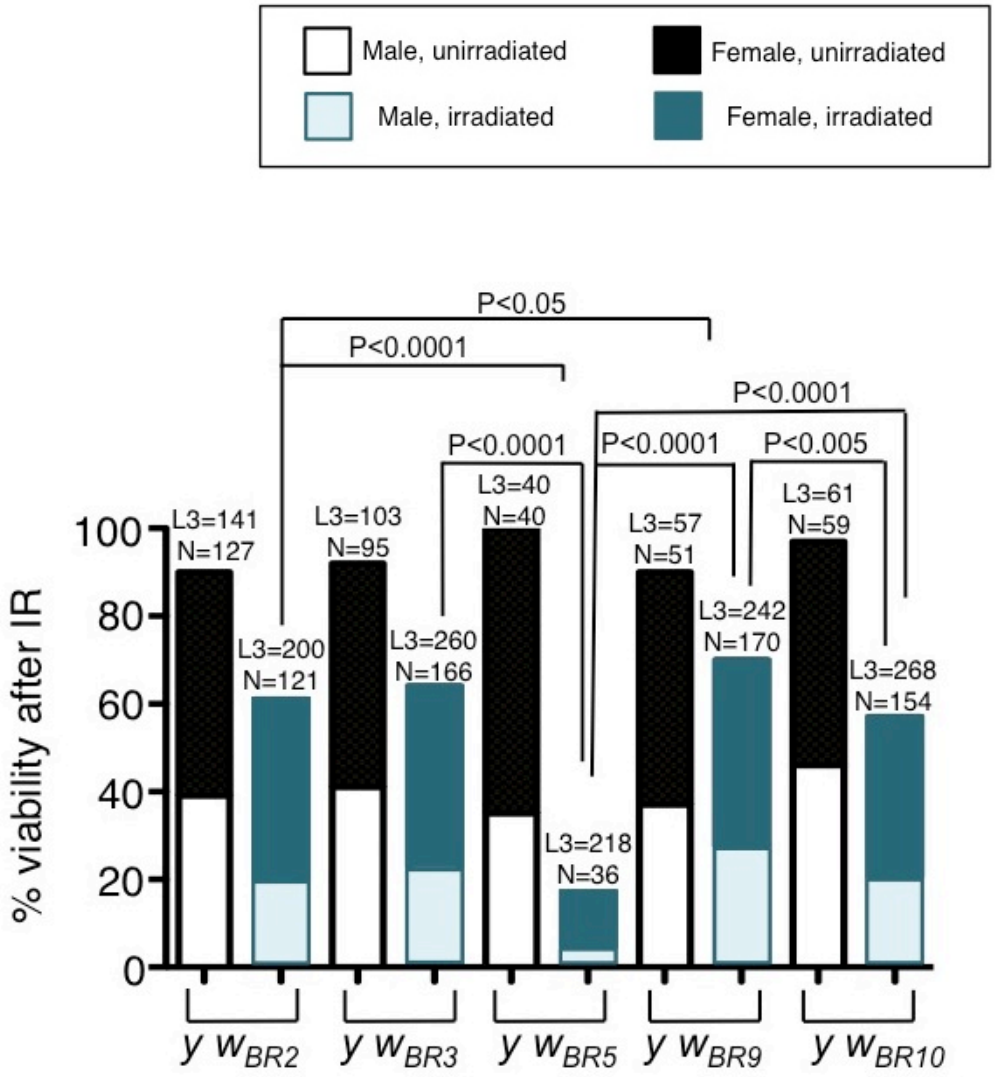
Male, unirradiated
Female, unirradiated
Male, irradiated
Female, irradiated
P<0.05
P<0.0001
P<0.0001
P<0.0001
P<0.0001
P<0.005
% viability after IR
100
80
60
40
20
0
L3=141
N=127
L3=200
N=121
L3=103
N=95
L3=260
N=166
L3=40
N=40
L3=218
N=36
L3=57
N=51
L3=242
N=170
L3=61
N=59
L3=268
N=154
y w BR2
y w BR3
y w BR5
y w BR9
y w BR10

Figure 23. The *y* w_{BR3}; $p53^{5A-1-4}$ null mutation sensitizes organisms to irradiation. Percent viability of males (black) to females (white) in yw_{BR3} and yw_{BR3}; $p53^{5A-1-4}$ homozygotes and heterozygotes is presented in graph. L3, total number of larvae irradiated; N, total number of adults eclosed. Larval irradiation was performed in petriplates coated with a moistened Whatmann paper.

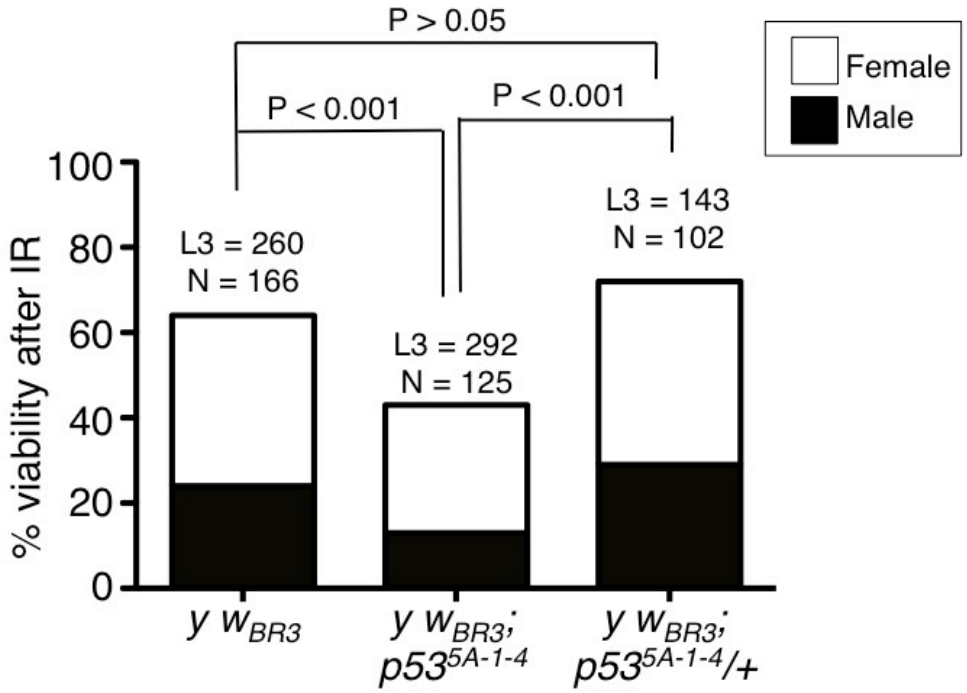
P > 0.05
P < 0.001
P < 0.001
Female
Male
% viability after IR
100
80
60
40
20
0
L3 = 260
N = 166
L3 = 292
N = 125
L3 = 143
N = 102
y w BR3
y w BR3; p53 5A-1-4
y w BR3; p53 5A-1-4/+

Figure 24. *corp*^{95B} mutants are sensitive to irradiation. (A) Percent viability of *corp*^{95B} with and without larval exposure to irradiation (IR), in empty petriplates without a moistened paper.
(B) In a second set of experiments, sex ratio of eclosed male to female progenies from four different crosses is presented in the graph. In this set, irradiation of larvae was performed on moistened paper coated petriplates. Two corp mutant lines, *corp*^{95B} and *corp*^{1A}, the *EP-corp*$^{+}$ and the *y* w_{BR3} males were individually crossed to *C(1)Dx/Y* females, such that all the male progenies inherit the *X* chromosome from their dad and the female progenies receive the *C(1)Dx* chromosome from their mom, ensuring that any effect on irradiation viability due to the mutant or the transgenic backgrounds would remain confined only to the male progenies. Sex ratio from the nonirradiated control cross, *corp*^{95B} x *C(1)Dx/Y* is also presented. L3, total number of larvae irradiated; N, total number of adults eclosed. Statistical significance calculated is presented in Table 8.
(C-E) Identifying deleted genomic regions of *corp* mutants. Genomic regions of *corp* and its neighboring gene, *CG1632*, are denoted along the length of the DNA. Black rectangles: exons, black connecting line: intron. Arrow denotes the direction of transcription of the genes. *corp* is located within the intron of *CG1632*. Genomic deletions of *95B* and *1A* corp mutants are identified by PCR amplification of *corp* genomic region. Primer pairs used: FW1, RV1, and FW2, RV2. Amplified products were run on the four lanes of a gel, marked 1 through 4: (1) *y w*; (2) *corp*^{1A}; (3) *corp*^{95B}; and (4) a third *corp* mutant. Both primer sets fail to detect any amplicon in *corp*^{95B}, while presence of an amplicon, similar in size to that of *y w* wildtype control, is detected in *corp*^{1A} by FW2, RV2. M1 is a 1 kb ladder and M2 is the 100 bp ladder. The horizontal red arrowhead points to the size expected in the *y w* control.

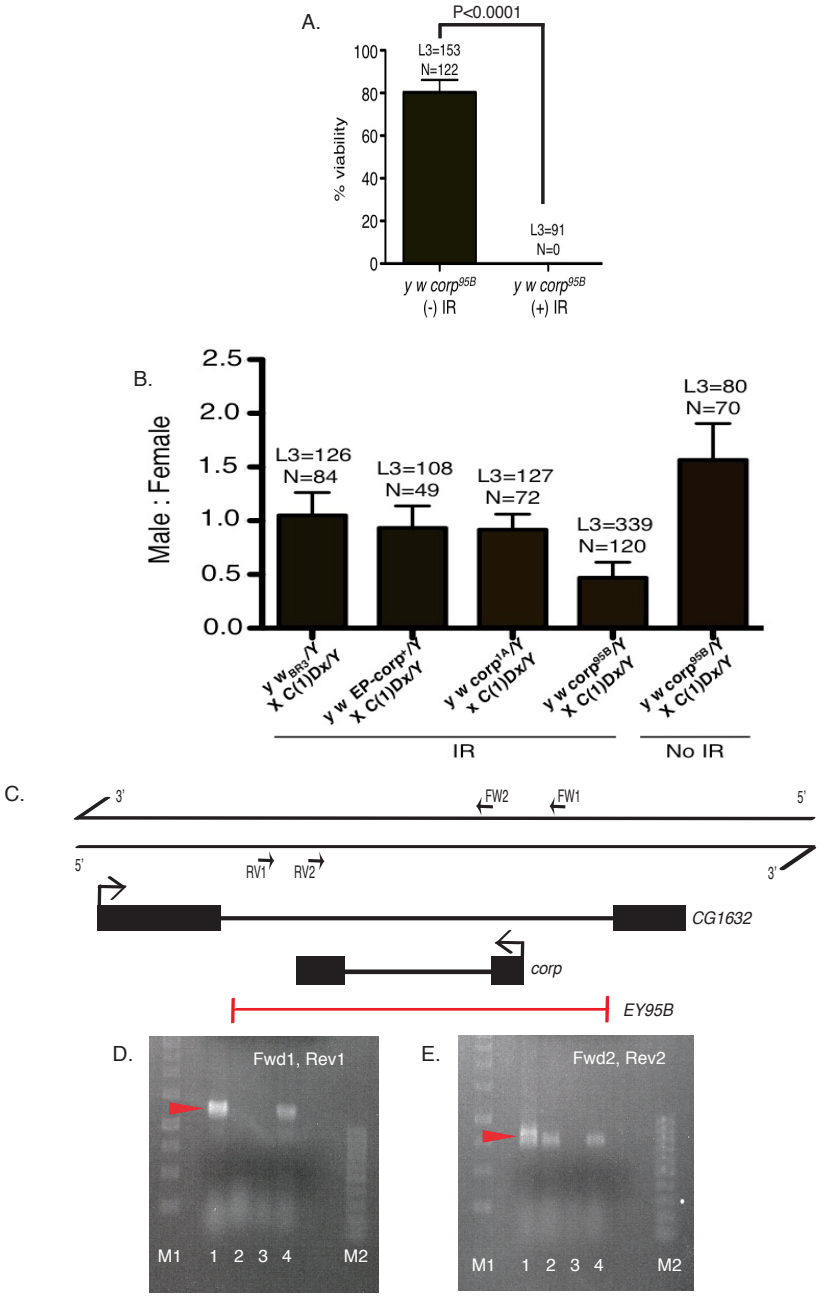
A.
P<0.0001
L3=153
N=122
L3=91
N=0
% viability
y w corp95B
(-) IR
y w corp95B
(+) IR
B.
Male : Female
L3=126
N=84
L3=108
N=49
L3=127
N=72
L3=339
N=120
L3=80
N=70
IR
No IR
C.
3'
5'
FW2
FW1
RV1
RV2
CG1632
corp
EY95B
D.
Fwd1, Rev1
M1 1 2 3 4 M2
E.
Fwd2, Rev2
M1 1 2 3 4 M2

Figure 25. *corp*$^{+}$ overexpression helps males to survive irradiation exposure. Percent viability of all the progeny classes from three different crosses (color-coded in the inset) are presented in the graph. The crosses are- (1) *y* w_{BR3}*/Y; UAS-GFP Actin-Gal4/CyO* x *y* w_{BR3} (Column 1: blue), (2) *y* w_{BR3}*/Y; UAS-GFP Actin-Gal4/CyO* x *y* w_{BR3} *EP-corp*$^{+}$ (Column 2: yellow), and (3) *y* w_{BR3} *EP-corp*$^{+}$*/Y* x *y* w_{BR3}*; UAS-GFP Actin-Gal4/CyO* (Column 3: pink), where *corp*$^{+}$ is overexpressed in none of the blue progeny classes, both yellow *Cy*$^{+}$ males and females and only pink *Cy*$^{+}$ females. L3, total number of larvae irradiated from each cross; N, total number of adults eclosed from each cross. Data are represented as mean + SEM. Statistical significance calculated is presented in Table 8.

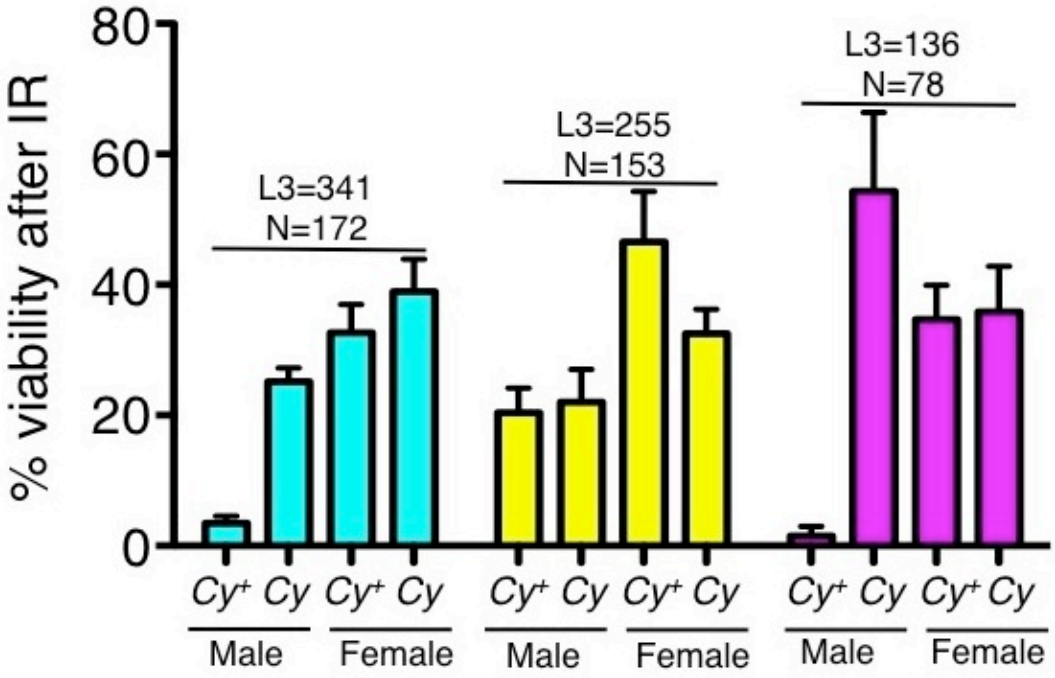
% viability after IR
80
60
40
20
0
L3=341
N=172
L3=255
N=153
L3=136
N=78
Cy+ Cy Cy+ Cy Cy+ Cy Cy+ Cy Cy+ Cy Cy+ Cy
Male Female Male Female Male Female

Table 8. Statistical significance of *corp* mutant or *corp*$^{+}$ overexpression-mediated variation of irradiation survival.

A. Experiment: *corp* mutant irradiation survival (Figure 19)					
Parameter compared: Proportion of eclosed males of the total larvae irradiated					
Crosses		**+ IR**			**- IR**
		***corp*^{1A}/Y x C(1)Dx**	***EP-corp*$^{+}$/Y x C(1)Dx**	***y w*$_{BR3}$/Y x C(1)Dx**	***corp*^{95B}/Y x C(1)Dx**
+ IR	***corp*^{95B}/Y x C(1)Dx**	P<0.0001	P<0.0004	P<0.0001	P<0.0001
	***EP-corp*$^{+}$/Y x C(1)Dx**	P>0.05	-	P>0.05	-

B. Experiment: *corp*$^{+}$ overexpression irradiation survival (Figure 20)		
1. Parameter compared: Proportion of eclosed *Cy*$^{+}$ to *Cy* males		
Parameters	**Column 1**	**Column 3**
Column 2	P<0.0001	P<0.0001
Column 3	P>0.05	-
2. Parameter compared: Proportion of eclosed *Cy*$^{+}$ to *Cy* females		
Parameters	**Column 1**	**Column 3**
Column 2	P>0.05	P>0.05
Column 3	P>0.05	-
3. Parameter compared: Proportion of *Cy*$^{+}$ eclosed males of the total larvae irradiated		
Parameters	**Column 1**	**Column 3**
Column 2	P<0.0001	P<0.0002
Column 3	P>0.05	-
4. Parameter compared: Proportion of *Cy*$^{+}$ eclosed females of the total larvae irradiated		
Parameters	**Column 1**	**Column 3**
Column 2	P>0.05	P>0.05
Column 3	P>0.05	-

Note. Statistical significance is calculated between two classes of crosses or parameters, as indicated row-wise and column-wise.

References

Hollstein, M., Sidransky, D., Vogelstein, B., and Harris, C.C. (1991). p53 mutations in human cancers. Science *253*, 49–53.

Jackson, S.P., and Bartek, J. (2009). The DNA-damage response in human biology and disease. Nature *461*, 1071–1078.

Jaklevic, B., Uyetake, L., Lemstra, W., Chang, J., Leary, W., Edwards, A., Vidwans, S., Sibon, O., and Tin Su, T. (2006). Contribution of Growth and Cell Cycle Checkpoints to Radiation Survival in Drosophila. Genetics *174*, 1963–1972.

Jaklevic, B.R., and Su, T.T. (2004). Relative contribution of DNA repair, cell cycle checkpoints, and cell death to survival after DNA damage in Drosophila larvae. Curr. Biol. *14*, 23–32.

Latonen, L., Taya, Y., and Laiho, M. (2001). UV-radiation induces dose-dependent regulation of p53 response and modulates p53-HDM2 interaction in human fibroblasts. Oncogene *20*, 6784–6793.

Li, G., and Ho, V.C. (1998). p53-dependent DNA repair and apoptosis respond differently to high- and low-dose ultraviolet radiation. British Journal of Dermatology *139*, 3–10.

McNamee, L.M., and Brodsky, M.H. (2009). p53-Independent Apoptosis Limits DNA Damage-Induced Aneuploidy. Genetics *182*, 423–435.

Morgan, W.F., Day, J.P., Kaplan, M.I., McGhee, E.M., and Limoli, C.L. (1996). Genomic Instability Induced by Ionizing Radiation. Radiat Res *146*, 247–258.

Sancar, A.A., Lindsey-Boltz, L.A.L., Unsal-Kaçmaz, K.K., and Linn, S.S. (2004). Molecular mechanisms of mammalian DNA repair and the DNA damage checkpoints. Biochemistry *73*, 39–85.

Sogame, N., Kim, M., and Abrams, J.M. (2003). Drosophila p53 preserves genomic stability by regulating cell death. Proc. Natl. Acad. Sci. U.S.a. *100*, 4696–4701.

Titen, S.W.A., and Golic, K.G. (2008). Telomere Loss Provokes Multiple Pathways to Apoptosis and Produces Genomic Instability in Drosophila melanogaster. Genetics *180*, 1821–1832.

van Bergeijk, P., Heimiller, J., Uyetake, L., and Su, T.T. (2012). Genome-Wide Expression Analysis Identifies a Modulator of Ionizing Radiation-Induced p53-Independent Apoptosis in Drosophila melanogaster. PLoS ONE *7*, e36539.

Vousden, K.H., and Lu, X. (2002). Live or let die: the cell's response to p53. Nat. Rev. Cancer. *2*, 594–604.

Wichmann, A., Jaklevic, B., and Su, T.T. (2006). Ionizing radiation induces caspase-dependent but Chk2- and p53-independent cell death in Drosophila melanogaster. Proc. Natl. Acad. Sci. U.S.a. *103*, 9952–9957.

Xie, H.B., and Golic, K.G. (2004). Gene Deletions by Ends-In Targeting in Drosophila melanogaster. Genetics *168*, 1477–1489.

Zhou, B.-B.S., and Elledge, S.J. (2000). The DNA damage response: putting checkpoints in perspective. Nature *408*, 433–439.

CHAPTER 6

DEFINED GENETIC PATHWAYS TO SURVIVE IRREPARABLE DNA DAMAGE: MAKING SENSE OF IT

Chromosomal rearrangements may promote mutation or loss or altered regulation of essential genes at or near the breakpoints and duplication or deletion would alter the gene dosage. If any of these events hinder the checkpoint or apoptotic pathway components, it would heighten the probability of survival of cells with unrepaired damage, thus precipitating the event of carcinogenesis. For example, by blocking the downstream effectors in the apoptotic pathways, the cells survive better (Colombani et al., 2006; Kurzhals et al., 2011; Peters et al., 2002; Titen and Golic, 2008). Our findings suggest that *fs(1)Yb*$^{+}$ plays a role in eliminating cells that have lost a telomere (Chapter 4). So, if *fs(1)Yb* is mutated, cells with a damaged genome may continue to survive, eventually enhancing genomic instability in the organism. On the other hand, there are components that directly promote suppression of cell death and upregulation of their levels would also increase cell survival and potentiate genome instability. For instance, we demonstrated that *corp*$^{+}$ overexpression exhibits anti-apoptosis by downregulating P53 levels (Chapter 3).

We have demonstrated the existence of two distinct pathways under p53 with opposite modes of function: the *hid*-, *reaper*-mediated pro-apoptotic pathway and *corp*-mediated anti-apoptotic pathway. Thus, it is intriguing that p53 can induce two apparently opposing functions. Previous works have reported that the different isoforms of p53 differentially regulate apoptosis and apoptosis-induced proliferation (Dichtel-Danjoy et al., 2012). It is yet to be found out if the pro-apoptotic (for example, *hid*) and anti-apoptotic (for example, *corp*) effectors of *p53* are also differentially regulated by the isoforms of *p53*. The different

functional consequences of P53 may also emerge from the multiple post-translational modifications of P53, including phosphorylation, acetylation, sumoylation that participate in controlling its function (Gatz and Wiesmüller, 2006; Mauri et al., 2008).

It is important to note that merely allowing cells to survive withstanding DNA damage by blocking the death inducers would not propagate a healthy living environment at the systemic level; it would affect the survival of the organism eventually through causing widespread genomic aberrations. In support, we found, similar to that reported previously (Jaklevic et al., 2006; Jaklevic and Su, 2004), that *p53* mutants are more sensitive to exposure to irradiation (Chapter 5). Even though $p53^{+}$-mediated apoptosis is blocked in these organisms, the load of an unstable genome, produced by blocking $p53^{+}$-mediated DNA repair, drives them to eventually die through aneuploidy-mediated and other p53-independent cell-death mechanisms (McNamee and Brodsky, 2009; Titen and Golic, 2008; van Bergeijk et al., 2012; Wichmann et al., 2006). So, some mode of permanently stemming the damaged DNA is desired to survive the loss.

This can be achieved by a third way where cells add a new telomere complex to the broken end, which cannot be otherwise repaired. Irreparably broken ends in the germline have been previously shown to be fixed by means of this mechanism in the male germline of *Drosophila* (Ahmad and Golic, 1998; Titen and Golic, 2010). In fact, seminal works by Barbara McClintock in the germline of maize showed that when a broken chromosome was delivered by the sperm to the egg, the breakage-fusion-bridge cycle continued in the endosperm

but ceased in the zygote, where it behaved as though it was healed at the broken end (McClintock, 1941). *De novo* telomere addition was also reported as a mechanism to rescue cells in yeast induced with dicentric-mediated chromosome break (Jager and Philippsen, 1989). The analogy between McClintock's findings in plant with that in yeast and *Drosophila* is quite obvious and a parallel to these phenomena is observed in mammals in the context of functional telomerase expression in the germline, suggesting that a telomere can be reconstituted at the broken end (Gao et al., 2008; Shay and Wright, 2001). The intervening steps between generation of a broken chromosome in the germline and recovery of a healed chromosome in the progeny are only partially characterized. Unpublished work from our lab by Dr. Rebeccah Kurzhals characterized a gene, *hiphop*, that plays a distinct role in inducing *de novo* telomere addition, resulting in suppression of apoptotic phenotype in the BARTL assay and highly increasing the rate of broken-and-healed chromosome transmission through the germline. As for the existence of the chromosome healing pathway in the soma, initial works reported the addition of new telomeres at the end of double-strand breaks in mouse embryonic stem cells and terminally deleted chromosomes in human lymphoblastoid cells lines (Flint et al., 1994; Sprung et al., 1999). However, telomerase was active in both the stem cells and tumor-derived cell line, which played a role in reconstituting the telomeric end. Some preliminary works in *Drosophila* show the possibility of somatic existence of chromosome healing (Sergio Pimpinelli, personal communication). Moreover, the fact that *hiphop*$^{+}$ produces wildtype-like eyes in the BARTL assay also supports the theory of

somatic *de novo* telomere addition. However, chromosome healing in the soma has not yet been well established or documented. Nevertheless, aberrant addition of *de novo* telomeres at broken, nontelomeric ends of chromosomes can also be proved deleterious by hindering DNA repair and leading to aneuploidy. Studies in yeast have shown that ATR mediates repression of telomerase function in response to DNA DSBs (Makovets and Blackburn, 2009; Zhang and Durocher, 2010).

Following extensive cell death, tissue recovery can also be mediated through compensatory proliferation of the neighboring cells triggered by the apoptotic cells, so that the organism can survive without compromising development. The longer that dying cells persist, the greater is the signal for compensatory proliferation to the surrounding cells. To date, multiple groups have reported the phenomenon of apoptosis-induced compensatory proliferation (Fan and Bergmann, 2008; Huh et al., 2004; Ryoo et al., 2004; Warner et al., 2010; Wells et al., 2006), although it is mostly the surrounding unaffected cells that proliferate to make up for the dead cells. Recent results demonstrated that dying cells signal other cells at their vicinity to become resistant to radiation-induced cell death by activation of an anti-apoptotic microRNA (Bilak et al., 2014). All these processes preserve tissue integrity and hence organismal survival.

Cell fate decisions: an important juncture

At the end, our findings, together with those previously reported by others, point to the fact that there are defined pathways that control the cell fate decisions following irreparable damage, both towards living and towards dying. So now the question is what are the deciding factors of a cell's ultimate destiny? The answer appears to lie in the tight control of a very complex gene regulatory network. My results can be encompassed to implicate multiple genes and levels of control in the regulation of recovery from tissue damage (Figure 26). Following telomere loss, the ATM and Chk2 activate *p53* to induce apoptosis. P53 also induces *corp* that acts on it in a negative feedback loop to protect the tissue from the deleterious effect of excessive cell death. The *fs(1)Yb*$^{+}$ plays a role in transposon silencing by ensuring the precise localization of Piwi and Armi proteins and piRNA generation. Telomere integrity has been found to be disrupted, probably through transposon desilencing in *piwi* pathway mutants, which also activates DDR genes (Chen et al., 2007; Khurana et al., 2010; Klattenhoff et al., 2007). Thus, it might look intriguing that being an upstream component, *fs(1)Yb*$^{+}$, when overexpressed induces DDR phenotype, like *piwi* pathway mutants. This can be explained by the hypothesis that an optimum level of Fs(1)Yb is necessary for correct localization and function of Armi and Piwi, and that both an upregulation and a downregulation would disrupt the protein localization process and produce similar disintegrated chromosome ends to trigger DDR. This possibility is open to investigation. It is also yet to be found out where exactly does the *fs(1)Yb* feed into the DDR pathway. Since we found that

corp^{+} is epistatic to *fs(1)Yb*$^{+}$, *fs(1)Yb* should be somewhere upstream to it, probably inducing a *p53*-dependent cell death. The apoptotic delay caused by *corp* may provide a window for allowing *de novo* telomere addition (for instance, by *hiphop* activation) or triggering compensatory cell proliferation pathway.

Thus, putting in a nutshell, it is essential that all these components must interact properly to ensure that healthy cells are encouraged and allowed to proliferate, and cells with damaged genomes are eliminated. An integral part of recovering from tissue injury is a tight balance: the intrinsic capability to repair and regenerate without succumbing to massive cell death, but not totally blocking cells from dying and accumulating damaged genome at the same time. For example, downstream of P53, upregulation of *hid*-, *reaper*-mediated apoptosis will lead to decreased survival and upregulation of *corp*-mediated anti-apoptosis will lead to over-proliferation and may sustain cells with an unstable genome. Thus, fine-tuning of closely controlled pathways with opposite functional consequences is essential. This limits the accumulation of defective cells and helps maintain the tissue homeostasis.

Figure 26. A model of pathways that determine cell fate following irreparable DNA damage. Following induction of a single telomere loss, ATM phosphorylates and activates, which in turn, activates P53. P53 transcriptionally activates genes (*grim, hid, reaper, sickle*) that induce apoptosis and *corp* that inhibits apoptosis, by acting on P53 in a negative feedback loop. The pro-apoptotic and anti-apoptotic are finely balanced, and their over-activation (denoted by two red-arrows) can respectively lead to decreased organismal survival due to massive cell-death and over-proliferation of genes with an unrepaired genome, probably leading to oncogenic transformation. *corp*-mediated inhibition and delay of apoptosis gives the cells an extended duration for triggering compensatory proliferation and *de novo* telomere addition (as mediated by *hiphop*). A second aneuploidy-driven, P53-independent JNK-mediated pathway also triggers apoptosis. The *fs(1)Yb* gene plays a role in recruitment and proper localization of piwi pathway proteins (piwi and armi) for transposon silencing, that is important for maintenance of telomere integrity. It is yet to be found out where exactly it feeds into the DDR pathway. As our results indicate, it acts upstream of *p53*, probably inducing *ATM* or *Chk2* or *p53* itself, or even acting as an inducer of DNA damage by disrupting telomere integrity.

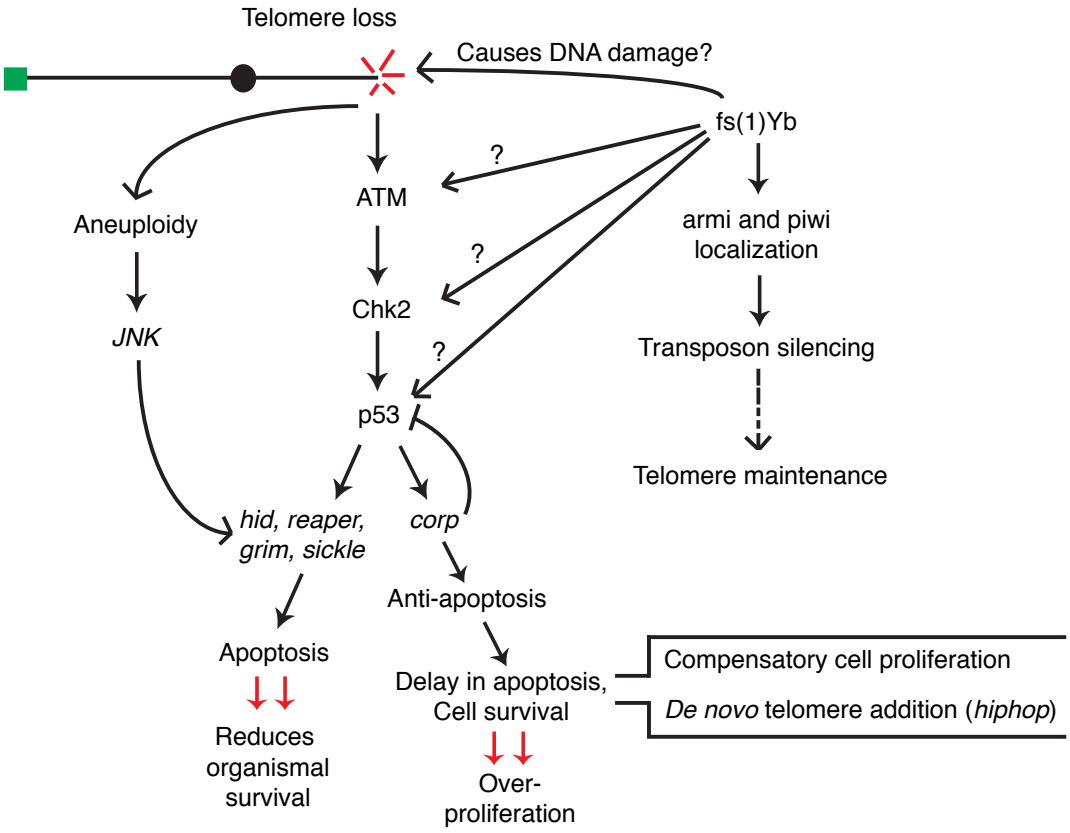
Telomere loss
Causes DNA damage?
fs(1)Yb
?
ATM
Aneuploidy
armi and piwi
localization
?
Chk2
JNK
Transposon silencing
?
p53
Telomere maintenance
hid, reaper,
grim, sickle
corp
Anti-apoptosis
Apoptosis
Delay in apoptosis,
Cell survival
Compensatory cell proliferation
De novo telomere addition (hiphop)
Reduces
organismal
survival
Over-
proliferation

References

Ahmad, K., and Golic, K.G. (1998). The transmission of fragmented chromosomes in Drosophila melanogaster. Genetics *148*, 775–792.

Bilak, A., Uyetake, L., and Su, T.T. (2014). Dying cells protect survivors from radiation-induced cell death in Drosophila. PLoS Genet *10*, e1004220.

Chen, Y.Y., Pane, A.A., and Schüpbach, T.T. (2007). cutoff and aubergine Mutations Result in Retrotransposon Upregulation and Checkpoint Activation in Drosophila. Curr. Biol. *17*, 6–6.

Colombani, J., Polesello, C., Josué, F., and Tapon, N. (2006). Dmp53 activates the Hippo pathway to promote cell death in response to DNA damage. Curr. Biol. *16*, 1453–1458.

Dichtel-Danjoy, M.-L., Ma, D., Dourlen, P., Chatelain, G., Napoletano, F., Robin, M., Corbet, M., Levet, C., Hafsi, H., Hainaut, P., et al. (2012). Drosophila p53 isoforms differentially regulate apoptosis and apoptosis-induced proliferation. *19*, 451–460.

Fan, Y., and Bergmann, A. (2008). Distinct Mechanisms of Apoptosis-Induced Compensatory Proliferation in Proliferating and Differentiating Tissues in the Drosophila Eye. Developmental Cell *14*, 399–410.

Flint, J.J., Craddock, C.F.C., Villegas, A.A., Bentley, D.P.D., Williams, H.J.H., Galanello, R.R., Cao, A.A., Wood, W.G.W., Ayyub, H.H., and Higgs, D.R.D. (1994). Healing of broken human chromosomes by the addition of telomeric repeats. Am J Hum Genet *55*, 505–512.

Gao, Q., Reynolds, G.E., Wilcox, A., Miller, D., Cheung, P., Artandi, S.E., and Murnane, J.P. (2008). Telomerase-dependent and -independent chromosome healing in mouse embryonic stem cells. DNA Repair (Amst) *7*, 17–17.

Gatz, S.A., and Wiesmüller, L. (2006). p53 in recombination and repair. Cell Death Differ *13*, 1003–1016.

Huh, J.R., Guo, M., and Hay, B.A. (2004). Compensatory Proliferation Induced by Cell Death in the Drosophila Wing Disc Requires Activity of the Apical Cell Death Caspase Dronc in a Nonapoptotic Role. Current Biology *14*, 1262–1266.

Jager, D., and Philippsen, P. (1989). Stabilization of dicentric chromosomes in Saccharomyces cerevisiae by telomere addition to broken ends or by centromere deletion. The EMBO Journal *8*, 247–254.

Jaklevic, B., Uyetake, L., Lemstra, W., Chang, J., Leary, W., Edwards, A., Vidwans, S., Sibon, O., and Tin Su, T. (2006). Contribution of Growth and Cell Cycle Checkpoints to Radiation Survival in Drosophila. Genetics *174*, 1963–1972.

Jaklevic, B.R., and Su, T.T. (2004). Relative contribution of DNA repair, cell cycle checkpoints, and cell death to survival after DNA damage in Drosophila larvae. Curr. Biol. *14*, 23–32.

Khurana, J.S., Xu, J., Weng, Z., and Theurkauf, W.E. (2010). Distinct Functions for the Drosophila piRNA Pathway in Genome Maintenance and Telomere Protection. PLoS Genet *6*, e1001246.

Klattenhoff, C.C., Bratu, D.P.D., McGinnis-Schultz, N.N., Koppetsch, B.S.B., Cook, H.A.H., and Theurkauf, W.E.W. (2007). Drosophila rasiRNA Pathway Mutations Disrupt Embryonic Axis Specification through Activation of an ATR/Chk2 DNA Damage Response. Developmental Cell *12*, 11–11.

Kurzhals, R.L., Titen, S.W.A., Xie, H.B., and Golic, K.G. (2011). Chk2 and p53 are haploinsufficient with dependent and independent functions to eliminate cells after telomere loss. PLoS Genet *7*, e1002103–e1002103.

Makovets, S., and Blackburn, E.H. (2009). DNA damage signalling prevents deleterious telomere addition at DNA breaks. Nat Cell Biol *11*, 1383–1386.

Mauri, F., McNamee, L.M., Lunardi, A., Chiacchiera, F., Del Sal, G., Brodsky, M.H., and Collavin, L. (2008). Modification of Drosophila p53 by SUMO Modulates Its Transactivation and Pro-apoptotic Functions. Journal of Biological Chemistry *283*, 20848–20856.

McClintock, B. (1941). The Stability of Broken Ends of Chromosomes in Zea Mays. Genetics *26*, 234–282.

McNamee, L.M., and Brodsky, M.H. (2009). p53-Independent Apoptosis Limits DNA Damage-Induced Aneuploidy. Genetics *182*, 423–435.

Peters, M., DeLuca, C., Hirao, A., Stambolic, V., Potter, J., Zhou, L., Liepa, J., Snow, B., Arya, S., Wong, J., et al. (2002). Chk2 regulates irradiation-induced, p53-mediated apoptosis in Drosophila. Proc Natl Acad Sci USA *99*, 11305–11310.

Ryoo, H.D., Gorenc, T., and Steller, H. (2004). Apoptotic cells can induce compensatory cell proliferation through the JNK and the Wingless signalingpathways. Developmental Cell *7*, 491–501.

Shay, J.W., and Wright, W.E. (2001). Telomeres and Telomerase: Implications for Cancer and Aging. Radiat Res *155*, 188–193.

Sprung, C.N.C., Reynolds, G.E.G., Jasin, M.M., and Murnane, J.P.J. (1999). Chromosome healing in mouse embryonic stem cells. Proc. Natl. Acad. Sci. U.S.a. *96*, 6781–6786.

Titen, S.W.A., and Golic, K.G. (2008). Telomere Loss Provokes Multiple

Pathways to Apoptosis and Produces Genomic Instability in Drosophila melanogaster. Genetics *180*, 1821–1832.

Titen, S.W.A., and Golic, K.G. (2010). Healing of euchromatic chromosome breaks by efficient de novo telomere addition in Drosophila melanogaster. Genetics *184*, 309–312.

van Bergeijk, P., Heimiller, J., Uyetake, L., and Su, T.T. (2012). Genome-Wide Expression Analysis Identifies a Modulator of Ionizing Radiation-Induced p53-Independent Apoptosis in Drosophila melanogaster. PLoS ONE *7*, e36539.

Warner, S.J., Yashiro, H., and Longmore, G.D. (2010). The Cdc42/Par6/aPKC Polarity Complex Regulates Apoptosis-Induced Compensatory Proliferation in Epithelia. Current Biology *20*, 677–686.

Wells, B.S., Yoshida, E., and Johnston, L.A. (2006). Compensatory Proliferation in Drosophila Imaginal Discs Requires Dronc-Dependent p53 Activity. Current Biology *16*, 1606–1615.

Wichmann, A., Jaklevic, B., and Su, T.T. (2006). Ionizing radiation induces caspase-dependent but Chk2- and p53-independent cell death in Drosophila melanogaster. Proc. Natl. Acad. Sci. U.S.a. *103*, 9952–9957.

Zhang, W., and Durocher, D. (2010). De novo telomere formation is suppressed by the Mec1-dependent inhibition of Cdc13 accumulation at DNA breaks. Genes & Development *24*, 502–515.

APPENDIX A

EP SCREEN DATASHEET

Stock	Cy^+ male eye phenotype						Notes
	B^S	1	2	3	4	5	
14818	14	0	0	1	0	0	
14821	0	0	0	0	18	0	suppressor
14830	8	0	5	10	0	0	
14833	4	0	0	3	0	0	
14841	8	0	0	2	0	0	
14846	8	0	1	5	0	0	
14851	5	0	1	8	0	0	
14854	-	-	-	-	-	-	
14862	5	0	2	7	0	0	
14865	-	-	-	-	-	-	
14866	7	-	-	-	-	-	
14995	18	0	2	0	0	0	
15002	8	0	5	1	0	0	
15004	-	-	-	-	-	-	
15008	-	-	-	-	-	-	
15037	-	-	-	-	-	-	
15038	8	0	7	43	-	-	
15044	6	0	0	5	0	0	
15049	-	-	-	-	-	-	
15058	28	0	0	1	0	0	

Stock	Cy^+ male eye phenotype						Notes
	B^S	1	2	3	4	5	
15060	5	0	1	1	0	0	
15065	8	1	0	0	0	0	
15083	14	0	0	0	0	0	
15087	18	0	2	3	0	0	
15299	10	0	2	0	0	0	
15300	12	0	1	7	0	0	
15305	35	0	2	3	0	0	
15318	18	0	4	0	0	0	
15324	9	0	6	2	0	0	
15347	17	0	0	7	0	0	
15349	5	0	2	10	0	0	
15361	17	0	1	8	0	0	
15368	6	0	0	0	0	0	
15386	9	0	2	8	0	0	
15388	10	0	0	0	0	0	
15389	8	0	10	12	0	0	
15392	19	0	1	2	0	0	
15393	5	0	2	0	0	0	
15394	4	0	1	0	0	0	
15395	4	0	2	14	0	0	

Stock	Cy^+ male eye phenotype						Notes
	B^S	1	2	3	4	5	
15397	9	0	2	1	0	0	
15398	24	0	0	0	0	0	
15400	7	0	3	8	0	0	
15401	6	0	0	8	0	0	
15407	4	0	2	7	0	0	
15410	9	0	0	0	0	0	
15411	12	0	0	4	0	0	
15412	13	0	2	10	0	0	
15414	15	0	1	3	0	0	
15416	8	0	0	4	0	0	
15419	11	0	3	5	0	0	
15425	-	-	-	-	-	-	
15431	7	0	4	6	0	0	
15432	18	0	3	5	0	0	
15434	11	0	0	3	0	0	
15436	11	0	2	4	0	0	
15438	12	0	7	4	0	0	
15439	11	1	0	0	0	0	
15444	12	0	4	1	0	0	
15445	15	0	7	3	0	0	

Stock	Cy^+ male eye phenotype						Notes
	B^S	1	2	3	4	5	
15448	11	0	2	2	0	0	
15449	11	0	1	0	0	0	
15450	12	0	4	2	0	0	
15459	4	0	0	0	0	0	
15472	-	-	-	-	-	-	
15490	20	-	-	5	-	-	
15492	11	0	5	1	0	0	
15497	11	0	1	2	0	0	
15500	14	0	4	1	0	0	
15528	7	0	0	2	0	0	
15529	7	0	2	5	0	0	
15541	12	0	10	2	0	0	
15543	15	0	0	3	0	0	
15544	8	0	12	8	0	0	
15577	19	0	2	4	0	0	
15592	10	0	2	4	0	0	
15595	8	0	4	7	0	0	
15623	16	0	7	1	0	0	
15634	14	0	0	3	0	0	
15637	8	0	11	29	0	0	

Stock	Cy^+ male eye phenotype						Notes
	B^S	1	2	3	4	5	
15646	8	0	0	0	0	0	
15647	22	0	4	2	0	0	
15650	0	0	0	0	0	18	suppressor
15653	5	0	0	6	0	0	
15662	8	0	12	18	0	0	
15669	14	0	3	3	0	0	
15673	8	0	4	2	0	0	
15675	6	0	5	0	0	0	
15677	5	0	3	0	0	0	
15679	18	0	1	8	0	0	
15681	6	0	5	7	0	0	
15688	12	0	2	5	0	0	
15689	1	0	1	3	0	0	
15690	12	0	2	5	0	0	
15701	12	0	0	2	0	0	
15702	4	0	0	10	0	0	
15703	15	0	10	12	0	0	
15704	5	0	0	5	0	0	
15705	18	0	7	6	0	0	
15713	-	-	-	-	-	-	

Stock	Cy^+ male eye phenotype						Notes
	B^S	1	2	3	4	5	
15715	9	0	12	16	0	0	
15724	20	0	6	2	0	0	
15725	-	-	-	-	-	-	
15726	22	0	4	9	0	0	
15734	8	0	10	2	0	0	
15742	1	0	0	0	15	0	suppressor
15744	7	0	0	4	0	0	
15748	14	0	4	2	0	0	
15755	19	0	9	3	0	0	
15765	0	0	2	6	0	0	
15769	22	0	2	4	0	0	
15778	0	18	9	2	0	0	enhancer
15779	16	0	3	7	0	0	
15783	16	0	7	0	0	0	
15784	12	0	8	11	0	0	
15788	25	0	6	5	0	0	
15790	19	0	1	2	0	0	
15791	-	-	-	-	-	-	
15795	16	0	16	1	0	0	
15806	12	0	0	1	0	0	

Stock	Cy^+ male eye phenotype						Notes
	B^S	1	2	3	4	5	
15811	21	0	9	4	0	0	
15829	7	0	5	6	0	0	
15830	6	0	9	1	0	0	
15836	34	0	9	2	0	0	
15844	25	0	7	6	0	0	
15862	22	0	1	7	0	0	
15870	22	0	15	1	0	0	
15872	-	-	-	-	-	-	
15876	-	-	-	-	-	-	
15877	-	-	-	-	-	-	
15879	15	0	2	6	0	0	
15881	2	0	1	0	0	0	
15883	35	0	7	22	0	0	
15885	19	-	4	0	0	0	
15886	8	0	0	5	0	0	
15887	12	0	3	2	0	0	
15888	31	0	6	3	0	0	
15894	0	12	1	0	0	0	Females also have small, rough eyes
15896	12	0	0	3	0	0	

Stock	Cy^+ male eye phenotype						Notes
	B^S	1	2	3	4	5	
15898	11	0	1	1	0	0	
15899	-	-	-	-	-	-	
15901	-	-	-	-	-	-	
15920	-	-	-	-	-	-	
15934	11	0	0	1	0	0	
15937	18	0	0	4	0	0	
15939	7	0	5	2	0	0	
15941	12	0	17	0	0	0	
15945	5	0	6	9	0	0	
15954	9	0	5	1	0	0	
15977	11	0	4	3	0	0	
16003	7	0	0	3	0	0	
16008	11	0	6	3	0	0	
16363	8	0	2	5	0	0	
16373	12	0	10	11	0	0	
16374	5	0	7	7	0	0	
16381	8	0	3	1	0	0	
16383	14	0	8	2	0	0	
16384	7	0	0	1	0	0	
16385	7	0	8	3	0	0	

Stock	Cy^+ male eye phenotype						Notes
	B^S	1	2	3	4	5	
16388	34	0	5	4	0	0	
16393	0	0	15	0	0	0	Females also have small eyes
16394	28	0	16	4	0	0	
16400	10	0	0	0	0	0	
16404	5	0	0	0	0	0	
16443	-	-	-	-	-	-	
16537	12	0	8	10	0	0	
16538	7	0	0	2	0	0	
16617	5	29	18	0	0	0	enhancer
16626	8	0	2	2	0	0	
16633	8	0	2	1	0	0	
16635	6	0	9	0	0	0	
16640	7	0	0	0	0	0	
16642	-	-	-	-	-	-	
16645	8	0	2	4	0	0	
16648	11	0	0	5	0	0	
16650	12	0	0	4	0	0	
16660	10	0	7	2	0	0	
16670	14	0	1	0	0	0	

Stock	Cy^+ male eye phenotype						Notes
	B^S	1	2	3	4	5	
16684	9	0	0	2	0	0	
16685	9	0	1	2	0	0	
16686	24	0	5	1	0	0	
16691	9	0	0	1	0	0	
16693	20	0	6	0	0	0	
16708	9	0	0	4	0	0	
16719	4	0	4	38	0	0	
16726	10	0	0	0	0	0	
16733	9	0	0	0	0	0	
16734	15	0	3	8	0	0	
16739	21	1	4	0	0	0	
16752	9	0	1	4	0	0	
16763	0	0	0	0	0	0	15 Cy^+ males, 8 Cy^+ and 9 *Cy* females
16771	9	0	0	0	0	0	
16772	8	0	1	2	0	0	
16779	12	0	0	4	0	0	
16781	15	0	0	6	0	0	
16782	21	0	6	3	0	0	
16785	10	1	0	0	0	0	

Stock	Cy^+ male eye phenotype						Notes
	B^S	1	2	3	4	5	
16786	3	0	1	2	0	3	
16789	3	0	1	0	0	0	
16796	15	0	5	2	0	0	
16803	14	0	5	1	0	0	
16809	7	0	1	2	0	0	
16811	16	0	3	0	0	0	
16813	6	0	0	0	0	0	
16817	22	0	3	2	0	0	
16824	14	0	1	2	0	0	
16827	11	0	5	1	0	0	
16835	7	0	0	0	0	0	
16836	18	0	3	2	0	0	
16858	0	18	0	0	0	0	No *Cy*+ females
16859	16	0	1	0	0	0	
16862	16	0	6	1	0	0	
16866	10	0	2	2	0	0	
16877	7	0	22	0	0	0	
16884	11	0	4	1	0	0	
16889	12	0	3	2	0	0	
16891	5	0	0	4	0	0	

Stock	Cy^+ male eye phenotype						Notes
	B^S	1	2	3	4	5	
16892	14	0	5	1	0	0	
16897	15	0	0	4	0	0	
16907	10	0	6	2	0	0	
16912	11	0	3	1	0	0	
16913	14	0	2	1	0	0	
16915	12	0	2	0	0	0	
16918	9	0	3	4	0	0	
16923	16	0	2	4	0	0	
16926	5	0	3	7	0	0	
16939	18	0	3	2	0	0	
16940	3	0	0	1	0	0	
16945	6	0	0	0	19	0	suppressor
16946	8	0	2	6	0	0	
16955	10	0	2	2	0	0	
16959	15	0	1	0	0	0	
16963	9	0	5	2	0	0	
16965	7	0	0	1	0	0	
16976	17	0	4	0	0	0	
16977	5	0	1	0	0	0	
17303	9	0	0	5	0	0	

Stock	Cy^+ male eye phenotype						Notes
	B^S	1	2	3	4	5	
17319	8	0	0	0	0	0	
17330	10	0	2	4	0	0	
17331	14	0	6	1	0	0	
17338	19	0	8	1	0	0	
17343	10	0	1	2	0	0	
17347	2	0	0	3	0	0	
17348	12	0	2	0	0	0	
17353	17	0	4	0	0	0	
17354	-	-	-	-	-	-	
17355	14	0	3	0	0	0	
17357	12	0	9	0	71	0	suppressor ?
17358	18	0	9	6	0	0	
17361	23	0	16	14	0	0	
17363	-	-	-	-	-	-	
17373	11	0	5	8	0	0	
17376	9	0	7	4	0	0	
17377	15	0	11	7	0	0	
17378	16	0	11	12	0	0	
17380	0	-	0	0	0	0	??
17381	6	0	18	2	0	0	

Stock	Cy^+ male eye phenotype						Notes
	B^S	1	2	3	4	5	
17386	14	0	12	0	0	0	
17395	19	0	15	0	0	0	
17397	15	0	17	14	0	0	
17403	8	0	2	5	0	0	
17411	7	0	11	9	0	0	
17416	19	0	5	1	0	0	
17420	16	0	18	21	0	0	
17439	7	0	8	9	0	0	
17440	12	0	10	9	0	0	
17443	4	0	7	9	0	0	
17445	19	0	14	9	0	0	
17447	10	0	8	2	0	0	
17453	22	0	3	2	0	0	
17455	19	0	13	8	0	0	
17458	19	0	9	11	0	0	
17477	17	0	16	20	0	0	
17478	12	0	7	9	0	0	
17482	11	0	8	9	0	0	
17491	27	0	22	0	0	0	
17494	16	0	5	2	0	0	

Stock	Cy^+ male eye phenotype						Notes
	B^S	1	2	3	4	5	
17496	5	0	3	32	0	0	suppressor ?
17497	15	0	4	0	0	0	
17507	16	0	0	24	0	0	
17509	14	0	14	3	0	0	
17512	8	0	1	0	6	0	
17529	17	0	4	0	0	40	suppressor ?
17535	10	0	12	5	0	0	
17541	12	0	9	6	0	0	
17544	17	0	4	7	0	0	
17545	-	-	-	-	-	-	
17549	11	0	10	2	0	0	
17557	8	0	3	6	0	0	
17560	10	0	5	0	0	0	
17563	51	0	1	8	0	0	
17565	10	0	0	2	0	0	
17566	8	0	5	2	0	0	
17571	11	0	3	0	0	0	
17585	12	0	0	3	0	0	
17590	15	0	11	0	33	0	suppressor ?
17592	22	0	0	15	0	0	

Stock	Cy^+ male eye phenotype						Notes
	B^S	1	2	3	4	5	
17596	11	0	7	9	0	0	
17598	2	0	4	2	0	0	
17602	8	0	0	6	0	0	
17604	21	0	18	12	0	0	
17606	12	0	0	8	0	0	
17608	-	-	-	-	-	-	
17609	18	0	9	11	0	0	
17613	19	0	8	9	0	0	
17616	-	-	-	-	-	-	
17631	12	0	11	9	0	0	
17648	4	0	12	0	0	0	
17674	0	0	0	0	0	104	suppressor
19646	22	0	14	12	0	0	
19666	16	0	0	0	0	0	
19685	19	0	11	14	0	0	
19689	24	0	0	0	0	0	
19697	18	0	0	0	0	0	
19717	19	0	6	2	0	0	
19730	8	0	11	4	0	0	
19731	12	0	4	1	0	0	

Stock	Cy^+ male eye phenotype						Notes
	B^S	1	2	3	4	5	
19732	22	0	0	0	0	0	
19733	21	0	18	11	0	0	
19744	11	0	7	2	0	0	
19773	31	0	12	11	0	0	
19779	25	0	0	0	0	0	
19797	17	0	3	8	0	0	
19802	3	0	4	1	0	0	
19817	8	0	5	1	0	0	
19822	22	0	11	9	0	0	
19823	15	0	8	2	0	0	
19833	11	0	4	0	0	0	
19839	18	0	8	6	0	0	
19866	13	0	7	2	0	0	
19892	16	0	8	2	0	0	
19898	2	0	1	9	0	0	
19900	14	0	11	5	0	0	
19902	6	0	4	0	0	0	
19934	15	0	8	2	0	0	
19942	16	0	1	0	27	0	suppressor ?
19943	11	0	5	2	0	0	

Stock	Cy^+ male eye phenotype						Notes
	B^S	1	2	3	4	5	
19947	17	0	12	9	0	0	
19949	5	0	7	2	0	0	
19950	12	0	8	9	0	0	
19954	-	-	-	-	-	-	
19957	17	0	8	7	0	0	
19963	24	0	0	0	0	0	
19964	19	0	13	11	0	0	
19969	7	0	9	2	0	0	
19976	8	0	12	6	0	0	
19990	15	0	11	8	0	0	
20005	12	0	7	5	0	0	
20006	0	0	8	0	0	0	inducer?
20010	32	0	0	14	0	0	
20011	19	0	0	0	0	0	
20024	23	0	17	14	0	0	
20044	15	0	8	0	12	0	
20065	0	0	0	2	0	0	
20069	7	0	9	3	0	0	
20074	12	0	9	6	0	0	
20077	7	0	1	4	0	0	

Stock	Cy^+ male eye phenotype						Notes
	B^S	1	2	3	4	5	
20101	5	0	1	1	0	0	
20116	3	0	1	1	0	0	
20118	14	0	12	10	0	0	
20126	13	0	0	9	0	0	
20144	19	0	14	12	0	0	
20177	9	0	0	2	0	0	
20194	21	0	16	0	0	0	
20197	12	0	4	7	0	0	
20216	7	0	1	4	0	0	
20217	17	0	0	12	0	0	
20218	24	0	21	0	0	0	
20256	22	0	0	21	0	0	
20257	18	0	11	14	0	0	
20258	9	0	5	0	58	0	suppressor ?
20269	18	0	8	3	0	0	
20294	13	0	11	9	0	0	
20295	9	0	4	3	0	0	
20297	12	0	0	14	0	0	
20299	17	0	`5	0	0	0	
20317	6	0	0	1	0	0	

Stock	Cy^+ male eye phenotype						Notes
	B^S	1	2	3	4	5	
20318	19	0	0	23	0	0	
20320	6	0	12	9	0	0	
20325	13	0	0	11	0	0	
20337	8	0	0	9	0	0	
20340	18	0	12	14	0	0	
20348	8	0	7	0	0	0	
20628	6	0	0	0	17	0	
20635	7	0	0	0	0	0	
20642	-	-	-	-	-	-	
20654	19	0	14	08	0	0	
20666	17	0	0	0	0	0	
20667	9	0	4	3	0	0	
20668	16	0	0	7	0	0	
20674	5	0	2	0	0	0	
20682	12	0	8	0	0	0	
20687	8	0	6	8	0	0	
20693	12	0	9	0	0	0	
20697	9	0	0	0	0	0	
20705	19	0	6	9	0	0	
20717	12	0	0	14	0	0	

Stock	Cy^+ male eye phenotype						Notes
	B^S	1	2	3	4	5	
20718	11	0	3	1	0	0	
20720	12	0	5	9	0	0	
20721	12	0	5	0	0	0	
20723	12	0	11	8	0	0	
20733	15	0	9	8	0	0	
20742	8	0	0	9	0	0	
20745	21	0	0	9	0	0	
20786	17	0	16	4	0	0	
20792	9	0	2	5	0	0	
20793	24	0	0	0	0	0	
20798	23	0	3	2	0	0	
20807	14	0	4	8	0	0	
20816	17	0	0	8	0	0	
20817	17	0	10	0	0	0	
20827	3	0	3	0	0	0	
20833	3	0	2	0	0	0	
20847	14	0	6	5	0	0	
20849	8	0	0	1	0	0	
20856	-	-	-	-	-	-	
20857	12	0	9	6	0	0	

Stock	Cy^+ male eye phenotype						Notes
	B^S	1	2	3	4	5	
20858	14	0	5	8	0	0	
20861	-	-	-	-	-	-	
20881	6	0	0	4	0	0	
20884	4	0	0	0	0	0	
20885	14	0	4	38	0	0	
20917	8	0	9	14	0	0	
20923	12	0	3	0	0	0	
20924	12	0	0	9	0	0	
20936	11	0	0	7	0	0	
20940	21	0	0	18	0	0	
20944	15	0	0	9	0	0	
20948	6	0	0	2	0	0	
20951	10	0	0	8	0	0	
20952	9	0	0	5	0	0	
20961	12	0	0	14	0	0	
20963	9	0	1	0	0	0	
20964	14	0	6	2	0	0	
21081	17	0	0	12	0	0	
21084	3	0	4	2	0	0	
21097	10	0	0	0	0	0	

Stock	Cy^+ male eye phenotype						Notes
	B^S	1	2	3	4	5	
21098	18	0	14	0	0	0	
21100	6	0	3	2	0	0	
21102	11	0	3	1	0	0	
21103	15	0	0	5	0	0	
21105	0	-	0	0	0	0	No *Cy* males too
21111	-	-	-	-	-	-	
21112	21	0	17	12	0	0	
21113	14	0	8	9	0	0	
21131	15	0	0	5	0	0	
21133	17	0	5	3	0	0	
21142	0	0	0	1	0	0	
21146	11	0	0	0	0	0	
21151	4	0	0	5	0	0	
21153	12	0	6	5	0	0	
21169	6	0	11	0	0	0	
21170	2	0	14	1	0	0	
21184	12	0	5	8	0	0	
21189	9	0	5	8	0	0	
21192	0	12	8	2	0	0	
21198	8	0	7	9	0	0	

Stock	Cy^+ male eye phenotype						Notes
	B^S	1	2	3	4	5	
21199	-	-	-	-	-	-	
21202	12	0	7	0	0	0	
21210	8	0	2	5	0	0	
21211	14	0	7	0	0	0	
21222	15	0	12	0	0	0	
21230	8	0	4	5	0	0	
21233	12	0	9	0	0	0	
21235	18	0	0	0	0	0	
21353	23	0	19	3	0	0	
21368	24	0	19	0	0	0	
21375	18	0	6	0	0	0	
21377	16	0	1	0	0	0	
21380	11	0	0	0	0	0	
21387	12	0	9	0	0	0	
21388	11	0	8	0	0	0	
21404	11	0	1	0	0	0	
21419	9	0	0	4	0	0	
21420	10	0	5	4	0	0	
21423	12	0	7	16	0	0	
21424	18	0	11	9	0	0	

Stock	Cy^+ male eye phenotype						Notes
	B^S	1	2	3	4	5	
21426	15	0	8	6	0	0	
21427	7	0	0	0	0	0	
21428	8	0	9	7	0	0	
21429	-	-	-	-	-	-	
21430	9	0	0	8	0	0	
21436	11	0	8	0	0	0	
21438	12	0	0	0	0	0	
21451	17	0	12	13	0	0	
21955	11	0	5	0	0	0	
22137	12	0	5	0	0	0	
22151	3	0	7	12	0	0	
22288	22	0	12	9	0	0	
22292	9	0	6	2	0	0	
22294	14	0	0	6	0	0	
22295	-	-	-	-	-	-	
22321	12	0	6	0	0	0	
22324	17	0	0	17	0	0	
22326	3	0	1	0	0	0	
22337	12	0	9	7	0	0	
22338	9	0	7	5	0	0	

Stock	Cy^+ male eye phenotype						Notes
	B^S	1	2	3	4	5	
22339	4	0	11	3	0	0	
22351	3	0	0	5	0	0	
22353	8	0	1	2	0	0	
22354	11	0	0	3	0	0	
22355	20	0	2	1	0	0	
22356	10	0	1	9	0	0	
22365	14	0	10	1	0	0	
22371	12	0	0	2	0	0	
22372	4	0	2	1	0	0	
22402	7	0	5	8	0	0	
22403	6	0	0	1	0	0	
22410	0	5	2	0	0	0	72 *Cy* males, 24 Cy^+ females (smaller rough eyes): Gene seems to effect eye and bristle.
22412	11	0	4	2	0	0	
22432	11	0	2	8	0	0	
22433	9	0	3	3	0	0	
22434	-	-	-	-	-	-	
22439	1	0	0	5	0	0	

Stock	Cy^+ male eye phenotype						Notes
	B^S	1	2	3	4	5	
22450	11	0	5	4	0	0	
22457	5	0	6	4	0	0	
22458	24	0	5	6	0	0	
22463	6	0	8	3	0	0	
22465	10	0	0	0	0	0	
22483	6	0	1	2	0	0	
22488	5	0	5	2	0	0	
22490	-	-	-	-	-	-	
22492	14	0	4	0	0	0	
22494	16	0	3	0	0	0	
22519	14	0	8	10	0	0	
22524	9	0	0	1	0	0	
22534	-	-	-	-	-	-	
22536	8	0	0	4	0	0	
22549	-	-	-	-	-	-	
22552	-	-	-	-	-	-	
22571	19	0	2	1	0	0	
22572	6	0	6	3	0	0	
22573	9	0	0	1	0	0	
22576	1	0	8	0	0	0	inducer?

Stock	Cy^+ male eye phenotype						Notes
	B^S	1	2	3	4	5	
22593	9	0	2	2	0	0	
22594	10	0	9	7	0	0	
22596	22	0	9	2	0	0	
22627	-	-	-	-	-	-	
22634	9	0	0	6	0	0	
22637	16	0	5	4	0	0	
22643	11	0	0	1	0	0	
22645	4	0	4	1	0	0	
22646	6	0	0	1	0	0	
22647	6	0	4	2	0	0	
22660	4	0	1	3	0	0	
23105	15	0	0	0	0	0	
23109	10	0	1	1	0	0	
23119	15	0	1	1	0	0	
24091	7	0	2	1	0	0	
24093	10	0	0	1	0	0	
24095	10	0	4	0	0	0	
24458	0	0	8	28	0	0	suppressor ?
24795	15	0	0	0	0	0	
17506	-	-	-	-	-	-	

Stock	Cy^+ male eye phenotype						Notes
	B^S	1	2	3	4	5	
21079	5	0	2	2	0	0	

APPENDIX B

CONSTRUCTED STOCKS

y w/H1; P{Gal4-ey.H}4.8 P{UAS-FLP1.D}JD1 or *eGUF4.8JD1/SM1, Cy*

y w/Y; P{Gal4-ey.H}4.8 P{UAS-FLP1.D}JD1 or *eGUF4.8JD1/SM1, Cy*

y w/H1; P{Gal4-ey.H}4.8 {UAS-FLP}2B or *eGUF4.82B/SM1, Cy*

y w EP-corp^{+}; Sco/s^{2}CyO

y w EP-corp^{+}; Sb/TM6, Ubx

y w EP-corp^{+}; 70FLP10/s^{2}CyO

y w EP-corp^{+}; EP-Chk2^{+}/s^{2}CyO

y w EP-corp^{+}; {UAS-p53}2/s^{2}CyO

y w EP-corp^{+}; {GMR-Gal4}/s^{2}CyO

y w EP-corp^{+}; p53^{5A-1-4}/TM6, Ubx

y w; UAS-corp$_{A1}$

y w; Sp/SM1, Cy; UAS-corp$_{A1}$/TM3, Sb

corp^{95B}; Sco/s^{2}CyO

corp^{95B}; UAS-corp$_{A1}$/TM6, Ubx

corp^{95B}; nanos-Gal4 UAS-FLP$_{95}$/TM6, Ubx

EP-fs(1)Yb^{+}; Sco/s^{2}CyO

EP-fs(1)Yb^{+}; 70FLP10/s^{2}CyO

EP 15778; HRH00A1/s^{2}CyO

EP 16617; Sb/TM6, Ubx

y w UAS-hid; Sco/s^{2}CyO

y w; UAS-rpr/SM1, Cy; p53^{5A-1-4}/TM6B, Tb

y w; GMR-Gal4/SM1, Cy; p53^{5A-1-4}/TM6B, Tb

y w$_{BR3}$

y w_{BR8}

y w_{BR9}

y w_{BR3}, *EP-corp*$^{+}$

y w_{BR3}; *Actin5C-Gal4 UAS-GFP/SM1, Cy*

y w_{BR3}; $p53^{5A-1-4}$